

Lars Falsen Habostad

# Evaluating the optimal portfolio of VRE capacity to be integrated into the power system

A case study of Zambia

Master's thesis in Energy and Environmental Engineering

Supervisor: Hossein Farahmand

Co-supervisor: Thomas Haugstenrød

June 2021



Lars Falsen Habostad

# **Evaluating the optimal portfolio of VRE capacity to be integrated into the power system**

A case study of Zambia

Master's thesis in Energy and Environmental Engineering  
Supervisor: Hossein Farahmand  
Co-supervisor: Thomas Haugstenrød  
June 2021

Norwegian University of Science and Technology  
Faculty of Information Technology and Electrical Engineering  
Department of Electric Power Engineering



Norwegian University of  
Science and Technology



---

# Abstract

The Republic of Zambia is located in Southern Africa. Like many of its neighboring countries, the electrification rate is low, and less than half the population has access to electricity. Also, the hydropower-dominated Zambian power system has proven vulnerable to changes in rainfall and drought. In recent years, low rainfalls, combined with increasing electricity demand, has led to massive power shortages, resulting in load shedding. Integrating variable renewable energy (VRE) has been proposed as a measure for diversifying the generation portfolio. Renewable energy integration has the potential to increase energy security and lower system operational cost.

This thesis evaluates the optimal portfolio of solar PV and wind power capacity to be integrated into the Zambian power system within 2030. A framework consisting of three steps is developed. First, the expected variations in VRE generation output and precipitation are investigated based on historical data from the Renewables.ninja database. Second, the optimal VRE portfolio is assessed through simulations in a single-node power system model in the open source software PowerGAMA. Finally, load flows are evaluated with the optimal portfolio of VRE integrated into the electricity grid, to identify potential grid constraints.

The results suggest that annual electricity output from solar PV and wind power plants is relatively stable, and negatively correlated with precipitation. VRE generation is therefore usually higher in dry years, compared to wet years. Also, the electricity production from VRE is highest in the dry season. These findings support the fact that increasing the VRE penetration in the system could increase energy security by diversifying the hydro-dominated generation portfolio.

The optimal VRE portfolio is found as the one minimizing the system cost. A portfolio of 2100 MW, consisting of 1470 MW (70%) solar PV capacity and 630 MW (30%) wind power capacity, provides the lowest cost, and is hence identified as optimal. This corresponds to a total VRE share of 37% of expected system generation capacity in 2030. When using a dynamic valuation of water stored in reservoirs, or a lower initial reservoir level, the optimal portfolio size changes to 2700 MW and 3100 MW, respectively. However, the distribution between solar PV and wind power capacity remains at 70/30, suggesting that this could be the optimal distribution of solar PV and wind power capacity.

The results from brief load flow analyses show that the existing electricity grid is suited for integrating the optimal portfolio of VRE, given the assumed distribution of new power plants in the grid. From a technical perspective, the flexibility of existing hydropower plants is therefore considered the most critical factor for increasing the VRE penetration in the system. Evaluating the technical impacts on hydropower plants from changed operations due to VRE integration is suggested as future work.

---

# Sammendrag

Republikken Zambia ligger i Sørlege Afrika. Som mange av sine naboland har landet en lav grad av elektrifisering, og under halvparten av befolkningen har tilgang til elektrisitet. I tillegg har det vannkraftdominerte Zambiske kraftsystemet vist seg å være sårbart for endringer i nedbør og tørke. De siste årene har lave nedbørsmengder, kombinert med økt etterspørsel etter elektrisitet, ført til et stort kraftunderskudd. Dette kraftunderskuddet har resultert i omfattende bruk av lastfrakobling. Økt integrasjon av variabel fornybar energi (VRE) har blitt foreslått som et tiltak for å diversifisere porteføljen av kraftverk i systemet. Fornybar energi kan potensielt øke forsyningssikkerheten og redusere kostnadene forbundet med elektrisitetsproduksjon.

Denne avhandlingen evaluerer den optimale porteføljen av solkraft og vindkraft som kan integreres i det Zambiske kraftsystemet innen 2030. En framgangsmåte bestående av tre steg er benyttet. I det første steget analyseres historiske data fra databasen Renewables.ninja for å undersøke forventet variasjon i kraftproduksjon fra VRE og variasjoner i nedbørsmengde. Andre steg finner den optimale porteføljen av VRE gjennom simuleringer i en enkeltnode-modell av kraftsystemet i open-source softwaren PowerGAMA. Tredje steg simulerer lastflyten med den optimale porteføljen av VRE integrert i kraftnettet, for å identifisere potensielle flaskehalsar i nettet.

Resultatene viser at den årlige elektrisitetsproduksjonen fra sol- og vindkraft er relativt stabil, og negativt korrelert med nedbørsmengde. Elektrisitetsproduksjonen fra VRE er derfor vanligvis høyere i tørre år sammenliknet med våte år. I tillegg er produksjonen fra VRE høyest i den tørre sesongen. Dette støtter antagelsen om at økt kapasitet av VRE i kraftsystemet kan øke forsyningssikkerheten ved å diversifisere den vannkraftdominerte kraftporteføljen.

Den optimale porteføljen av VRE blir i denne avhandlingen funnet som den porteføljen som minimerer systemkostnaden. En portefølje på 2100 MW, bestående av 1470 MW (70%) solkraft og 630 MW (30%) vindkraft resulterer i den laveste kostnaden, og er derfor identifisert som optimal. Dette tilsvarer en VRE-andel på 37% av forventet produksjonskapasitet i systemet i 2030. Bruker man en dynamisk verdsettelse av vann lagret i vannkraftreservoarer, eller et lavere startnivå for fyllingsgraden i reservoarer, endrer den optimale porteføljestørrelsen seg til henholdsvis 2700 MW og 3100 MW. Fordelingen mellom solkraft og vindkraft holder seg imidlertid på 70/30, som indikerer at dette kan være en optimal fordeling.

Resultatene fra enkle lastflytanalyser viser at det eksisterende strømmettet kan håndtere integrasjonen av den optimale porteføljen av VRE, gitt den antatte plasseringen av nye kraftverk i nettet. I et teknisk perspektiv er det derfor fleksibiliteten til eksisterende vannkraftverk som vurderes som den mest kritiske faktoren for å øke andelen VRE i systemet. Studier av de tekniske konsekvensene av endrede operasjonsmønstre på vannkraftverk, som følge av innfasing av VRE, er derfor foreslått som tema for fremtidig arbeid.

---

# Preface

This master's thesis was written at the Department of Electric Power Engineering at the Norwegian University of Science and Technology (NTNU) during the spring semester of 2021. It was supervised by Professor Hossein Farahmand (NTNU) and co-supervised by Senior Advisor Thomas Haugstenrød (Multiconsult).

I want to thank Hossein and Thomas for their invaluable help and guidance during the thesis. They have trusted me to work independently, but have also been available for discussing the thesis whenever needed. Combining the academic knowledge of Hossein with the practical experience of Thomas, has led to a strong supervisory team.

Further, I would like to thank Zambia Electricity Supply Corporation Limited (ZESCO), and George Muyunda in particular. Without data and guidance from George, this thesis would not have been possible.

The abstract of this thesis has been submitted for review to the Renewable Energy Grid Integration Week, which is a conference taking place in September 2021 in Berlin.

Trondheim, June 18, 2021

Lars Falsen Habostad



---

# Contents

<b>Abstract</b>	<b>i</b>
<b>Sammendrag</b>	<b>ii</b>
<b>Preface</b>	<b>iii</b>
<b>List of Figures</b>	<b>vii</b>
<b>List of Tables</b>	<b>x</b>
<b>Abbreviations</b>	<b>xi</b>
<b>1 Introduction</b>	<b>1</b>
1.1 Scope . . . . .	2
1.2 Contribution . . . . .	4
1.3 Structure . . . . .	5
<b>2 Literature review</b>	<b>6</b>
2.1 Benefits of integrating VRE into power systems . . . . .	6
2.1.1 Increasing energy security in Southern Africa with VRE . . . . .	6
2.2 Challenges of increasing the VRE penetration in power systems . . . . .	7
2.3 Using hydropower for flexibility operations . . . . .	8
2.4 Optimal power system planning through portfolio optimization . . . . .	9
<b>3 Theory and methods</b>	<b>11</b>
3.1 Variations in renewable energy resource availability . . . . .	11
3.1.1 Determining the spatial distribution of new power plants . . . . .	11
3.1.2 Extracting data from Renewables.ninja . . . . .	12
3.2 Modeling power systems in PowerGAMA . . . . .	12
3.3 Portfolio optimization methodology . . . . .	13
3.3.1 $Generation_{cost}$ - the annual cost of generation from existing power plants . . . . .	15
3.3.2 $VRE_{cost}$ - the annual cost of new VRE power plants . . . . .	16
3.3.3 $LoadShed_{cost}$ - the annual cost of load shedding . . . . .	17
3.3.4 $ReservoirFilling_{cost}$ - the cost of changed reservoir levels . . . . .	17
3.4 Modeling the impact of different climatic years . . . . .	19
3.5 Creating a multi-node model of the power system . . . . .	20
<b>4 The Zambian power system</b>	<b>21</b>
4.1 Geography, population and the economy of Zambia . . . . .	21
4.2 Power plants . . . . .	23
4.2.1 Kafue Gorge Upper and Itzhi-Tezhi hydropower stations . . . . .	23
4.2.2 Kariba North Bank hydropower station . . . . .	24
4.2.3 Maamba and Ndola thermal power plants . . . . .	24
4.3 Consumers . . . . .	25



---

4.4	Transmission network . . . . .	27
4.4.1	Interconnection with neighboring countries . . . . .	27
4.5	Electricity tariffs and power market in Zambia . . . . .	28
4.6	Drought and load shedding . . . . .	29
4.7	Current status of VRE in Zambia . . . . .	30
<b>5</b>	<b>Case study: A 2030 scenario of the Zambian power system</b>	<b>32</b>
5.1	Variations in renewable generation output and precipitation in Zambia . . . . .	32
5.1.1	Solar power generation . . . . .	32
5.1.2	Wind power generation . . . . .	35
5.1.3	Precipitation . . . . .	37
5.2	Modeling different climatic years . . . . .	37
5.3	Single-node model of the Zambian power system . . . . .	38
5.3.1	System operating reserve requirements . . . . .	38
5.3.2	Power plants . . . . .	39
5.3.3	System load . . . . .	43
5.3.4	Exports/imports . . . . .	44
5.4	Cost parameters . . . . .	45
5.4.1	Marginal cost of power plants . . . . .	45
5.4.2	Value of lost load (VoLL) . . . . .	46
5.4.3	Water values . . . . .	46
5.4.4	Cost of new solar PV and wind power capacity . . . . .	47
5.5	Grid model of the Zambian power system . . . . .	48
<b>6</b>	<b>Results and discussion</b>	<b>52</b>
6.1	Variations in renewable generation output and precipitation . . . . .	52
6.1.1	Solar PV . . . . .	52
6.1.2	Wind power . . . . .	54
6.1.3	Daily variations in VRE generation output . . . . .	55
6.1.4	Precipitation . . . . .	56
6.1.5	Correlation between VRE generation and precipitation . . . . .	57
6.1.6	Diversifying the generation portfolio with VRE in a changing climate . . . . .	58
6.2	Single-node model validation . . . . .	60
6.3	Portfolio simulation results . . . . .	62
6.3.1	Average year results . . . . .	62
6.3.2	Dry year results . . . . .	63
6.3.3	Wet year results . . . . .	65
6.3.4	Weighted average results . . . . .	66
6.3.5	Impacts on system operations from different VRE portfolios . . . . .	68
6.4	Sensitivities . . . . .	74
6.4.1	Dynamic water values . . . . .	74
6.4.2	Projected 2030 system load . . . . .	75
6.4.3	Initial reservoir filling levels . . . . .	77
6.5	Grid model simulation results . . . . .	79
6.6	Potential sources of error . . . . .	82
6.6.1	Sources of error from modeling the system in PowerGAMA . . . . .	83

---

---

<b>7 Conclusion</b>	<b>84</b>
7.1 Scope of future work . . . . .	85
<b>Bibliography</b>	<b>86</b>
<b>Appendix</b>	<b>93</b>
A Sources used for modeling the Zambian system . . . . .	93
B Sensitivity analysis: Dynamic water values . . . . .	94
C Sensitivity analysis: Low load . . . . .	96
D Sensitivity analysis: Low initial reservoir level . . . . .	98
E Distribution of VRE power plants in the grid model . . . . .	100

---

## List of Figures

1	Flowchart describing the portfolio optimization model. . . . .	15
2	Zambia marked with blue on the map of Africa. Source: [61] . . . . .	21
3	Map of Zambia showing the altitude of the landscape in meters above sea level. The major river systems and the Kariba Dam are also shown. Source: [62] . . . . .	22
4	National electricity consumption by economic sector. Source: [10] . . . . .	26
5	Load profile for an average day in 2018. Note that the vertical axis is starting at 1400 MW. Source: [44] . . . . .	26
6	The Zambian transmission network. Red lines represent 330 kV, green lines represent 220 kV and purple lines represent 132 kV. The dotted lines represent planned transmission lines. Source: [44] . . . . .	27
7	Zambian electricity imports and exports. Source: [10] . . . . .	28
8	Solar PV power potential in Zambia. Source: [75] . . . . .	33
9	Geographical coordinates chosen for mapping out the variability in generation output from future solar PV power plants in Zambia. . . . .	34
10	Average wind speeds 150 m above ground level in Zambia. Source: [51] . . . . .	35
11	Geographical coordinates chosen for mapping out the variability in generation output from future wind power plants in Zambia. . . . .	36
12	The grid used in the grid model in PowerFactory. Source: [91], edited by author . . . . .	49
13	Simulated annual electricity generation from solar PV in Zambia. The results were obtained as an average of the simulated output from the eight selected locations. . . . .	53
14	Average monthly simulated electricity generation from solar power in Zambia for the years 2000-2019. . . . .	53
15	Simulated annual electricity generation from wind power in Zambia. The results were obtained as an average of the simulated output from the eight selected locations. . . . .	54
16	Average monthly simulated electricity generation from wind power in Zambia for the years 2000-2019. . . . .	55
17	Simulated hourly VRE generation output for an average day (local time). . . . .	56
18	Historical average precipitation in Zambia, weighted by land area. . . . .	56
19	Average monthly precipitation in Zambia. . . . .	57
20	The daily average generation output from KGU+KNB in 2018 and simulated output from the Large Hydro power plant in the PowerGAMA model. . . . .	61
21	Total annual system cost for 121 different portfolios of solar PV and wind power capacity integrated into the system in an average year. The y-axis shows the solar PV share of the portfolio, implying that the upmost row corresponds to VRE-portfolios consisting of only wind power capacity (0.0 solar PV share), while the lowermost row corresponds to VRE-portfolios consisting of only solar PV capacity (1.0 solar PV share). . . . .	63

---

22	Total annual system cost for 121 different portfolios of solar PV and wind power capacity integrated into the system in a dry year. The y-axis shows the solar PV share of the portfolio, meaning that the upmost row corresponds to VRE-portfolios consisting of only wind power capacity (0.0 solar PV share), while the lowermost row corresponds to VRE-portfolios consisting of only solar PV capacity (1.0 solar PV share). . . . .	64
23	Total annual system cost for 121 different portfolios of solar PV and wind power capacity integrated into the system in a wet year. The y-axis shows the solar PV share of the portfolio, meaning that the upmost row corresponds to VRE-portfolios consisting of only wind power capacity (0.0 solar PV share), while the lowermost row corresponds to VRE-portfolios consisting of only solar PV capacity (1.0 solar PV share). . . . .	66
24	Weighted average system cost for the average, dry and wet year. . . . .	67
25	Simulated generation output and load shedding for three selected days in January (from hour 360 to hour 432). A VRE portfolio of 1470 MW solar PV and 630 MW wind power capacity in an average climatic year was used in the simulations. . . . .	69
26	Load shedding as a weighted average of the three climatic years. . . . .	70
27	Curtailed VRE and RoR hydropower as a weighted average of the three climatic years. . . . .	71
28	Simulated average daily generation output from the Large Hydro power plant in a dry year. A VRE portfolio size of 2100 MW was used in the simulations. 0% solar PV corresponds to a portfolio consisting of only wind power capacity, while 100% solar PV corresponds to a VRE portfolio with only solar PV. Note that the y-axis is starting at 800. . . . .	72
29	Weighted average system cost for different VRE portfolios, when using dynamic water values. . . . .	75
30	Weighted average system cost for different VRE portfolios, when using the low load profile in the simulations. Note that the x-axis is starting at 500 MW instead of 1500 MW used in the previous plots. . . . .	77
31	Weighted average system cost for different VRE portfolios when having an initial reservoir filling level of 30%. . . . .	78
32	The overloaded lines in the Lusaka area market with red color. . . . .	80
33	Water value profile obtained from [55] and scaled to fit the VoLL in Zambia. The curve shows a steep decrease in water value when the reservoir level is less than 20%. The static water value of 52 USD/MWh used in the base case is obtained for a reservoir level of 73%, which is close to the initial reservoir level of 75% at the beginning of the year. . . . .	94
34	System cost for different VRE portfolios in an average year, when using dynamic water values. . . . .	94
35	System cost for different VRE portfolios in a dry year, when using dynamic water values. . . . .	95
36	System cost for different VRE portfolios in a wet year, when using dynamic water values. . . . .	95

---

---

37	System cost for different VRE portfolios in an average year, when modeling the system with low load. . . . .	96
38	System cost for different VRE portfolios in a dry year, when modeling the system with low load. . . . .	96
39	System cost for different VRE portfolios in a wet year, when modeling the system with low load. . . . .	97
40	System cost for different VRE portfolios in an average year with a low initial reservoir level. . . . .	98
41	System cost for different VRE portfolios in a dry year with a low initial reservoir level. . . . .	98
42	System cost for different VRE portfolios in a wet year with a low initial reservoir level. . . . .	99

---

## List of Tables

1	Grid-connected power plants in the Zambian power system by the end of 2019. Source: [10], [11] . . . . .	25
2	Planned solar PV and wind power plants in the Zambian power system. Source: [11] . . . . .	31
3	Inputs used for each coordinate in the simulations of solar power generation.	34
4	Inputs used for each coordinate in the simulations of wind power generation.	36
5	The climatic years selected to represent a dry year, an average year and a wet year. . . . .	37
6	Thermal power plants modeled in PowerGAMA. Source: [74], [44] . . . . .	39
7	Run of river power plants modeled in PowerGAMA. Source: [74], [44], [59] . . . . .	41
8	KGU, KGL and KNB aggregated into the Large Hydro power plant. Note that the capacity of the Large Hydro power plant is 310 MW lower than the sum of the three aggregated power plants due to the reserve requirement. Source: [11], [74], [44], [59] . . . . .	42
9	Solar PV power plants modeled in PowerGAMA. Source: [74], [52] . . . . .	43
10	Wind power plants modeled in PowerGAMA. Source: [52] . . . . .	43
11	The projected load and system losses in the Zambian power system in 2030. Source: [11], [44] . . . . .	44
12	Projected CAPEX and OPEX of solar PV and wind power. Source: [86], [21], [11] . . . . .	48
13	Model parameters used to calculate the total system cost for different portfolios of VRE. . . . .	48
14	The correlation coefficients between solar PV generation, wind power generation and precipitation in Zambia. . . . .	58
15	Economically optimal portfolios of new solar PV and wind power capacity for the three climatic years, and the weighted average result. . . . .	68
16	The system load used in the base case and in the sensitivity analysis. . . . .	76
17	Sources used for modeling the Zambian system in PowerGAMA, and the cost parameters used in the portfolio optimization. . . . .	93
18	The optimal new solar PV capacity distributed in the grid model. . . . .	100
19	The optimal new wind power capacity distributed in the grid model. . . . .	100

---

## Abbreviations

CAPEX	Capital Expenditure
ERB	Energy Regulation Board
GHG	Greenhouse Gas
HFO	Heavy Fuel Oil
IPP	Independent Power Producer
IRENA	International Renewable Energy Agency
KGL	Kafue Gorge Lower
KGU	Kafue Gorge Upper
KNB	Kariba North Bank
LCOE	Levelized Cost of Electricity
OPEX	Operating Expenditure
PHS	Pumped Hydro Storage
PPA	Power Purchase Agreement
PV	Photovoltaic
REFiT	Renewable Energy Feed-in Tariff
RoR	Run-of-the-River
SAPP	Southern African Power Pool
VoLL	Value of Lost Load
VRE	Variable Renewable Energy





# 1 Introduction

Securing access to affordable and clean energy for all, is stated in the UN Sustainable Development Goal number 7 as an important measure for ending poverty and protecting the planet. Currently, nearly 9/10 people have access to electricity globally, but electricity access is unevenly distributed [1]. In sub-Saharan Africa, electricity reaches only around half of the population, and the lack of reliable and cheap energy stifles the economic development in this area. Southern Africa is rich in solar and wind resources, and falling prices on renewable energy technologies have made solar and wind energy viable options for increasing electricity access [2], [3].

The Republic of Zambia is located in Southern Africa. Like many of its neighboring countries, the population is poor, and less than half of the population has access to electricity [4], [5]. In addition to the low degree of electrification, challenges have also been experienced in the power system in recent years. The Zambian power system is dominated by hydropower, which makes it vulnerable to changes in rainfall and drought. Abnormally low rainfalls, combined with increasing electricity demand, has led to massive power shortages. The result has been extensive use of load shedding<sup>1</sup> performed by the public utility ZESCO [7], [3].

Increasing the generation capacity in the system is considered an important measure to meet the growing electricity demand, and reduce load shedding. The 300 MW Maamba coal fired power plant was commissioned in 2016. Further, a doubling of the installed capacity at the Maamba power plant was originally proposed [8], [3]. However, investing in thermal power plants with high greenhouse gas (GHG) emissions is not a sustainable solution.

In Zambia, the government is now looking to increase the integration of variable renewable energy (VRE<sup>2</sup>) into the power system to diversify the generation portfolio, and reduce the risk of power shortages [10], [11]. Increasing the penetration of VRE in the power system also has the potential to lower the total cost of electricity generation and lower the GHG emissions [12], [13], [3].

Nevertheless, integrating VRE into power systems can lead to several challenges. Most importantly, these energy sources are non-dispatchable, meaning that the generation output cannot be regulated to meet changes in power demand, but rather depends on e.g. variable solar radiation and wind speeds. In power systems with a large fraction of VRE, the system operator must therefore ensure that the flexibility of the system is continuously sufficient to balance variations in load and renewable energy generation [3].

When integrating VRE into power systems, both economical and technical evaluations should be conducted. This thesis evaluates the optimal portfolio of solar PV and wind

---

<sup>1</sup>Load shedding can be defined as an intentionally engineered power shutdown where electricity delivery to consumers is stopped [6].

<sup>2</sup>VRE can be defined as non-dispatchable renewable energy, and typically refers to solar PV and wind power [9].

power capacity to be integrated into the Zambian power system in an economic perspective, when taking into account the technical constraints of the system. This is done by simulating system operations in the software PowerGAMA. Potential impacts on load shedding, VRE curtailment and hydropower operations from different VRE portfolios are also discussed. In addition, the potential overloading of the existing power grid from implementing the optimal VRE portfolio is assessed.

Finding the optimal VRE portfolio could be important for several reasons. First, the findings presented in this thesis can serve as a basis for government strategies for power system generation expansion. In particular, ZESCO could benefit from such strategies when planning for new generation capacity. This could reduce the future cost of electricity, and increase energy security. Second, the findings can inform other stakeholders such as investors and non-profit organizations on the potential benefits and challenges of investing in renewable energy in Zambia. Finally, the framework developed in this thesis can be used for assessing VRE integration in similar countries in Southern Africa.

## 1.1 Scope

The main objective of this thesis is to assess the economically optimal portfolio of VRE to be integrated into the Zambian power system, when taking into account the technical constraints of the system. A techno-economic framework is presented, and both economic and technical analyses are conducted. Only new solar PV and wind power capacity is evaluated in this thesis, and VRE will refer to these two technologies from now on.

The most important question to be answered in this thesis, can be formulated as follows: *What is the optimal portfolio of new solar PV and wind power capacity to be integrated into the Zambian power system within 2030?*

This question is answered through a three-step procedure:

1. **Evaluate the variability of renewable energy resources in Zambia from historical data.** This includes assessing the geographical distribution of resources and the variability of resources in time. Historical solar irradiation and wind speed data are converted into hourly generation profiles, and extracted from the open-source database Renewables.ninja. Historical precipitation is also evaluated. Further, literature regarding the potential future development of renewable energy resources in Southern Africa is reviewed.
2. **Assess the economically optimal portfolio of solar PV and wind power capacity to be integrated into the system.** A single-node model of the system in the software PowerGAMA is used for determining the annual system cost of different portfolio alternatives. The single-node model is also used for evaluating the impacts on load shedding, VRE curtailment and hydropower operations from different VRE portfolios.
3. **Simulate the operations in the Zambian power system, with the optimal portfolio of VRE implemented in the current electricity grid, to map out potential**

**grid constraints.** The optimal portfolio of solar PV and wind capacity is translated into power plants in the system, and the simulations are performed in a multi-node model of the Zambian system in PowerGAMA.

The main emphasis is put on evaluating the economically optimal VRE portfolio (step 2). Since there is uncertainty related to many of the model parameters, this includes sensitivity analyses of the most crucial inputs. Evaluating the renewable energy resource potential (step 1) is done mostly to lay the foundation for the two next steps. The renewable energy generation profiles extracted in this step are used in the single-node model and the multi-node model simulations. In addition, understanding how renewable energy resources vary, makes it easier to interpret the results from the portfolio assessments. Simulating the power flows in the multi-node PowerGAMA model (step 3) is conducted to obtain an indication of whether or not the existing grid can handle the proposed VRE integration.

PowerGAMA is an open-source, flow-based market simulation tool implemented in Python, which allows for the simulation of large scale integration of renewable energy in power systems [14]. PowerGAMA provides a techno-economic model of the power system, and takes into account the transmission constraints in the power grid. This allows for a vast range of use areas, from pure economic assessments, to technical evaluations of power flows in the grid [3].

The metric *system cost* captures the most important factors for evaluating the economic performance of different VRE portfolios in a system perspective. It includes the cost of operating existing power plants, the cost of building and operating new VRE power plants, the cost of load shedding and the cost/benefit of changed hydropower reservoir levels. A simplified version of the water value method<sup>3</sup> is used for determining the economic value of energy stored in reservoirs.

To capture the differences in inflow to reservoirs and VRE generation output, a dry year, a wet year and an average climatic year are modeled. This selection is made based on the annual precipitation for each of the years. None of the model parameters are stochastic, but the modeling of different climatic years represents a partly stochastic element through scenario analysis.

The data used in this thesis is mostly extracted from publicly available sources, but some data is received through cooperation with ZESCO and Multiconsult. This applies to historical load profiles, generation profiles and technical data on power lines and loads in the current system.

The scope of the thesis is limited to the year 2030. Thus, the timeline of the VRE integration leading to an optimal result in 2030 is not evaluated. Also, the scope is limited to evaluating the Zambian system without considering interconnections with neighboring countries. This represents a simplification of the real system. Moreover, this thesis only focuses on the optimal solar PV and wind power capacity to be integrated into the system,

---

<sup>3</sup>The water value method normally refers to the the valuation of water stored in reservoirs used in optimal hydropower production planning [15].

and not other technologies such as new hydropower and thermal generation capacity. Only grid connected systems are included in this evaluation.

This thesis is building on the work conducted by the author in the specialization project during the fall 2020 semester. Some parts of the thesis are taken directly from [3], which is the specialization project report. These parts are cited accordingly.

## 1.2 Contribution

To identify potential research gaps, existing literature was reviewed. Several papers evaluate renewable energy integration in Zambia. In [16], the impacts of solar PV integration into the Zambian power system are studied, with the ramp rate constraints of existing hydropower plants included as a constraint. The authors find that large-scale integration of solar energy could be limited by the ramp rate restrictions of the hydropower generators. A case study on the integration of electric vehicles and decentralized VRE in the Lusaka area is performed in [17]. Shifting the charging of the vehicles to consume the mid-day generation peak, and limiting the afternoon load peak, is described as an enabler for high penetration of solar PV in the system. The International Renewable Energy Agency (IRENA) evaluates the renewable energy potential in Zambia in [18]. Microgrids are mentioned as a potential solution for providing electricity to the rural population. Renewable energy integration in Zambia is further studied in [19], mostly focusing on the regulatory framework and risks from an investor perspective. Multiconsult conducts a cumulative impact assessment of integrating 120 MW of new solar PV capacity into the Zambian power system in [20]. The report includes detailed assessments of power flows, fault analyses and stability analyses.

However, [11] is the most relevant paper for the work conducted in this thesis. It evaluates the optimal portfolio of renewable energy that can be integrated in Zambia towards 2030. Several scenarios are evaluated, and the paper finds that the optimal VRE portfolio to be integrated into the Zambian system consists of 1376 MW solar PV and 1400 MW wind power capacity (when assuming no interconnections). The report is used both as a source of data, and as a benchmark for the results obtained in this thesis.

The literature mentioned above provides a range of different studies of renewable energy integration in Zambia. Nevertheless, most of the existing literature focuses on case studies of solar PV integration, or discusses renewable energy integration on a high level. The existing paper evaluating optimal renewable energy integration [11], selects the optimal portfolio based on the objective of minimizing load shedding and VRE curtailment.

This thesis contributes to the existing literature by finding the economically optimal portfolio of new VRE capacity by the use of water values in the system cost calculation. Using the water value method allows for evaluating the cost/benefit of changed hydropower reservoir filling levels. This is highly relevant for assessing the value of increased reservoir levels resulting from a higher VRE penetration in the system. The evaluation of portfolio performance based on system cost separates this thesis from [11].

In addition, the framework in this thesis separates from the current literature on renewable energy integration in Zambia in a number of ways. First, the evaluation of historical solar, wind and rainfall data conducted in this thesis is (to the best knowledge of the author) more comprehensive than in the existing literature. This provides a good basis for evaluating the performance of VRE portfolios in different climatic years. Further, this thesis focuses on displaying the system cost and impact on power system operations resulting from a large number of VRE portfolios, and not only the optimal one. The framework allows for analyzing different economic and technical drivers of the system cost. Also, the results provide a good basis for informing the Zambian government on the potential benefits and challenges of integrating different VRE portfolios. Finally, the use of only open-source software separates this thesis from most of the current literature.

### **1.3 Structure**

Section 2 presents a brief literature review. The objective is to provide the reader with a broader background knowledge within the topic of optimal VRE integration. This is done through a review of existing literature regarding benefits/challenges of renewable energy integration, hydropower flexibility and VRE portfolio optimization. The specific theory and methods applied in this thesis are presented in Section 3. The software *Renewables.ninja* and *PowerGAMA* are described, and the portfolio optimization model is explained in detail.

The thesis then shifts focus towards Zambia. Section 4 presents a detailed description of the Zambian power system. The objective is to inform the reader about the current state of the system, and the challenges experienced in recent years. Section 5 describes how a 2030 scenario of the Zambian power system was developed. This includes both data extraction, and modeling the system in *PowerGAMA*.

Section 6 presents and discusses the results from the Zambian case study. System costs resulting from different portfolios are shown, and impacts on system operations from the different portfolios are discussed. Sensitivity analyses are conducted. Further, potential overloading of lines in the power grid from integrating the optimal portfolio of VRE is evaluated. Finally, a conclusion is drawn in Section 7 on what could be the optimal portfolio of new VRE capacity in the Zambian power system. The most important results are summarized, and the scope of future work is proposed.

## 2 Literature review

In addition to the papers evaluating renewable energy integration in Zambia, presented in Section 1, a somewhat broader literature review was conducted. The review was based on the work conducted in the specialization project. Some of the material is therefore taken from [3].

In this section, the benefits of integrating VRE into power systems are discussed, emphasising the ability of VRE to increase energy security in a changing climate. Some of the main challenges associated with VRE are also reviewed, followed by the role of hydropower in providing power system flexibility. This includes some brief comments regarding the potential increased wear and tear on hydropower plants from changed operations following VRE integration. The use of portfolio optimization methodologies in power system planning is discussed at the end of the section.

### 2.1 Benefits of integrating VRE into power systems

The most prominent reason for integrating VRE into power systems, is the environmental benefit associated with such energy sources in many countries. Solar PV and wind power have the potential to reduce pollution-related environmental impacts from electricity production, such as GHG emissions, freshwater ecotoxicity and particle emissions [13], [21].

Another advantage of implementing VRE into power systems, is that these technologies today represent the cheapest form of electricity generation in many locations worldwide. Levelized cost of electricity (LCOE) of solar PV has decreased by more than 80% in the last decade, and the LCOE of wind power has fallen by around 40% in the same period [22]. The trend of falling costs is expected to continue for both technologies in the coming years [9].

#### 2.1.1 Increasing energy security in Southern Africa with VRE

VRE could also increase energy security in power systems. This is particularly relevant for power systems dominated by hydropower [23], such as in Zambia. The findings in [11] suggest that the annual electricity output from VRE could be more stable than hydropower output, and hence decrease the risk of power shortages in dry years. In addition to the uncertainty in annual inflow to hydropower plants, there is also uncertainty related to the future impact of climate change on rainfall and temperature. Integrating VRE to diversify the generation portfolio could therefore be even more relevant in the future.

Several papers evaluate the potential impacts of climate change on the future water availability in Southern Africa. In [24], the authors conclude that climate change could lead to 10-30% lower hydropower output from the large hydropower plants in the Zambezi river basin. The article underlines the need for including climate change and upstream development considerations into national and regional energy planning. Similarly, the findings in [25] indicate that the high and increasing dependency on hydropower of several countries in Southern Africa increases the risk of climate-related electricity supply disruption.

The article suggests diversifying generation portfolios with VRE as a viable option for mitigating the impact on electricity supply in dry years. These findings are supported by the results obtained in [26], which project that future temperatures could increase and that rainfall could decrease in Zambia. A potential reduction of water availability of 13% in 2050 could be the result. Further, [27] presents a review of existing literature on the projected impacts on hydropower operations in sub-Saharan Africa from climate change. Despite high uncertainty, the article underlines that existing studies seem to be consistent in projecting a negative impact on hydropower operations in Southern Africa.

VRE is also highly dependent on weather, and can therefore be affected by changes in climate. The potential impacts on wind and solar resources in Southern Africa from climate change is evaluated in [28]. The article concludes that the mean wind and solar resource potential will most likely remain unchanged by 2050, but that the uncertainty is high. A high resolution study of renewable energy resource potential development in Africa towards 2060 is conducted in [29]. The findings indicate a likely decrease in solar PV potential of up to 2%, but a significant increase in wind power output of up to 20%. The results vary between different regions in Africa, and the changes are likely to be smaller in the Southern Africa Region.

In total, the current literature suggests that diversifying hydro-dominated portfolios with VRE could increase energy security in Southern Africa. While several papers expect in-flow to hydropower plants to decrease in the future, solar PV and wind power output are expected to remain relatively constant or increase.

## 2.2 Challenges of increasing the VRE penetration in power systems

Despite the mentioned advantages, there are some challenges associated with integrating large amounts of VRE into power systems. The main challenge is that these energy sources are non-dispatchable, meaning that the output cannot be determined by the operator, but rather depends on variable solar irradiation and wind speeds. This can imply challenges on different timescales.

### **Power system stability (sub-seconds to minutes)**

The stability of a power system can be defined as the ability of the system to return to normal conditions after a disturbance. Traditionally, the inertia of rotating masses of synchronous generators has contributed to the system stability during transients [30]. VRE is mostly connected to the grid through power converters that do not provide the same inertia to the system. Also, most synchronous generators are equipped with a governor that can regulate the power generation based on frequency measurements in the grid. VRE has very limited ability to regulate the generation, and is therefore unable to perform primary frequency control on the same level as conventional generation technologies [31].

### **Load following (tens of minutes to hours)**

Load following can be defined as the system generation resources' ability to meet natural changes in load throughout the day. To achieve this balance, generators must be able

to adjust their output, and generators must be brought on/off line in the order of tens of minutes [30]. VRE has limited ability to regulate output, which could, e.g., lead to over-generation in systems dominated by renewable energy [32]. Another challenge, is that the dispatchable power plants in the system must have a ramp rate<sup>4</sup> that is high enough to balance the short-term variations of VRE production and load. Fast-drifting clouds temporarily shading solar power plants could e.g. change the power output substantially within minutes. The decrease in generation must be picked up by dispatchable units able to ramp up sufficient power [34].

### **Scheduling (day)**

Daily scheduling is the planning of generation to meet daily energy and peak power requirements [30]. In power systems with high shares of VRE, scheduling is challenging both because forecasting the exact generation from renewable sources can be difficult, and also because the dispatchable generation in the system must be able to adapt to the net demand<sup>5</sup> during the day. In systems with a high penetration of solar PV, the net demand is often low mid-day when the output from solar plants is high. A sharp increase in net demand in the afternoon can often be seen as the afternoon load peak occurs simultaneously with the sunset. This shape is commonly referred to as the "duck curve" [35]. Challenges could be experienced because the dispatchable generators in the system must be able to ramp up their production fast enough to follow the changes in net demand.

### **Long-term planning (months to years)**

Long-term system operation planning can be defined as securing that the generation capacity in the system can meet the power and energy requirements throughout seasons and years. The output from VRE sources can vary substantially seasonally [36]. In addition to seasonal variations, systems with high penetration of renewable energy must provide reliability also in years with abnormal weather conditions. The importance of running multi-year simulations to address rare events of long periods with low renewable energy resource availability, is underlined in [37].

## **2.3 Using hydropower for flexibility operations**

The mentioned challenges emphasize the need for enhancing power system flexibility, which can be defined as a system's ability to respond to changes in demand and supply at all timescales [33]. Flexibility can be provided by several different sources, such as batteries, pumped hydro storage, flexible demand and dispatchable power plants. In Zambia, the most important flexibility source is large hydropower plants with reservoirs.

Such plants can provide flexibility on all time-scales: Rotating synchronous generators provide instantaneous system inertia, and the governor adjusts the flow of water through the turbine to regulate frequency. Some plants can go from zero to maximum generation

---

<sup>4</sup>The rate at which generators can change power output is constrained by e.g. physical limitations of the turbine, power system operating rules and potential environmental constraints limiting the rate of change of water flow downstream of hydropower plants. This is known as ramp rate constraints [16], [33]

<sup>5</sup>Net demand can be defined as the load in the system minus the generation from VRE.



within minutes, and are therefore well suited for following variations in load throughout the day. Large reservoirs can store energy throughout seasons/years, and can hence provide long-term flexibility [38].

The potential of Norwegian hydropower to balance future variations in VRE output in Central-West Europe is investigated in [39]. The article finds that flexible hydropower can provide large benefits to the system, in terms of reduced peak power prices and reduced load shedding. In [40], the reservoir operations in the Zambezi basin are optimized to offset wind power intermittence in South Africa. Considering the synergies between wind power and hydropower in the design/operations of new hydropower plants, is found to increase the benefit of integrating both technologies. Further, the use of hydropower as a flexibility source can decrease the wear and tear on South African coal power plants from cycling.

When providing baseload, hydropower units are typically operated around the best efficiency point, and generate stable power output. Flexible operations can, on the other hand, be defined as any operation that is not baseload operations. This typically involves more starting/stopping of units, and running the turbines at reduced or maximum power levels [41].

In general, the wear and tear on hydropower assets will increase when using the turbines for flexible operations with higher VRE penetration in the system. The average efficiency will also decrease because the turbines are operated more outside the best efficiency point [42]. In most cases, this will lead to increased maintenance cost for hydropower operators, but the magnitude of cost increase is site specific [43]. This is considered highly relevant for Zambia. ZESCO is concerned that increased penetration of VRE will lead to increased wear and tear on hydropower generation equipment, and that the units will be unable to adapt to the new operational patterns [44].

## **2.4 Optimal power system planning through portfolio optimization**

Portfolio-theory ideas in the context of renewable energy integration in power systems are described in [45]. The article underlines the importance of portfolio based planning, meaning that the stand-alone generation cost of different technologies is de-emphasized. Instead, the cost interrelationship between the generation alternatives is analyzed. Further, the article argues that alternative generation resources should not be evaluated against each other, but rather alternative resource portfolios should be compared.

Optimization models used for power system planning are reviewed in [46]. The goal is to map out the differences between traditional power system planning and current planning involving large scale VRE portfolio integration. One of the key differences identified, is that models have been extended to include multi-objective functions. Instead of minimizing system cost, objectives such as climate change mitigation and renewable energy targets have been included to a larger degree. In addition, different flexibility options such as storage technology and demand side management are often included when optimizing renewable energy integration.

Current methodologies used for capturing the short-term variations in load and VRE generation output in long-term integrated system models, is investigated in [47]. Such models are highly relevant for evaluating renewable energy integration from a system perspective. The article highlights the challenge of having models with a sufficient time-resolution and degree of detail, while still keeping the computational time feasible. An option is to identify representative days of variations in load/VRE output, and base the simulations on these. However, this methodology fails to capture the chronology of the problem, making modeling of storage operations impossible. Also, the article argues that long-term planning models often underestimate the level of flexibility required in the system when integrating VRE. The result could be an over-estimation of the optimal capacity of renewable energy in the system.

A system level optimization model of the Kenyan generation system is used to examine the economic benefit of adding solar PV capacity into the system in [48]. This is considered a highly relevant study, due to the similarities between the Zambian and Kenyan power system. Both systems have a rapidly growing electricity demand, and a high fraction of hydropower in the generation mix.

Despite the LCOE of solar PV might be lower than other alternatives, the authors point out that LCOE does not capture the total cost to the system of VRE integration. Therefore, the paper uses the metric avoided production cost. This metric subtracts the total annual generation cost with solar PV added in the system, from the total cost in a base case with no solar PV. The economic value of adding solar PV capacity is hence found as the difference in the total annual production cost. By using the metric avoided production cost, the economic impacts of changed operations at the existing power plants are captured. In addition, the synergies between the solar PV generation and the demand is included [48].

The output from solar PV is found to displace hydropower during the day, and hydropower displaces expensive diesel generators in the evening. Having hydropower plants with reservoirs is identified as a key-enabler for the integration of solar PV, because there is no need for additional storage investments. The authors propose that new hydropower capacity is deployed alongside VRE, and that this could be a viable option for many African countries [48].

### 3 Theory and methods

The framework applied in this thesis follows the three-step procedure described in Section 1, and is further explained in this section. First, the methods used for evaluating the variability of renewable energy resources are described (step 1). Second, the PowerGAMA software is introduced. Having a basic knowledge of the software is considered useful for understanding the models and results presented throughout the thesis. Further, the portfolio optimization methodology is explained (step 2). The framework used for modeling different climatic years is also briefly discussed. Finally, the methods used to evaluate the load flows in the grid with the optimal VRE portfolio integrated into the system are presented (step 3).

#### 3.1 Variations in renewable energy resource availability

Variability in VRE generation output can be measured both in time and space. In this thesis, the scope was to examine how the total generation output from new solar PV and wind power plants is expected to vary, when considering the expected spatial distribution of new power plants. Hourly, monthly and annual variations in generation output were investigated based on historical weather data. Also, historical precipitation data was evaluated.

The objective of these evaluations was twofold. Most importantly, assessing the expected variations in solar PV and wind power output can inform how these energy sources can complement each other to mitigate the variations in total VRE output. Particularly, it is interesting to observe the variations of these resources in relation to precipitation, to better understand the role of VRE in diversifying a hydro-dominated power system. In addition, obtaining VRE generation profiles for multiple climatic years provides input data to be used in the portfolio optimization.

##### 3.1.1 Determining the spatial distribution of new power plants

When evaluating future scenarios, understanding how new VRE capacity is expected to be distributed geographically could be important. Spreading new power plants over a large area could reduce the magnitude of variability in generation output [49]. Also, having power plants distributed over a large area could mitigate VRE resource shortages [37].

Three different data sources were used to determine the expected locations of new power plants; maps of solar PV and wind power resource potential, maps of the existing power grid and literature studying future renewable energy integration for the selected country. A map showing the solar PV potential across the majority of the world is provided in [50]. Similarly, [51] illustrates the wind power potential for the entire globe. These maps have high enough resolution to be used for brief assessments of the resource distribution within countries. Seeing these maps in relation to the current electricity grid map, provided indications on where new power plants are likely to be constructed. However, the most important source of information was existing literature and data sources describing the currently planned VRE power plants. This is further explained in Section 5.

The goal of this step was not to predict the exact location of new power plants. Rather, the goal was to obtain a set of coordinates to be used in Renewables.ninja to evaluate the fluctuations in VRE generation output for the country as a whole.

### 3.1.2 Extracting data from Renewables.ninja

Generation profiles for solar PV and wind power, and historical rainfall data, were gathered through the simulation tool Renewables.ninja [52]. This open-source software is developed by researchers at ETH Zürich and Imperial College London. Based on historical satellite data, the software simulates the hourly output from solar and wind power plants located anywhere in the world [53], [54]. In addition, hourly historical weather data, such as air temperature, rainfall and cloud cover, can be extracted.

In this thesis, the generation output from solar PV power plants and wind power plants were simulated based on historical weather data for the years 2000-2019. Each of the selected geographical coordinates were modeled with a power plant with a theoretical capacity of 1 kW. For each of the two technologies, simulated hourly generation output from the power plants were aggregated into a generation profile representing the hourly output for the country as a whole. This was done for all the years, and resulted in 20 years of simulated hourly generation output.

Historical precipitation data was gathered for the country as a whole from the Renewables.ninja database. Several additional factors such as air temperature, irrigation and the operation of upstream dams determine the inflow to hydropower plants. Precipitation is, however, considered the most important factor [26], and can indicate annual variations in inflow. The simulated generation output and the precipitation data were compared to evaluate the correlation between VRE output and precipitation.

## 3.2 Modeling power systems in PowerGAMA

Generation profiles and precipitation data obtained from Renewables.ninja were used as input data for modeling the power system in PowerGAMA. This subsection aims to give the reader a basic understanding of the software, and the majority of the material is taken from the specialization project [3].

PowerGAMA (Power Grid and Market Analysis) is an open source Python-based software developed by SINTEF Energy Research [14]. The simulation tool is inspired by SINTEF's Power System Simulation Tool (PSST), and is used for high level analyses of renewable energy integration in power systems. Previously, PowerGAMA has been used for e.g. modeling the European power system, evaluating the integration of renewable energy in Morocco and simulating pumped hydro storage (PHS) plant operations in Spain [55].

PowerGAMA optimizes generation dispatch in a power system for each time step based on the marginal cost of each power plant. The software will determine the dispatch resulting in the minimum total system generation cost, considering the grid structure, grid capacity

constraints and limits on maximum/minimum dispatch for each generation unit. Further, variations in generation from solar, wind and run-of-the-river (RoR) hydropower plants, and variations in demand are included in the model [14].

All generators are modeled with inflow profiles. For hydropower plants with reservoirs, this represents the hourly inflow of water to the reservoirs. The water can either be stored in the reservoirs, or used for power generation in each time step. Reservoirs are modeled with time coupling, meaning that storage levels will change in time based on the output from the generator connected to the storage, and inflow to the storage. For RoR hydropower, solar PV and wind power plants, the inflow profiles describe the power generation, as long as the generators are not coupled with storage.

Since the marginal cost of hydropower is low, plant owners must decide whether to discharge from reservoirs based on the expected value of having stored energy. This is modeled in PowerGAMA as a storage value, which reflects the value of having an additional unit of water in the reservoir. Whether or not to discharge power from the reservoir depends on the cost of alternative generation (equivalent to nodal price) and the storage value. If the storage value is lower than the nodal price, the storage will discharge to the generators, and if the storage value is higher, the storage will not discharge [14]. Storage values are equivalent to water values used in the Norwegian power system.

If the output from generators exceed the load in the system, or the transmission capacity is not sufficient to evacuate the generated power at one or several nodes, curtailment of VRE power plants will occur. Similarly, load shedding is conducted in PowerGAMA if generation is not able to meet load at one or several nodes. Load shedding is modeled as a generator with a high marginal cost, equal to the value of lost load (VoLL).

PowerGAMA is flow-based, meaning that the power flow in the grid is determined by physical power flow equations. DC power flow equations are used as a linear approximation for the power flow equations. Combined with the linear optimization, the method is known as DC Optimal Power Flow. This method does not capture losses in the system, and reactive power, which is a simplification. Also, the software does not include ramp rate constraints, start-up costs of generators, forecast errors, varying efficiency of generators, spinning reserve requirements and unit commitment [14]. The validity of these assumptions is discussed in Section 6.

Simulations in PowerGAMA are usually performed with an hourly granularity, and the same resolution was used in this thesis. Therefore, the model does not include sub-hourly variations in load and renewable energy generation, and hence does not capture all challenges related to system stability.

### **3.3 Portfolio optimization methodology**

To find the optimal portfolio of VRE to be integrated into the power system, a program was built around a single-node power system model in PowerGAMA. This program runs the single-node model to simulate one year of system operations with different portfolios of

new solar PV and wind power capacity integrated into the system. All other model parameters, such as the hourly system load profile, thermal/RoR hydropower dispatch and the solar/wind power generation profiles are the same for all portfolio combinations. Despite this model being referred to as an "optimization model", it is in reality using exhaustive search<sup>6</sup> to find the optimal portfolio of new VRE capacity. A total of 121 different portfolios of solar PV and wind power capacity were evaluated.

Using exhaustive search to find the optimal portfolio of VRE, is a time-consuming method, and a more efficient optimization model could quite easily have been developed. However, basing the optimization model on a large number of simulations in PowerGAMA has several advantages. First, it allows for comparing the system cost resulting from many different portfolio combinations. This makes it possible to understand the drivers of system cost. Further, the optimization model allows for evaluating the impact on system operations from a large number of VRE portfolios. Different portfolios could potentially imply similar system costs, but quite different impacts on e.g. load shedding, VRE curtailment and hydropower operations. The use of exhaustive search was inspired by the methodology applied in [37].

In the single-node model, all the generators and loads in the system are connected to one node. This corresponds to modeling the underlying power grid as a copper plate, where power can flow unconstrained between all nodes in the system. For a power system with bottlenecks in the grid, this simplification could result in an inaccurate model of the real system. If the transfer capacity in the grid is sufficient, a single-node model could however provide a decent representation of system operations. The validity of the single-node model compared to a complete power system model is further discussed in Section 6.

The main reason for using a single-node model was to reduce the simulation time. The optimization model simulates a year (8760 hours) of power system operations for each portfolio combination, and using a complete model of the power system would have resulted in an infeasible simulation time.

The two main components of the single-node model are the load and the generators. These are modeled with hourly profiles describing the variations in load and variations in inflow to generators. System reserve requirements are not included in the PowerGAMA software, but were approximated by modifying the maximum and minimum generation limits of dispatchable power plants. Using a single-node model for simulating power system operations for a large number of different portfolios of VRE implemented in the system, was inspired by the methods used in [48].

To find the optimal portfolio of VRE to be integrated into the system, the annual system cost associated with each of the portfolios was calculated. This cost metric is explained in detail in the coming subsections. For now, it can be noted that the optimal portfolio was identified as the one resulting in the lowest system cost. Figure 1 shows a flow chart of the portfolio optimization model.

---

<sup>6</sup>Also known as "brute force". A large number of candidate solutions are simulated to find the optimal one.

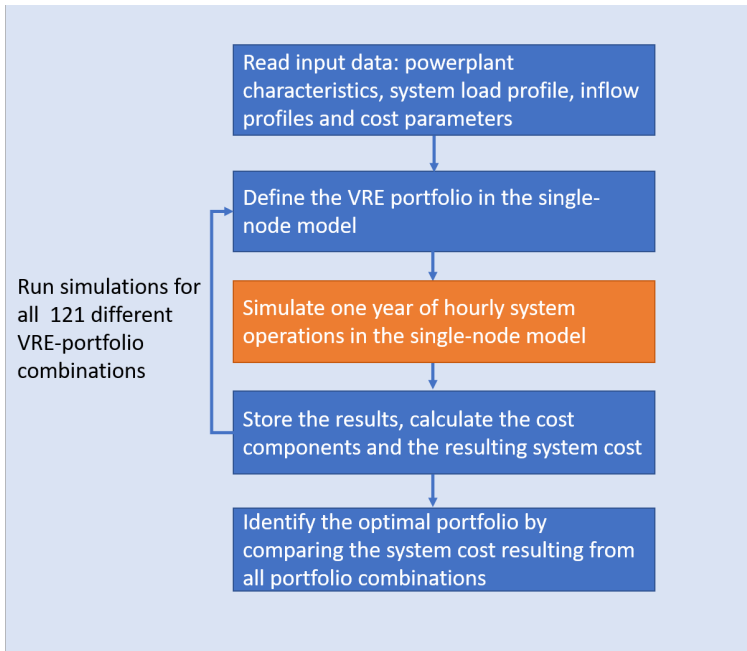


**Figure 1:** Flowchart describing the portfolio optimization model.

The annual system cost consists of four components, as seen in Equation 1. System cost is not an attempt to capture all the costs related to operating the system and expanding generation capacity, but rather an approximation of the costs relevant for determining the economic impact of integrating different VRE portfolios. It includes the cost of operating existing generators, the cost of building and operating new VRE power plants, the economic cost of load shedding and the cost/benefit of decreased/increased reservoir filling levels. Each of the cost components is explained more thoroughly in the following subsections.

$$\text{System}_{cost} = \text{Generation}_{cost} + \text{VRE}_{cost} + \text{LoadShed}_{cost} + \text{ReservoirFilling}_{cost} \quad (1)$$

### 3.3.1 $\text{Generation}_{cost}$ - the annual cost of generation from existing power plants

The cost of generation for the system as a whole is calculated in PowerGAMA based on the marginal cost of operating generators. It is assumed that the marginal cost is constant for all power plants, regardless of the generation output. The annual cost of generation from existing power plants is hence a sum of total energy output from each generator, multiplied by the respective marginal cost of the generator. VRE power plants were assumed to have zero marginal cost, as explained further in the next subsection. Equation 2 shows the mathematical formulation of the  $\text{Generation}_{cost}$ .

$$\text{Generation}_{cost} = \sum_{i=1}^{N_G} \sum_{t=1}^{8760} c_i P_i(t) \quad (2)$$

$N_G$  : Number of generators in the system

$c_i$  : Marginal cost of generator  $i$  [USD/MWh]

$P_i(t)$  : Dispatch of generator  $i$  in hour  $t$  [MWh]

### 3.3.2 VRE<sub>cost</sub> - the annual cost of new VRE power plants

Annualized average CAPEX and OPEX of new VRE power plants were assumed fixed per installed MW, and not dependent on the generation output. The annual cost of new VRE power plants in the system is found by multiplying the total new solar PV and wind capacity by the annualized CAPEX + OPEX per MW for each technology. This is shown in Equation 3. Costs related to potential grid upgrades following renewable energy integration were not included. This simplification was made because these costs are difficult to determine, and are often relatively small compared to the investment cost of VRE power plants [11]. This is discussed further in Section 6.

Both solar PV and wind power plants were assumed curtailable, meaning that in hours where the generation in the system exceeds the load, curtailment of power output will occur. No additional cost of curtailing power production was assumed. However, because the annual cost of new VRE power plants was assumed fixed, the cost of curtailment is captured implicitly to a certain degree; having a VRE portfolio with a high degree of curtailment implies a high VRE<sub>cost</sub>, compared to the economic benefit of the VRE power plants.

$$\text{VRE}_{cost} = K_{pv} G_{pv} + K_w G_w \quad (3)$$

$K_{pv}$  : Sum of annualized CAPEX and OPEX of new solar PV capacity [USD/MW]

$G_{pv}$  : New solar PV capacity [MW]

$K_w$  : Sum of annualized CAPEX and OPEX of new wind power capacity [USD/MW]

$G_w$  : New wind power capacity [MW]



### 3.3.3 LoadShed<sub>cost</sub> - the annual cost of load shedding

A major advantage of implementing new generation capacity in power systems in sub-Saharan Africa, is the potential reduction in load shedding. Calculating the economic cost of load shedding can be challenging, because the value of lost load (VoLL) varies greatly between different consumers. Also, the value can vary significantly between countries [56]. Obtaining a country-specific VoLL, which reflects the average cost of non-served energy is therefore important. In the model, the annual economic cost of load shedding is calculated as the total magnitude of non-served energy multiplied by the VoLL.

$$\text{LoadShed}_{\text{cost}} = \sum_{t=1}^{8760} c_v P_L(t) \quad (4)$$

$c_v$  : The value of lost load (VoLL) [USD/MWh]

$P_L(t)$  : Non-served energy in the system in hour  $t$  [MWh]

### 3.3.4 ReservoirFilling<sub>cost</sub> - the cost of changed reservoir levels

One of the benefits of adding VRE generation capacity into hydro-dominated power systems, is that hydropower reservoirs can store a larger fraction of the inflow, and increase the resilience against supply disruptions in dry years. With a higher degree of filling, power could also be exported to neighboring countries (if assuming interconnected country), and displace expensive thermal power plants from a long-term perspective. Hence, having an additional unit of water in the reservoir certainly has a value.

This is commonly referred to as the water value [39], [57]. Assigning a value to the stored water is necessary also from a modeling perspective. Without any value on stored energy, the optimal portfolio could be a combination of solar PV and wind power capacity leading to close to empty reservoirs. The cost of changed reservoir levels was calculated by using two different methods; with a constant water value and with dynamic water values.

#### Constant water value

With a large portfolio of VRE integrated into the system, the filling level of the hydropower reservoirs at the end of the simulation period will generally be higher than for a smaller VRE portfolio. This is because the electricity output from VRE power plants displaces hydropower generation, allowing the reservoirs to store a higher fraction of the inflow. To capture the value added to the system from increased water levels, the difference in filling level between the beginning and the end of the simulation period is multiplied with a constant water value. If the reservoir filling level is lower at the end of the year compared to the beginning, this represents a net cost to the system, due to less stored energy. On the other hand, having a higher reservoir level at the end of the year, represents a net benefit to the system (negative ReservoirFilling<sub>cost</sub>). The constant water value method was applied in the base case in this thesis, and is shown mathematically in Equation 5.

$$\text{ReservoirFilling}_{\text{cost}} = \sum_{i=1}^{N_R} [R_i(0) - R_i(8760)]w_c \quad (5)$$

$N_R$  : Number of reservoirs in the model

$R_i(t)$  : Filling level of reservoir  $i$  in hour  $t$  [MWh]

$w_c$  : Constant water value for the system [USD/MWh]

### Dynamic water values

As an alternative to the use of a constant water value, dynamic water values were applied. In liberalized power markets, hydropower producers rely on dynamic water values for production planning. These are usually calculated based on advanced optimization models, and used to determine the optimal dispatch throughout the year for hydropower plants with reservoirs [15]. In this thesis, dynamic water values were mainly used for calculating the total cost of changed reservoir levels.

When using dynamic water values, the  $\text{ReservoirFilling}_{\text{cost}}$  is calculated as the sum of net change in reservoir level multiplied by the water value for each time step, as seen in Equation 6. The water value is a function of the reservoir filling level, which depends on time, since the model updates the reservoir level at each time step. The relation between filling level and water value was evaluated specifically for Zambia, and is discussed in Section 5.

$$\text{ReservoirFilling}_{\text{cost}} = \sum_{i=1}^{N_R} \sum_{t=1}^{8760} [P_i(t) - I_i(t)]w_i(R_i(t)) \quad (6)$$

$N_R$  : Number of reservoirs in the model

$P_i(t)$  : Dispatch of the generator connected to reservoir  $i$  in hour  $t$  [MWh]

$I_i(t)$  : Inflow to reservoir  $i$  in hour  $t$  [MWh]

$w_i(R_i(t))$  : Water value for reservoir  $i$  in hour  $t$  calculated from the filling level [USD/MWh]

$R_i(t)$  : Filling level of reservoir  $i$  in hour  $t$  [MWh]

A difference between the calculation of the  $\text{ReservoirFilling}_{\text{cost}}$  with a constant water value, and a dynamic water value, is that Equation 6 captures the risk of emptying/filling the reservoirs during the simulation period. When only considering the reservoir level at the start/end of the simulation period (base case), the reservoirs could in theory be close

to empty/full during the simulation period, without any impact on the system cost. Calculating the water values dynamically makes it possible to put a cost on the risk of load shedding and spilling from reservoirs.

In general, care should be taken when including the changes in the value of stored water in the system cost, because it is not necessarily a direct economic cost. In particular, care should be taken when calculating the cost based on dynamic water values. In a year with low reservoir levels most of the year, but no load shedding, the  $\text{ReservoirFilling}_{\text{cost}}$  could be high when using dynamic water values. Nevertheless, the experienced economic impact might be equal to a normal year, as long as load shedding does not occur.

However, load shedding will in reality be practiced long before reservoirs are completely empty in many power systems in Southern Africa [6], [48]. Putting a high value on the stored water, when having low reservoir levels, could hence make sense in an economic perspective. Similarly, the value of generating an additional unit of electricity in wet years, when the filling level is high, could in reality be low. This is because the output from other hydropower plants is most likely high. Using dynamic water values could therefore capture the risk of emptying/filling the reservoirs, and some of the direct economic impacts from low/high reservoir levels that are not captured when using a constant water value. Dynamic water values were applied in the sensitivity analyses in this thesis.

### **3.4 Modeling the impact of different climatic years**

Inflow to hydropower reservoirs can in general vary substantially between years in most countries [58], [59]. Also, the output from solar PV and wind power plants vary. Three representative climatic years were selected from the historical data, to capture the impacts of different climatic years on the system cost. The years represent a dry year, an average year and a wet year, and were selected based on annual precipitation.

The optimization model was simulated for each of the climatic years. In practice, this was done by running the simulations with the inflow to reservoirs and VRE generation profiles belonging to each of the selected years. For the sake of simplicity, it was assumed that the inflow to all reservoirs/RoR hydropower plants in the model follow the same annual variations as the precipitation.

To determine the optimal portfolio, the results from each of the climatic years were weighted by the fraction of years they were assumed to represent. If e.g. 15% of all years can be categorized as dry years, 15% are wet years and 70% are normal climatic years, the weighting factors would be 0.15, 0.15 and 0.70, respectively. The optimal portfolio was then found as the portfolio providing the lowest weighted average system cost. This adds a partly stochastic element to the optimization model. By using scenario analysis of inflow and VRE generation in different climatic years, the stochastic nature of weather variations is captured to some degree.

### **3.5 Creating a multi-node model of the power system**

Because the portfolio optimization model is based on the single-node model in PowerGAMA, it does not consider the underlying electricity grid. Integrating new VRE capacity into the grid could potentially lead to overloading of transmission infrastructure, making grid upgrades necessary. To evaluate the possible impacts of integrating the optimal VRE portfolio into the grid, the portfolio found optimal in the optimization model was translated into power plants in the electricity grid. Simulations were then performed in a multi-node model in PowerGAMA, to evaluate possible bottlenecks in the transmission system. This model is from now referred to as "the grid model".

Connecting new power plants to the grid also requires e.g. contingency analyses, fault analyses and system stability evaluations. In this thesis, the objective was not to evaluate all possible consequences of renewable energy integration in detail. The goal was to indicate whether or not the existing transmission system can handle the integration of the optimal VRE portfolio. This can be viewed as a supplement to the results obtained in the portfolio optimization model.

## 4 The Zambian power system

To understand the topic of renewable energy integration in Zambia, a brief understanding of the country is useful. This section aims to give the reader a basic knowledge of the geography, population and economy, followed by a more detailed description of the Zambian power system. Current challenges are discussed, and the status of renewable energy integration is also presented. These topics were treated in the project preceding this thesis, and the material in this section is mostly taken from [3].

### 4.1 Geography, population and the economy of Zambia

The Republic of Zambia is located in Southern Africa, as seen in Figure 2. Most of the country forms a part of a high plateau 900-1500 meters above sea level, shown in Figure 3. The largest river systems are Zambezi, Kafue and Luangwa. The Zambezi forms the fourth largest river system in Africa. It passes through the famous Victoria Falls and Lake Kariba, and flows further along the border to Zimbabwe into Mozambique [60]. On the way to Mozambique, the Zambezi river forms a confluence with the Kafue river. These two rivers form the basis for the vast majority of power production in Zambia.



Figure 2: Zambia marked with blue on the map of Africa. Source: [61]

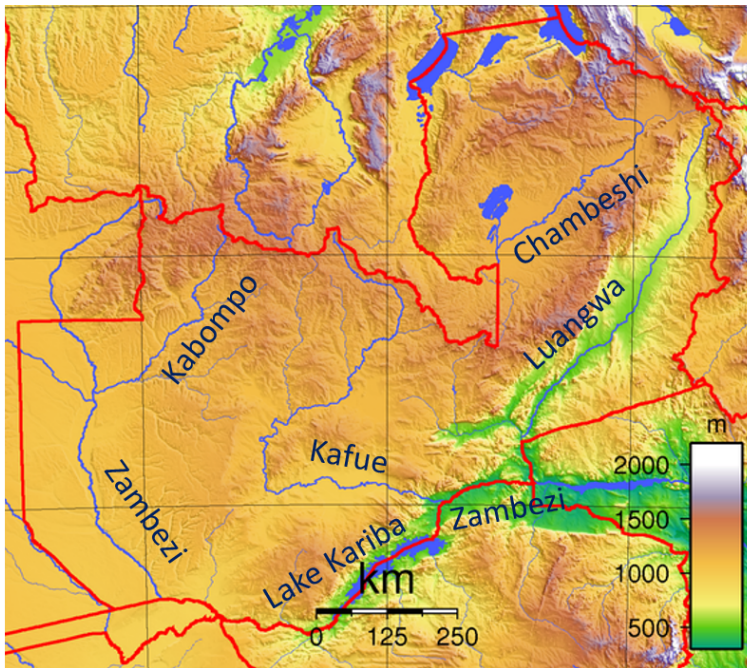


**Figure 3:** Map of Zambia showing the altitude of the landscape in meters above sea level. The major river systems and the Kariba Dam are also shown. Source: [62]

The Zambian climate is tropical, but the relatively high altitude of the country modifies the temperature, and it is in general comfortable to humans [60]. The year can roughly be divided into three seasons. The warm and wet season lasts from November until April, and the country receives the majority of yearly rainfall during this period. The temperature is usually in the range  $20\text{-}25\text{C}^\circ$ . The cool and dry season lasts from May until August, with temperatures between  $10\text{C}^\circ$  and  $20\text{C}^\circ$ , followed by the hot and dry season from September to October. Usually the temperature in this season can reach up to  $30\text{C}^\circ$  [60].

The population in Zambia was 17.9 million by the end of 2019, and is growing rapidly at a rate of 2.8% per year. The steep population increase has made the Zambian population one of the youngest in the world [63]. Zambia is a poor country, and 57% of the population is living in extreme poverty, defined as living on less than \$1.90 per day [4].

The Zambian economy has grown by an average rate of 6.8% between 2000 and 2014. However, the growth has decreased in recent years, and the average growth rate between 2015 and 2019 was 3.1% per annum [63]. One of the main reasons for the decrease in growth, is falling copper prices. The economy is highly dependent on copper mining, which accounts for around 80% of total exports [64]. Another reason for the stalling growth, is the drought experienced in recent years. The lack of water has reduced the output from the agriculture sector, and has lead to a power shortage due to reduced generation from hydropower plants [63].

Electricity only composes around 20% of the total energy consumption in Zambia. Bioenergy (mostly wood and charcoal collected by households) is by far the most important energy source, and accounts for around 70% of final energy consumption [65], [66]. However, electricity is a cornerstone of economic and social development, and an indispensable energy source in all developed societies. The power system therefore plays a vital role in the development of the Zambian population and economy.

The Zambian power sector comprises the public utility ZESCO, independent power producers (IPPs) and power distribution companies. It is out of the scope of this thesis to explain the ownership models and the regulations of the Zambian power system in detail. However, it can be noted that ZESCO currently operates around 80% of the system generation, and the vast majority of the transmission grid [10].

## 4.2 Power plants

The generation side of the Zambian power system is dominated by hydropower plants, and between 80-90% of the electricity production comes from hydropower [10]. In addition to hydropower, some thermal capacity and solar PV power plants are connected to the grid. Table 1 shows an overview of all the power plants at the end of the subsection.

### 4.2.1 Kafue Gorge Upper and Itezhi-Tezhi hydropower stations

Kafue Gorge Upper (KGU) has an installed capacity of 990 MW. The power station normally covers around half of the yearly electricity demand in Zambia, and is hence of utterly high importance to the power system. KGU is operated with primary and secondary frequency control, and is used as a load-following plant. This means that the generation at KGU is constantly adjusted to meet the changes in net load in the system.

The power plant is connected to a reservoir with storage capacity of  $700 \text{ Mm}^3$ , which corresponds to approximately 856 GWh of storage. However, the main reservoir for the power station is the  $7000 \text{ Mm}^3$  Itezhi-Tezhi dam located 400 km upstream of the KGU power station. This reservoir regulates the flow of water in the Kafue River, and it takes 2-4 months for the water to flow from the Itezhi-Tezhi reservoir to the KGU reservoir [59]. The Itezhi-Tezhi reservoir was constructed in 1976 to store water from the rainy season to be used for power generation in the dry season at the KGU power plant, and to regulate the flooding of the Kafue Flats upstream of KGU [67], [44].

In 2016, the 120 MW Itezhi-Tezhi hydropower station was commissioned. Even though being connected to the large Itezhi-Tezhi reservoir, this power station is mostly operated with a steady daily power output, consistent with the purpose of the reservoir of providing a stable river flow. The power plant is operated by the IPP Itezhi-Tezhi Power Corporation [10].

### **4.2.2 Kariba North Bank hydropower station**

Kariba North Bank (KNB) is the largest power station in the Zambian system, with an installed capacity of 1080 MW. The generators are not equipped with automatic generation control, and therefore respond slower to changes in net load than KGU, because they must be manually controlled.

KNB is connected to the Kariba Dam, which is the largest man-made lake in the world. Zambia shares the water resources in the dam with Zimbabwe, which has a 1050 MW hydropower plant discharging from the dam. The dispatch at KNB is governed by the water level of the reservoir and bilateral agreements with Zimbabwe. Low water levels correspond to constrained generation output to avoid emptying the reservoir [44].

### **4.2.3 Maamba and Ndola thermal power plants**

The Maamba coal power plant and the Ndola heavy fuel oil (HFO) plant make up the majority of the thermal generation in the system. These two power plants are operated by IPPs, and ZESCO is buying the power through power purchase agreements (PPAs) [44].

Small and medium sized diesel power plants are located in the Copperbelt region, and are used for securing the electricity supply to the mines. Installing new diesel generators has been discussed as a measure to increase energy security in other parts of Zambia as well, but the plans seem to have been stranded due to financial challenges [68].



Power plant	Technology	Installed Capacity [MW]	Type
Kafue Gorge Upper	Hydro	990	Reservoir
Kariba North Bank	Hydro	1080	Reservoir
Itezhi-Tezhi	Hydro	120	Reservoir
Victoria Falls	Hydro	108	RoR
Mulungushi	Hydro	32	RoR
Lusemfwa	Hydro	24	RoR
Lunzua River	Hydro	14.80	RoR
Lusiwasi	Hydro	12	RoR
Musonda Falls	Hydro	10	RoR
Micro hydro	Hydro	7.7	RoR
<b>Total</b>	<b>Hydro</b>	<b>2398.5</b>	
Maamba	Coal	300	
Ndola	HFO	110	
Luano	Diesel	40	
Bancroft	Diesel	20	
Small diesel plants ( $\leq 10MW$ )	Diesel	23.60	
<b>Total</b>	<b>Thermal</b>	<b>493.6</b>	
Bangwelu	Solar PV	54	
Ngoyne	Solar PV	34	
Small solar power plants	Solar PV	1.1	
<b>Total</b>	<b>Solar PV</b>	<b>89.13</b>	
<b>Total System Generation Capacity</b>		<b>2981.2</b>	

**Table 1:** Grid-connected power plants in the Zambian power system by the end of 2019. Source: [10], [11]

### 4.3 Consumers

Around 40% of the Zambian population has access to electricity [5]. Lack of electricity access is typical for countries in sub-Saharan Africa. The electricity access is also typically unevenly distributed between the population living in urban areas and the rural population. In Zambia, around 80% of the urban population has access to electricity, while only 12% of the rural population has electricity access [5].

The low degree of electrification among households is reflected in the distribution of load between different economic sectors, seen in Figure 4. The mining industry consumes around half of all electricity, while the domestic sector (including households and commercial buildings) contributes to one third of electricity consumption. The remaining electricity consumption is distributed as seen in the figure.

The electricity demand has been growing in recent years as the population and economy has been growing. In the years 2012-2018, the annual electricity consumption growth rate was around 3.3% per year on average [44].

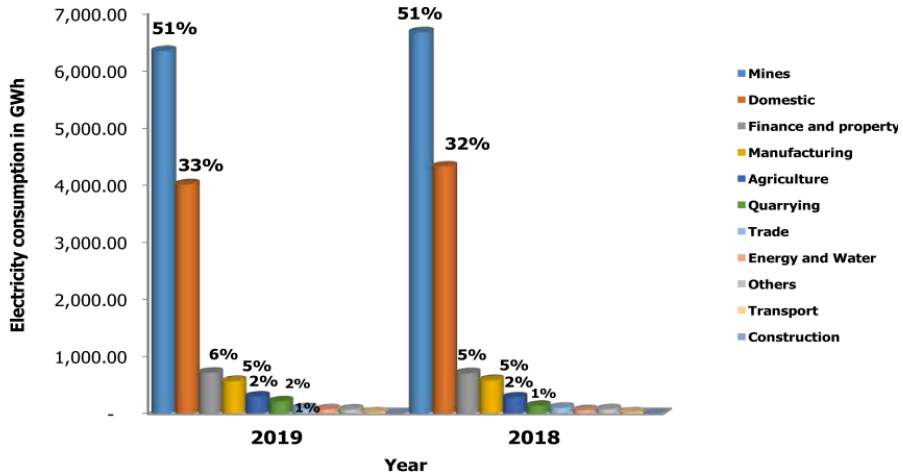


**Figure 4:** National electricity consumption by economic sector. Source: [10]

The average daily load profile for 2018 is shown in Figure 5. The curve shows a peak at 8 pm, with a following decrease in load during the night. An increasing share of the Zambian population is using electricity for cooking in the evening, contributing to the peak [69].

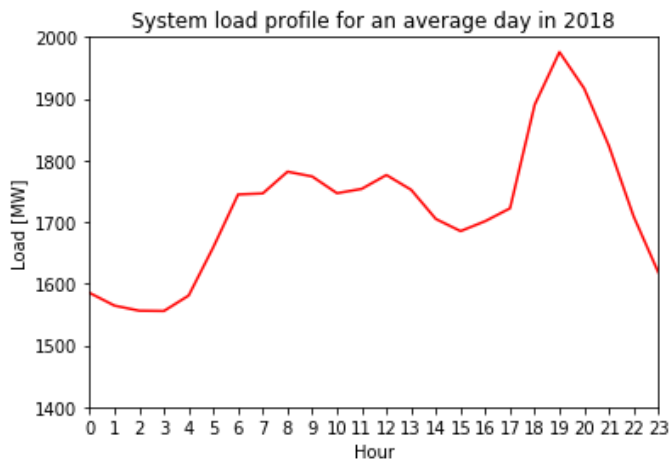


**Figure 5:** Load profile for an average day in 2018. Note that the vertical axis is starting at 1400 MW. Source: [44]

## 4.4 Transmission network

The Zambian transmission network can be seen in Figure 6. The major loads in the system consist of the mining loads and residential loads in the Copperbelt area, and residential loads in the densely populated Lusaka area. The majority of generation resources are located in the south, and connected to the load centres through the 330 kV lines stretching from south to the north in parallel on the map. A newly commissioned double 330 kV line closes the loop between north and south.

A single 330 kV line connects the eastern part of the country to the main grid. In general, the population is rural, and the loads are moderate in the east. The south-western part of the country is also relatively sparsely populated, and the connection to the main grid is weak.

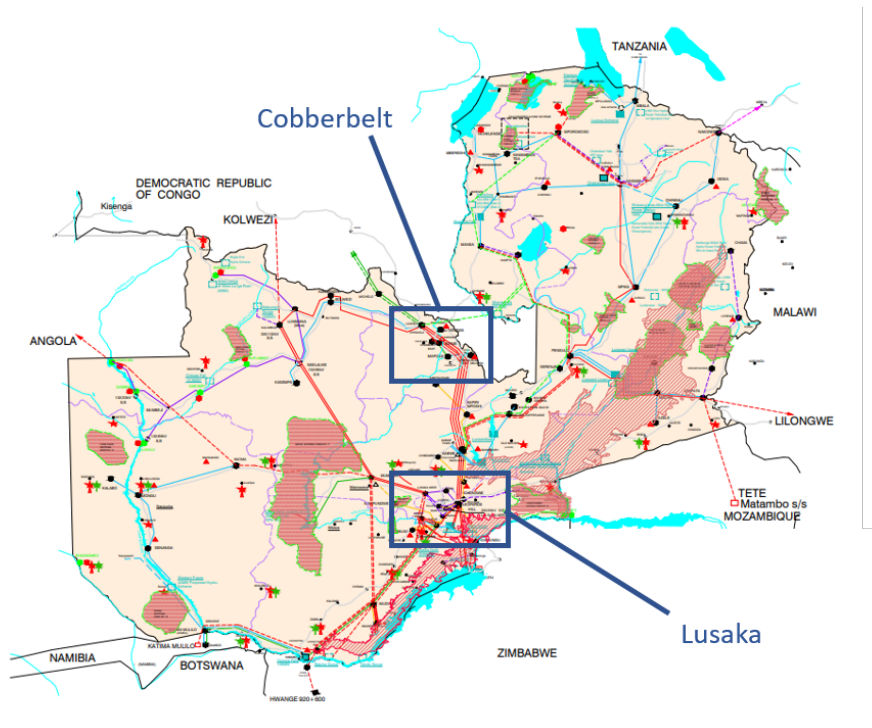


**Figure 6:** The Zambian transmission network. Red lines represent 330 kV, green lines represent 220 kV and purple lines represent 132 kV. The dotted lines represent planned transmission lines. Source: [44]

### 4.4.1 Interconnection with neighboring countries

Zambia has interconnectors to the Democratic Republic of Congo in the north, Zimbabwe and Namibia in the south, and Malawi in the east. The total active transfer capacity is 1250 MW (import) and 1000 MW (export) [11].

As a member of the Southern African Power Pool (SAPP), Zambia is trading power with neighboring countries both in the spot market, and on long-term contracts. Figure 7 shows the imports and exports of electricity from 2011 to 2019. As seen from the figure, the export volumes have been relatively stable around 1000-1250 GWh the last eight years. The imports have in general been low, but surged in 2015, 2016 and 2017. In 2016, the imported volume reached almost 2200 GWh, making Zambia a net importer of electricity. The main reason for the surge was low domestic hydropower generation caused by drought, combined with increased electricity demand.

An interesting observation, is that although 2016 was an extreme year with record high imports and extensive use of load shedding due to power shortage, the change in exported volume was quite modest. Protocol agreements for power exports, which binds ZESCO to exporting power, regardless of domestic generation, is a reason for this [70].

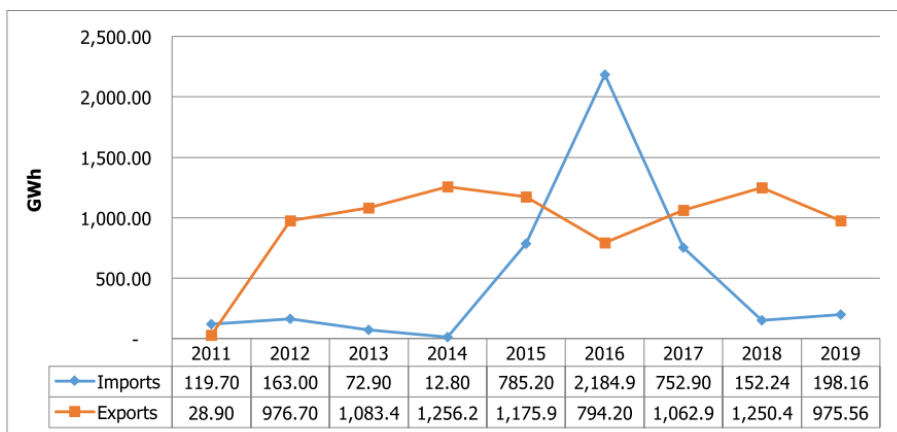


**Figure 7:** Zambian electricity imports and exports. Source: [10]

## 4.5 Electricity tariffs and power market in Zambia

In Zambia, electricity is not traded as in liberalized power markets in e.g. Europe. Instead, ZESCO has traditionally been the only power producer, transporting power through its own grid and selling it to consumers at fixed tariffs. The tariffs are set by the Energy Regulation Board of Zambia (ERB) every year, and vary in magnitude between different customer types [10].

Recent years, private power producers have been allowed into the electricity market through power purchase agreements (PPAs) with ZESCO. Typically, these contracts last for 5-25 years, and determine a fixed price at which ZESCO buys the electricity from the power producer. In the Copperbelt area, the agreement is different, with ZESCO selling electricity to the Copperbelt Energy Corporation, which distributes the electricity to the mines in the area [71].

One of the current market structure challenges, is that the electricity tariffs are set by the ERB, and do not reflect the actual cost of electricity generation experienced by ZESCO. The electricity tariffs have hence been substantially lower than the cost of generating and distributing a unit of electricity, leading to financial problems for ZESCO. Increasing the number of IPPs through PPAs has made the situation more challenging, since the price paid by ZESCO to the power producers is often higher than the electricity tariffs. In other words, ZESCO is buying electricity at a higher price than it gets when selling to consumers. As a result, ZESCO has struggled with increasing deficits in recent years. Including IPPs however seems like the only option for expanding system generation, since ZESCO has insufficient funds to invest in the new generation capacity [72].

In 2019, the ERB approved ZESCO's application for increasing the electricity tariffs by 113% on average. The regulating authorities hope this increase in tariffs can cover operating expenses and debt payments [10], and also make investments in new power generation more attractive to private investors. However, a doubling of electricity tariffs will impact the poor population, and it is estimated that such an increase could cause more than 180,000 people to drop below the poverty line [73].

The low electricity tariffs and the financial situation of ZESCO are also reasons why Zambia has experienced extensive use of load shedding. Importing power from neighboring countries is expensive, and implies losses to ZESCO when selling the power in Zambia. Even though current transmission lines have capacity to cover the shortage of power in dry years, the imports have been constrained by ZESCO's lack of funds [73].

## **4.6 Drought and load shedding**

Load shedding is not a new concept in Zambia, and has happened in the past. However, the last years have been more challenging than ever. Poor rainfall in the 2014/2015 wet season resulted in low water levels in the hydropower reservoirs, leading to reduced hydropower generation. The reduction in electricity production, combined with an increase in electricity demand from 2014 to 2015 of 6.8%, led to an energy crisis [7].

In 2015, the generation output from KGU (990 MW installed capacity) was limited to 540 MW, and the production at KNB (1080 MW installed capacity) was kept below 760 MW. Moreover, ZESCO could not meet the demand in the system, and introduced rotating load shedding lasting eight hours. This implies cutting the electricity supply to one or several areas for eight consecutive hours, before rotating the load shedding to new areas [7].

During the rainy season of 2016/2017, reservoir levels rose. In addition, the 300 MW Maamba coal power plant and the 120 MW Itezhi Tezhi hydropower plant were commissioned. The load shedding regime started in 2015 could therefore be ended in March 2017. However, the country experienced another drought in the 2018/2019 wet season. ZESCO had to resume load shedding with record-breaking magnitude in 2019, with load shedding cycles up to 20 hours per day in certain areas [73].

Several studies have investigated the impacts of load shedding on households and commercial businesses in Zambia. It is out of the scope of this thesis to describe these findings in detail. Nevertheless, it can be mentioned that load shedding leads to severe negative economic, environmental, health, and social impacts [7], [6].

#### **4.7 Current status of VRE in Zambia**

To improve the current situation in Zambia, the government has presented different strategies. The *Power System Development Master Plan 2010-2030* presented in 2011, argues that only 30% of available hydropower resources are utilized, and that generation expansion plans should be centered around hydropower [59].

However, this report was published prior to the load shedding experienced from 2015-2017 and 2019-2020, and the government strategy now involves plans for diversifying the generation mix to reduce the risk of power shortages in dry years. The Renewable Energy Feed-in Tariff (REFiT) programme, launched by the Zambian government, is an initiative to encourage private small to medium scale investments in renewable energy. The Scaling Solar Programme is another initiative aiming at introducing 500 MW of solar power financed by private investors into the Zambian power system [19]. Combined with other proposed incentives, the VRE integration is expected to increase in Zambia [74].

Zambia is rich in renewable energy resources. Solar, wind, hydro and geothermal energy are resources with a high potential [11]. Forest and agricultural waste is in addition mentioned in literature as a potential energy source which can be used for electricity generation [19]. In this thesis, only solar PV and wind power are evaluated. These technologies are considered to have the highest potential in terms of exploitable resources in Zambia. Also, the trend of falling costs of solar PV and wind power capacity is expected to continue, making them increasingly competitive [9].

Currently, only the Bangwelu and Ngoyne solar PV power plants constitute the utility scale VRE generation capacity in the system. However, several projects are planned to be commissioned in the coming years. Table 2, shows an overview of the currently planned VRE power plants. The vast majority of the new capacity is solar PV. When it comes to new wind power capacity, only a single power plant of 130 MW is planned.

<b>Power plant</b>	<b>Capacity [MW]</b>	<b>Location</b>	<b>Technology</b>
Bulemu East/West	40	Bulemu	solar PV
Garneton North/South	40	Kitwe	solar PV
Globeleq Solar One/Two	40	Kafue	solar PV
Kanona	100	Serenje	solar PV
Muzuma	100	Muzuma	solar PV
Green Field	50	Lusaka	solar PV
Globeleq project	100	Lusaka	solar PV
MGC project	100	Mumbwa	solar PV
Hive project	90	Siavonga	solar PV
Serenje	130	Pensulo	wind
<b>Total</b>	<b>790</b>	-	-

**Table 2:** Planned solar PV and wind power plants in the Zambian power system. Source: [11]

## **5 Case study: A 2030 scenario of the Zambian power system**

To improve energy security, increase access to electricity and keep up with the growing electricity demand, expanding the generation portfolio is of high importance in Zambia. As discussed, solar PV and wind power could be attractive options for increasing the generation capacity in the system.

In this section, the methods presented in Section 3 are applied on a 2030 scenario of the Zambian power system. First, the methods used for mapping out the variations in renewable energy generation output and precipitation in Zambia are shown. Second, the methods used for extracting data and modeling the Zambian power system in a single-node model in PowerGAMA are explained. Also, the cost parameters used in the optimization model are obtained. Finally, the power system is modeled in a multi-node model. A summary of all the data sources used for modeling the system and the cost parameters is included in Appendix A.

### **5.1 Variations in renewable generation output and precipitation in Zambia**

#### **5.1.1 Solar power generation**

As seen from Figure 8, the average daily solar PV power potential in Zambia is in the range of 4.1 - 4.7 kWh/kWp per day. The potential is largest in the southwestern part of the country, and smallest in the eastern regions. However, the power potential is large for the entire country, with relatively small variations. Therefore, it is likely that the geographical locations of new solar PV plants will be determined mainly by factors such as grid infrastructure, proximity to load and available land, rather than differences in resource potential.



## 5.1 Variations in renewable generation output and precipitation in Zambia

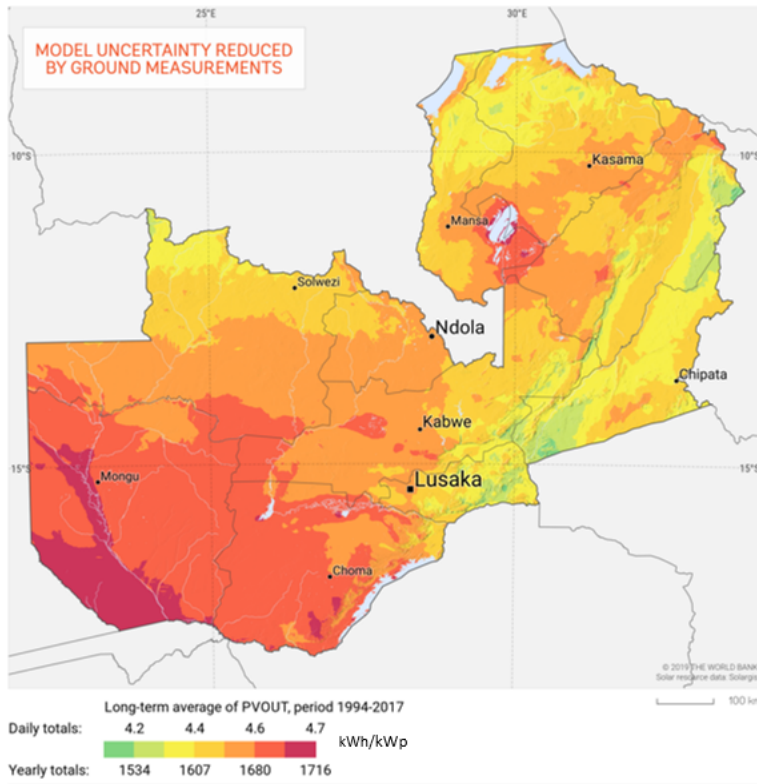


**Figure 8:** Solar PV power potential in Zambia. Source: [75]

The locations of the currently planned solar PV plants (described in Section 4) indicate where to expect new power plants. In addition, the coordinates chosen for solar PV power plants in [11] suggest where additional plants can be located. Based on these sources, the geographical coordinates selected to map out the variations in solar generation were chosen as seen in Figure 9.

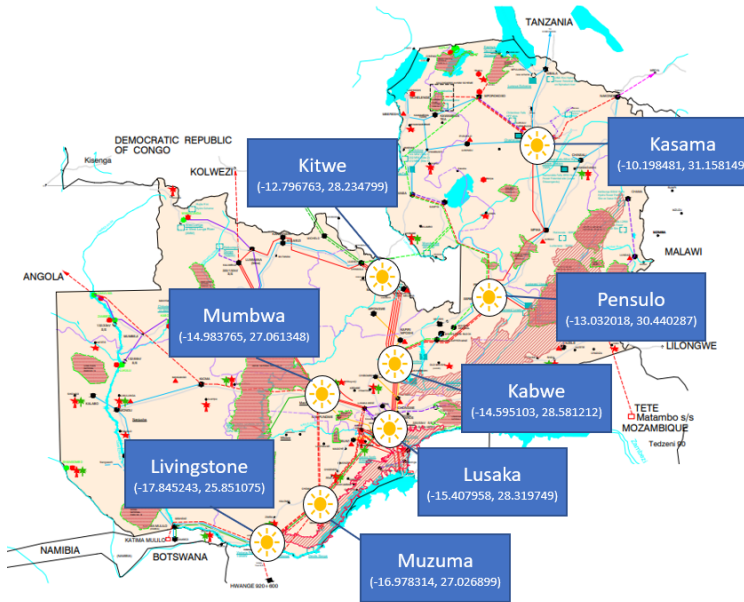


**Figure 9:** Geographical coordinates chosen for mapping out the variability in generation output from future solar PV power plants in Zambia.

The hourly solar PV generation output for the selected coordinates were simulated based on historical satellite data from the years 2000-2019 in Renewables.ninja. The tilt angle was set to 22 degrees for all locations, which is on average the optimal fixed tilt angle for solar power production in Zambia [76]. An overview of all the inputs used in the simulations can be seen in Table 3.

The simulated generation profiles for the eight selected coordinates were aggregated into one profile representing the solar PV generation output for Zambia as a whole. Each of the profiles were weighted equally, even though some of the locations are likely to have higher installed generation capacity than others. This was done for simplicity reasons, and because of the uncertainty related to the exact location of new power plants.

Input	Value
Years	2000-2019
Dataset	MERRA-2
Capacity	1 kW
System loss	10%
Tilt	22°
Azimuth	180°
Tracking	None

**Table 3:** Inputs used for each coordinate in the simulations of solar power generation.

### 5.1.2 Wind power generation

The wind resources vary more geographically than the solar resources, as seen from Figure 10. The map is based on both data from satellites, and on measurements at various heights above ground level [51], [77]. Average wind speed 150 m above ground level is up to 9.0 m/s in some areas, and [77] argues that some parts of the country have potential for grid-scale wind power generation.

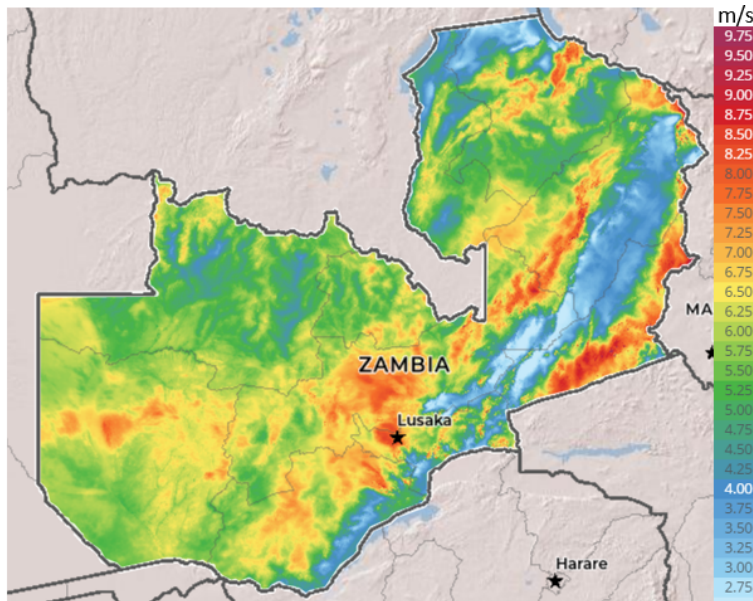


**Figure 10:** Average wind speeds 150 m above ground level in Zambia. Source: [51]

As mentioned in Section 4, there is currently only one candidate wind power project in Zambia. Potential locations for new wind power plants is suggested in [11], based on the best available wind resources and network availability. The same locations were chosen in this thesis to evaluate the variability of wind power generation, and can be seen in Figure 11. The area around Lusaka has both a high potential for wind power, and a strong electricity grid infrastructure, and is therefore likely to be relevant for future wind power plants.

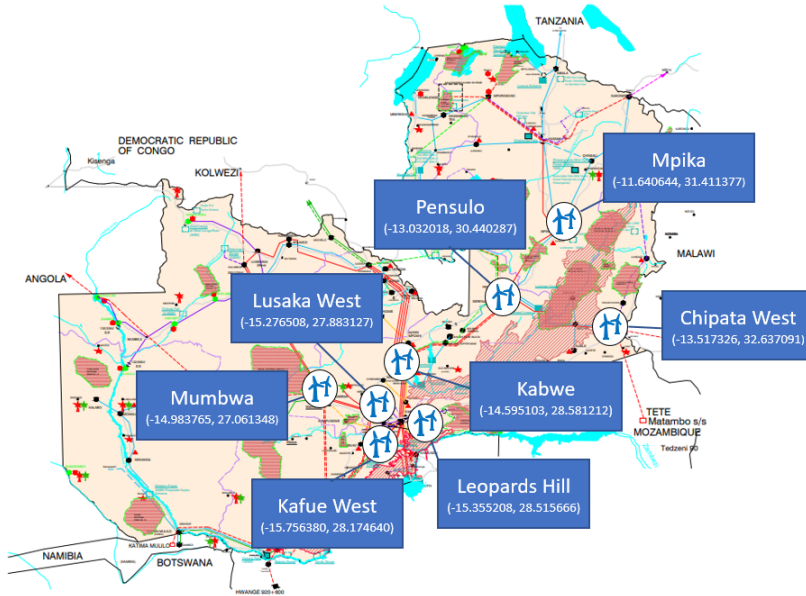


**Figure 11:** Geographical coordinates chosen for mapping out the variability in generation output from future wind power plants in Zambia.

The hourly wind power generation for the selected locations were simulated for the years 2000-2019 in Renewables.ninja. Wind turbines with a hub-height of 130 meters, and a rated capacity of 4.0 MW is projected in [11] in the short-and-mid-term in Zambia. In the long term, the report projects turbines with hub-heights of 150 meters and rated capacity of 4.2 MW. A similar conclusion is drawn in [77], where the authors suggest 4 MW turbines with hub heights of 130 meters to be used in Zambia.

To map out the variability of generation from potential wind power plants in 2030, the Vestas V136 4000 turbine with a hub height of 136 meters was chosen for the simulations in Renewable.ninja. A theoretical installed capacity of 1 kW was used to obtain the hourly generation profiles. An overview of the inputs used in the simulations can be seen in Table 4. As for the solar generation data, the simulated wind generation profiles from the eight selected locations were aggregated into one profile, and equally weighted in the aggregation.

Input	Value
Years	2000-2019
Dataset	MERRA-2
Capacity	1 kW
Hub height	136 m
Turbine model	Vestas V136 4000

**Table 4:** Inputs used for each coordinate in the simulations of wind power generation.

### 5.1.3 Precipitation

As described in Section 4, hydropower is by far the most important electricity source in Zambia. Variations in inflow to the large hydropower reservoirs and to the RoR hydropower plants can therefore have a high impact on the energy security of the country. The catchment areas of the large rivers exceed the borders of Zambia, but the domestic rainfall was considered a sufficient indication on the variability of inflow to hydropower reservoirs. Data on hourly precipitation was extracted for the country as a whole for the years 2000-2019.

## 5.2 Modeling different climatic years

Based on studies of the annual precipitation in Zambia, three years were selected to represent a dry, average and wet climatic year. Data for these years was used in the portfolio optimization model. An overview of the chosen climatic years can be seen in Table 5. 2003 was the the second driest year in the 20 year period, and 2007 was the second wettest year in the period. The two years were chosen as the median-years in the lower 15% and upper 15% of precipitation years, and it was assumed that they represent the 15% driest and 15% wettest years, respectively. 2011 was selected as the normal year, as it was the year with median precipitation in the 20 selected years. This year was assumed to represent 70% of all climatic years.

Assuming that each of the three years represents a certain fraction of climatic years, is a simplification. Also, climate change could potentially make the variations in precipitation larger in Zambia in the future, which could make historical data invalid for modeling the future variations [24]. However, these model simplifications were considered necessary due to the limited time and scope of this thesis.

The inflow profiles to reservoirs and RoR hydropower plants were scaled based on the differences in precipitation. 2003 was assumed to have 25% lower inflow than the normal year, and 2007 was assumed to have 20% higher inflow, since the precipitation in these years was 25% lower and 20% higher than in the average year, respectively.

Data from [59] supports the fact that the flow in the large rivers can vary substantially between years. In [11], a dry year is modeled as a year with -33% water availability compared to average conditions, and a wet year is modeled with +44% hydropower availability compared to average conditions. These variations are considered extreme scenarios, and the variability modeled in this thesis is somewhat more modest.

	Dry year	Normal year	Wet year
Year selected	2003	2011	2007
Inflow compared to normal year	-25%	0%	+20%
Fraction of years assumed to fall into category	15%	70%	15%

**Table 5:** The climatic years selected to represent a dry year, an average year and a wet year.

## 5.3 Single-node model of the Zambian power system

A single node model of the 2030 Zambian power system was built in PowerGAMA. Since this model reflects a future scenario of the system, projections had to be made on the development of future system load and installation of new hydro/thermal power plants. The projections were obtained from literature, and this section describes both how the input data was obtained, and how the system was modeled in PowerGAMA.

### 5.3.1 System operating reserve requirements

Operating reserves are defined in the SAPP Operating Manual [78] as the sum of spinning reserves<sup>7</sup> and quick reserves<sup>8</sup>. As mentioned in Section 4, the large dispatchable hydropower plants are regulating power output to ensure that system generation constantly equals system load in Zambia. With an increasing penetration of VRE, the reserve requirement is likely to be increased at these plants.

Today, the spinning reserve requirement is 100 MW when Zambia is not exporting/importing power (operating in island mode) [44]. The quick reserve requirement is unknown, but is assumed to equal the spinning reserve requirement [11]. Estimating the required reserves in 2030 can be done through several methodologies, and no universal methodology exists [79]. A comprehensive assessment of operational reserve requirements based on stochastic modeling of forecast errors of load and VRE generation is conducted in [11]. The result is dynamic requirements for operating reserves throughout all hours of the year.

For the sake of simplicity, only a static operating reserve requirement was used in this thesis. The upward regulating reserve requirement was set equal to 310 MW, which is the average reserve requirement presented in [11]. This might seem like a low operational reserve requirement, but this constraint will in reality only be binding when the generation from VRE power plants is low, with following less reserve requirements (explained further in Subsection 5.3.2).

For the downwards regulating reserve, the average value presented in [11] is 220 MW. However, it was assumed that a minimum of three generators at the dispatchable hydropower plants must be running at all time, implying a minimum downwards regulating reserve of 300 MW (further explained in Subsection 5.3.2).

Although the thermal power plants can contribute with operating reserves, it was assumed that all operating reserves must be provided by the large hydropower plants. This is because the thermal generation is governed by PPAs, and to the best knowledge of the author, providing operating reserves is not a part of those contracts.

---

<sup>7</sup>Unused generation capacity synchronized to the system and available to follow load without manual intervention [78].

<sup>8</sup>Non-spinning generation capacity that can come online within ten minutes, or load that can be interrupted within ten minutes [78].

### 5.3.2 Power plants

Several large power plants are planned in Zambia [80]. However, the construction of large power plants is often associated with uncertainty in terms of e.g. financing and commissioning date. Therefore, only the projects considered most likely to be in operation within 2030 were included in the scenario.

#### Thermal power plants

Today, the 300 MW Maamba coal power plant constitutes the majority of the thermal power capacity in the Zambian system [10]. An expansion of the power plant capacity to 600 MW was originally planned, but seems to have been stranded due to the lack of financing. As in [11], the capacity of 300 MW was therefore assumed to be valid in a 2030 scenario. Also, the capacity of the Ndola 110 MW HFO power plant, and the capacity of the diesel power plants in the system were assumed to remain the same in 2030 as today. To the author's best knowledge, no new thermal power plants are planned, and the thermal power plants in the 2030 scenario were hence the same as today.

The Maamba coal fired plant was modeled with constant generation output, equal to the average output of 233 MW in 2018 [74]. Despite some cycling observed in the historical generation data [44], the constant output is considered a decent assumption, due to the high capacity factor and long periods with constant generation output.

Constant generation output equal to the 2018 average was also assumed for the heavy fuel oil plant, and the diesel plants in the model. From the historical generation data [44], variations in generation output was, however, observed for some of these plants. Assuming constant generation output is therefore a simplification implying some error.

Because a liberalized power market does not govern the dispatch of power plants in Zambia, modeling the generation output could in general be challenging. This particularly applies for the thermal generators governed by confidential PPAs. Since the rules governing the dispatch at these plants are unknown, constant generation output is considered a necessary simplification.

An overview of the thermal plants included in the model is shown in Table 6. The power plants were modeled with constant inflow profiles and no storage in PowerGAMA, and the generation hence equals the average inflow factor multiplied by the capacity of each plant.

Power plant	Cap. [MW]	Avg. inflow fac.	Inflow profile
Maamba	300	0.78	const
Ndola	110	0.49	const
Diesel plants	83.6	0.49	const

**Table 6:** Thermal power plants modeled in PowerGAMA. Source: [74], [44]

**RoR hydropower plants**

The currently planned Batoka Gorge hydropower project on the Zambezi river could imply 2400 MW of new RoR hydropower capacity, shared equally between Zambia and Zimbabwe [80]. An additional 1200 MW shared between the two countries is planned at the Devil's Gorge hydropower plant. These two projects could add a total generation capacity of 1800 MW to the Zambian power system. However, as done in [11], these power plants were not included in the 2030 scenario. This is mainly because of the uncertainty related to large hydropower plant construction projects. The construction work has not begun at either of the two projects, and it is unknown whether or not these power plants will be in operation within 2030. Assuming that these projects are not online within 2030, is one of the major uncertainties of this thesis, and is further discussed in Section 6. Moderate extensions of the Lusiwasi and Chisimba Falls hydropower plants were the only new RoR hydropower capacity additions included in the model.

Even though climate change could change the patterns and magnitude of rainfall, as discussed in Section 2, it was assumed that historical inflow profiles could be used for modeling the variations in inflow to RoR hydropower plants in 2030. Only monthly variations were modeled, meaning that every hour within each month has the same inflow. All profiles were normalized to make it easy to simulate wet/dry years by adjusting the average inflow factor.

In reality, the Itezhi-Tezhi power plant is connected to a large reservoir, but as described in Section 4, the daily generation output is relatively stable. Therefore, the power plant was modeled as a RoR power plant where the dispatch is governed by a monthly profile, based on historical generation data from 2018 and 2019 [44].

The generation profile for the Victoria Falls power station was based on historical data for the years 1978-2007 extracted from [59]. Due to the lack of data, this profile was also used for all the other RoR power plants in the system, which is a simplification. However, the other RoR power plants only constitute around 7% of installed hydropower capacity, and the potential error following this assumption is considered relatively small.

An overview of the RoR hydropower plants included in the model can be seen in Table 7. The inflow factors shown in the table represent the inflow as a fraction of installed capacity for an average climatic year.



Power plant	Cap. [MW]	Avg. inflow fac.	Inflow profile
Itezhi Tezhi	120	0.62	Itezhi-Tezhi
Lusiwasi	101	0.58	Vic. Falls.
Victoria Falls	108	0.70	Vic. Falls.
Mulungushi	32	0.60	Vic. Falls.
Lunsemfwa	24	0.60	Vic. Falls.
Lunzua River	14.8	0.49	Vic. Falls.
Musonda Falls	10	0.57	Vic. Falls.
Micro Hydro	16.8	0.27	Vic. Falls.

**Table 7:** Run of river power plants modeled in PowerGAMA. Source: [74], [44], [59]

### Large hydropower plants with reservoirs

In addition to the two existing large hydropower plants, the Kafue Gorge Lower (KGL) hydropower plant is currently under construction, and is planned to be commissioned by the end of 2021. When completed, the installed capacity will be 750 MW. Located 17.3 km downstream of the existing KGU power plant, the two power plants will form a cascade. KGL is built and operated by an IPP [81].

The three largest hydropower plants in the 2030 system scenario are hence KGU, KGL and KNB. In the single-node model, these were aggregated into one power plant, called "Large Hydro". The aggregation was performed due to the challenges experienced when modeling the large hydropower plants in the Specialization project [3]. As described, dispatch is determined by the storage values for hydropower plants with reservoirs in PowerGAMA. In the Zambian system, one of the three large hydropower plants will always have the lowest storage value when modeling them as separate units. One of the plants will thus be generating at maximum capacity, and the other plants will generate at low capacity, or not at all [3]. This is not considered a representative model of the real hydropower operations. By aggregating the three hydropower plants, the resulting Large Hydro power plant models the sum of dispatch from the actual plants. The generation capacity, reservoir capacity and inflows were therefore added together.

The initial reservoir level in the aggregated reservoir was set to 75%, which represents a relatively high filling level in a historical context [59], [82]. This model parameter is discussed further in Section 6.

The upward regulating reserve requirement described in Subsection 5.3.1 was implemented by setting the maximum generation capacity 310 MW lower than the sum of generation capacity from the three plants. In practice, this implies that the Large Hydro power plant cannot generate at max capacity, but must save some generation capacity as reserves. This constraint will only be binding when the output from VRE generators is low, and the generation output from the Large Hydro power plant is high. Because the output from VRE generators is low when the spinning reserve requirement is a binding constraint, the relatively low reserve requirement can be justified.

Similarly, the downwards regulating reserve requirement of 300 MW was implemented as a minimum generation limit for the Large Hydro power plant. In reality, this implies that a total of three generators at KGU, KGL and KNB must be running at all time<sup>9</sup>.

The model does not take into account the distribution of generation output between the three different plants constituting the Large Hydro power plant, or the distribution between the generators within each power plant. Thus, all generation output levels between the minimum and maximum limits are assumed feasible for the Large Hydro power plant. In reality, the minimum generation limit for each generator will make some output levels infeasible. Also, it is assumed that the reserve requirements can be met for all output levels between the upper and lower generation limit.

Ramp rate constraints were not included in the model. In general, the hydropower generators are considered fast ramping [44]. However, current literature suggests that ramp rate constraints could limit VRE integration in Zambia [16]. Despite not included in the model, this topic is therefore evaluated in Section 6.

The inflow profile for the aggregated reservoir was modeled as the inflow to the KGU reservoir. This is because this profile will govern both the inflow to KGU and partly KGL, which makes up the majority of generation capacity in the aggregated plant. No data was obtained for the inflow profile to KGU, but the inflow was assumed to equal the outflow from the Itzhi-Tezhi reservoir. Since it takes 2-4 months for the water to flow from the Itzhi-Tezhi reservoir to KGU, the inflow profile was approximated by shifting the Itzhi-Tezhi generation profile by three months. This simplification is also made in [11].

The inflow factor for the Large Hydro power plant was found as a weighted average of the inflow factors of the three plants, based on data from [11] and [74]. Table 8 shows key parameters for the three power plants, and the resulting parameters for the Large Hydro power plant used in the model.

Power plant	Cap. [MW]	Reservoir cap. [GWh]	Inflow fac. (avg. year)
Kafue Gorge Upper (KGU)	990	855.7	0.69
Kafue Gorge Lower (KGL)	750	43.6	0.46
Kariba North Bank (KNB)	1080	7938.7	0.48
Large Hydro	2510	8838.0	0.62

**Table 8:** KGU, KGL and KNB aggregated into the Large Hydro power plant. Note that the capacity of the Large Hydro power plant is 310 MW lower than the sum of the three aggregated power plants due to the reserve requirement. Source: [11], [74], [44], [59]

### Solar PV power plants

As presented in Section 4, several solar power plants are currently planned in Zambia. The expected locations of these new plants were used for mapping out the VRE potential in Zambia, as seen in Subsection 5.1. When it comes to finding the optimal VRE portfolio

<sup>9</sup>The minimum generation limit of each generator is around 100 MW [44].

to be integrated into the system within 2030, the planned power plants were however not included in the scenario. This is because the main objective in this thesis is to find the optimal VRE portfolio to be integrated, regardless of the current plans. Only the existing power plants were hence included in the scenario, while the new solar PV capacity was varied to find the optimal portfolio.

As described in Subsection 5.1, the hourly generation profiles for the eight selected geographical locations in Zambia were aggregated into a single profile. This profile represents the hourly generation output per installed kW of solar PV capacity in Zambia as a whole, and was used as the inflow profile for both the existing and the new solar PV capacity in the single-node model. New solar PV capacity was modeled as a single power plant, and the capacity was varied in the simulations. Table 9 shows the solar PV power plants included in the model.

Power plant	Cap. [MW]	Inflow fac. (avg. year)	Inflow profile
Bangwelu/Ngoyne	88	0.209	Avg. Zambia
Micro Solar	1.1	0.209	Avg. Zambia
New solar PV cap.	varying	0.209	Avg. Zambia

**Table 9:** Solar PV power plants modeled in PowerGAMA. Source: [74], [52]

### Wind power plants

Since no wind power plants currently exist in Zambia, only new wind power capacity was included in the model. As for the new solar PV capacity, the wind power capacity was modeled as a single power plant with the aggregated wind power profile as inflow profile. An overview of the inputs describing the wind power plant included in the model can be seen in Table 10.

Power plant	Cap. [MW]	Inflow fac. (avg. year)	Inflow profile
New wind power cap.	varying	0.37	Avg. Zambia

**Table 10:** Wind power plants modeled in PowerGAMA. Source: [52]

### 5.3.3 System load

The hourly profile describing the total load in the system, is an important parameter in the 2030 scenario. The historical load profile for 2018 obtained from [44] was used as a baseline profile, and was modified to represent 2030 based on electricity demand forecasts from literature. 2018 was chosen as a baseline year because it is the most recent year not affected by load shedding, and the hourly demand profile in this year is considered representative for the system under normal conditions [3].

Literature was reviewed to find projections for electricity and peak power demand in 2030. A relatively comprehensive demand forecast was conducted in [11], which includes population growth, increased household electricity access, economic growth, development in mining loads and system losses. The forecast includes projections for both peak power and

electricity demand, and is to the best knowledge of the author, the most updated demand forecast for Zambia. The findings were therefore used for adjusting the 2018 load profile to a 2030 scenario.

Based on data from the Chamber of Mines, [11] projects a total mining industry load of 1385 MW in 2031, and it was assumed to be the same in 2030. As in [3], the mining load was modeled constant for all hours in this thesis, which is relatively close to reality [44]. Non-mining loads were assumed to follow the same hourly profile in 2030 as non-mining loads in 2018, but scaled to the projected average non-mining load of 1057 MW in 2030. Added together, the constant mining load and the non-mining load profile constitute the power system hourly load profile for 2030. Transmission system losses were included by scaling the total load by a factor corresponding to the expected system losses [74], [11].

As seen in Table 11, the total electricity demand resulting from this profile is 24870 GWh, and the peak demand is 3489 MW, including system losses. Both of these numbers are almost the same as used in [11], suggesting that scaling the 2018 load profile to match total electricity output implies a correct scaling of the maximum peak demand as well. The projected system load was implemented as a single load in the model.

Demand type	Peak load [MW]	Average load [MW]	Annual el. demand [GWh]
Mine loads	1385	1385	12133
Non-mining loads	1615	1057	9259
Losses	489	397	3478
<b>Total</b>	<b>3489</b>	<b>2839</b>	<b>24870</b>

**Table 11:** The projected load and system losses in the Zambian power system in 2030. Source: [11], [44]

### 5.3.4 Exports/imports

As shown in Section 4, Zambia is usually a net exporter of electricity on an annual basis. However, it was assumed that the power system is operated without interconnectors to neighboring countries (island mode) in this thesis. Therefore, no exports/imports were included. This assumption was made mainly to simplify the system model and evaluate the costs and implications of being self-sufficient with electricity in Zambia. Interconnectors to neighboring countries make it technically feasible to export/import electricity during periods with surplus/shortage of power in Zambia, but other factors could constrain the physical flows. As an example, load shedding has been practiced in Zambia because the cost of importing power is too high [73]. Also, neighboring countries have power systems highly dependent on hydropower, and could experience the same power shortages during dry years as Zambia, with following restrictions on exports [25].

In the future, more non-dispatchable energy sources could lead to changes in the SAPP electricity market. Several Southern African countries are implementing increasing solar PV capacity, and this trend is expected to continue with the expected decrease in LCOE of new power plants [83], [84]. Experience from wind power generation in Northern Europe

suggests that adding a large VRE generation capacity in a limited geographical area could lead to periods with over-generation, with following low, or even negative, power prices [32]. In Southern Africa, over-generation from solar PV power plants mid-day could potentially become a challenge, making the future export market more uncertain.

Over-dimensioning the VRE generation capacity in Zambia to benefit from future exports during hours with high production, could hence be associated with risk. As explained, under-dimensioning new installed capacity to rely on imports in dry years, could also be risky. Modeling the system without exports/imports could therefore be a good way of determining the optimal portfolio of VRE to cover the domestic electricity demand.

## 5.4 Cost parameters

This subsection shows the different cost parameters used in the 2030 scenario. Table 13 at the end of the subsection summarizes the most important cost parameters.

### 5.4.1 Marginal cost of power plants

PowerGAMA optimizes the generation in the system based on the marginal cost of different power plants. In large power systems with a liberalized power market, this could be an accurate model of the dispatch in the real system. In such systems, the generators with the lowest marginal costs will be generating most of the time because they outbid generators with higher marginal costs. Thus, the generators with high marginal cost will only generate when the electricity price is high.

In the Zambian system, the electricity tariffs are fixed, and the generators are either operated by ZESCO, or owned by IPPs and operated through PPAs. As explained, the dispatch from thermal generators was therefore modeled with constant output. The generation output from RoR hydropower plants and VRE power plants will similarly be governed by the previously described inflow profiles. In total, the only dispatchable plant in the model is the Large Hydro power plant. This plant will output power equal to the difference between the load and the generation quantity produced by the non-dispatchable power plants. Therefore, having the correct marginal cost of generators is not critical for modeling the dispatch in the system.

Nevertheless, the marginal costs of generators were also used for calculating the total cost of operating power plants in the optimization model. Having a decent estimation of the marginal costs was therefore necessary. The cost of operating the thermal power plants was obtained from [44]. Since the thermal power plants are regulated through confidential PPAs, the marginal costs will not be shown in this thesis. For the sake of simplicity, it was assumed that the marginal cost of these power plants will be the same in 2030 as today.

The VRE power plants were assumed to have zero marginal cost in the model. Hydropower plants were assumed to have a marginal cost of 0.005 USD/kWh, which is in line with the assumptions made in previous studies using PowerGAMA [55].

### 5.4.2 Value of lost load (VoLL)

A VoLL between 1.0 USD/kWh and 3.0 USD/kWh is applied for the countries in Southern Africa in [80]. In [6], a VoLL of 0.95 USD/kWh is found for small businesses experiencing load shedding in Zambia. Households and small businesses are the consumers bearing the majority of the burden of load shedding in Zambia [10], and the relatively low VoLL of 0.95 USD/kWh was therefore used in this thesis.

### 5.4.3 Water values

Having a correct water value for governing the Large Hydro power plant dispatch in the model is not critical, because it is the only dispatchable power plant in the model. As long as the water value is always lower than the VoLL in the system, the Large Hydro power plant will cover the difference between non-dispatchable generation output and load. As explained in Section 3, the water values were also used to calculate the cost of changed reservoir levels in the optimization model. Consequently, a constant water value and a water value function for the Zambian system were obtained. The two different methods used for calculating the water values do not result in different dispatch from the aggregated reservoir, but leads to different valuation of changed reservoir level during the simulation period.

#### Constant water value

The water-power nexus in the SAPP is investigated in [85], and average water values for all member countries for a range of climatic years are presented. For Zambia, the average water value for the KGU reservoir is estimated to 0.075 USD/kWh, and the average water value at KNB is estimated to 0.050 USD/kWh. Weighting these quantities by the storage capacities of the KGU and KNB reservoirs yields a water value of 0.052 USD/kWh for the aggregated reservoir used in the PowerGAMA model. This water value might change within 2030 as both the demand and the generation portfolio in Zambia and neighboring countries is changing, but the estimate is considered a relevant approximation for capturing the value of stored water.

#### Dynamic water values

PowerGAMA allows for modeling water values with both a reservoir filling component, and a time component. For simplicity reasons, only a filling component was used in this thesis, implying that the storage value is a function only of the reservoir filling level. For a filling level of 100%, an additional water unit in the reservoir would imply spilling water, and the water value is hence zero. If the reservoir is empty, the consequence would be load shedding, and the water value with 0% filling level would equal the VoLL. Between these two extremes, the water value is however harder to determine. In this thesis, the relation between reservoir level and water value used in [55] was applied, but scaled to the VoLL in Zambia. A figure showing the water value as a function of reservoir level is included in Appendix B.

#### 5.4.4 Cost of new solar PV and wind power capacity

To find the optimal VRE portfolio to be integrated into the Zambian power system, the development in the cost of solar PV and wind power technology is of high importance. The cost of building and operating VRE power plants will in reality vary between specific projects, and develop in time as the cost of technology is changing. In this thesis, cost projections from existing literature for both capital expenditure (CAPEX) and operating expenditure (OPEX) towards 2030 were used to estimate the average annualized cost of new power plants.

Multiconsult and the African Development Bank (AfDB) present an analysis of the investments needed to realize the so-called New Deal on Energy for Africa in [86]. In this report, projections for CAPEX and OPEX for onshore wind and solar PV in Africa are made for the years 2020, 2025 and 2030. A linear decrease in CAPEX is expected for wind, while the CAPEX of solar PV is expected to have a steeper decrease in the first half of the decade compared to the second half. The unit of the OPEX is USD/kW/year, meaning that the operational cost is assumed fixed, and does not depend on the amount of generated electricity.

A similar forecast for the costs of solar PV and wind power capacity for each year from 2020-2030 is presented in [11]. The projections for CAPEX are close to the values obtained in [86] for both wind and solar PV. However, the values are generally lower for OPEX in [11] than in [86]. In particular, the OPEX for onshore wind power is less than half. As a reference, [87] reviews the OPEX of wind power in the United States, and finds that operating cost spanned from 33 USD/kW-yr to 59 USD/kW-yr in 2018, with a expected decrease of only 10-20% the next two decades. This indicates a potential underestimation of OPEX in [11]. The projections for both CAPEX and OPEX from [86] were therefore used in this thesis.

The lifetime of solar PV power plants was assumed to be 30 years, and the lifetime of wind power plants was assumed to be 20 years, based on the most frequently used lifetimes in [21]. The discount rate was set to 10%, as in [11]. This is higher than the discount rate used for solar PV and onshore wind in most developed economies [88], but the risk associated with large investments is in general higher in sub-Saharan African countries, contributing to a higher discount rate.

The resulting levelized cost of electricity (LCOE) was calculated with the average capacity factors for solar PV and wind power in Zambia. LCOE was not used as model input, but can inform about the electricity cost resulting from the assumptions made. The CAPEX, OPEX and resulting LCOE for the two technologies can be seen in Table 12.

Whether or not the projected LCOE-values are realistic, is hard to determine. In 2016, the winning bids in two solar PV tenders of 0.060 USD/kWh and 0.078 USD/kWh were considered record-breaking in Zambia [89]. Three years later, the lowest accepted bid in the 120 MW GET FiT auction was 0.039 USD/kWh [90]. This rapid decrease in PPA-price indicates that the LCOE-values of solar PV in Table 12 might be too high. However,

none of the GET FiT power plants have been constructed yet, and it remains uncertain when the power plants associated with the record-low bid will be commissioned. Thus, the costs and implied LCOE of solar PV, seen in Table 12, are considered somewhat conservative, but realistic. This is supported by [11], which displays a broad range of LCOE from committed solar PV projects. For wind power, no historical LCOE data for Zambia exists, and hence the calculated LCOE values are hard to validate.

Technology, year	CAPEX [USD/kW]	OPEX [USD/kW-yr]	LCOE [USD/kWh]
Solar PV, 2020	850	18.06	0.059
Solar PV, 2025	690	18.06	0.049
Solar PV, 2030	600	18.06	0.045
Onshore wind, 2020	1330	57.52	0.060
Onshore wind, 2025	1280	46.19	0.056
Onshore wind, 2030	1230	44.91	0.054

**Table 12:** Projected CAPEX and OPEX of solar PV and wind power. Source: [86], [21], [11]

The installation of solar PV generation capacity was assumed to be distributed uniformly in time between 2020 and 2030. The CAPEX and OPEX of the installed solar PV capacity in 2030 was hence calculated as an average of the projected values in 2020, 2025 and 2030. From the average CAPEX and OPEX values, the 10% discount rate, and 30 years lifetime, the annualized cost of 1 kW solar PV capacity was calculated to 93.7 USD/kW-yr. The same assumptions were applied for the wind power capacity. Annualized cost over the lifetime of 20 years for 1 kW wind power capacity was calculated to 199.9 USD/kW-yr.

Table 13 shows an overview of the most important cost parameters presented in this subsection.

Model parameter	Value	Unit
Value of lost load (VoLL)	0.95	USD/kWh
Constant water value	0.052	USD/kWh
Annualized CAPEX + OPEX of new solar PV plants	93.7	USD/kW
Annualized CAPEX + OPEX of new wind power plants	199.9	USD/kW

**Table 13:** Model parameters used to calculate the total system cost for different portfolios of VRE.

## 5.5 Grid model of the Zambian power system

Building the multi-node model of the Zambian power system was done after the optimal portfolio of new VRE capacity was obtained from the optimization model. This allowed for modeling the system with the optimal VRE capacity integrated into the grid.

Despite the fact that this thesis evaluates renewable energy integration within 2030, the grid was modeled as of today (2021). This can be justified for several reasons. Even though grid upgrades are planned between 2021 and 2030 [11], there is always uncertainty related to the commissioning date of infrastructure projects. Also, implementing



the optimal new VRE portfolio within 2030 implies connecting new power plants to the grid before potential upgrades are commissioned. Simulating the load flows in the 2021 grid can therefore be viewed as a worst case scenario, where no new grid upgrades are commissioned, but the new VRE capacity and load increases to 2030 level.

### Nodes and branches

The grid model was based on a model of the Zambian power system in the software Digsi-lent PowerFactory, obtained from ZESCO [44]. It models the Zambian power system as of 2023, and was therefore adjusted to represent the current power system. Only the substations and lines at the three highest voltage levels (132 kV, 220 kV and 330 kV) were included in the model. Generators and loads connected at lower voltage levels in the system were modeled as connected directly to the buses at the higher voltage levels. Thus, the model represents all loads and generators in the system.

Figure 12 shows the 48 nodes and 72 branches included in the grid model. As seen from the figure, the grid is meshed in the Lusaka area and the Copperbelt region, and mostly radial in the rest of the country. The reactance and thermal rating of lines were included in the model. Transformers were not included, due to lack of data. However, this is considered a minor simplification.

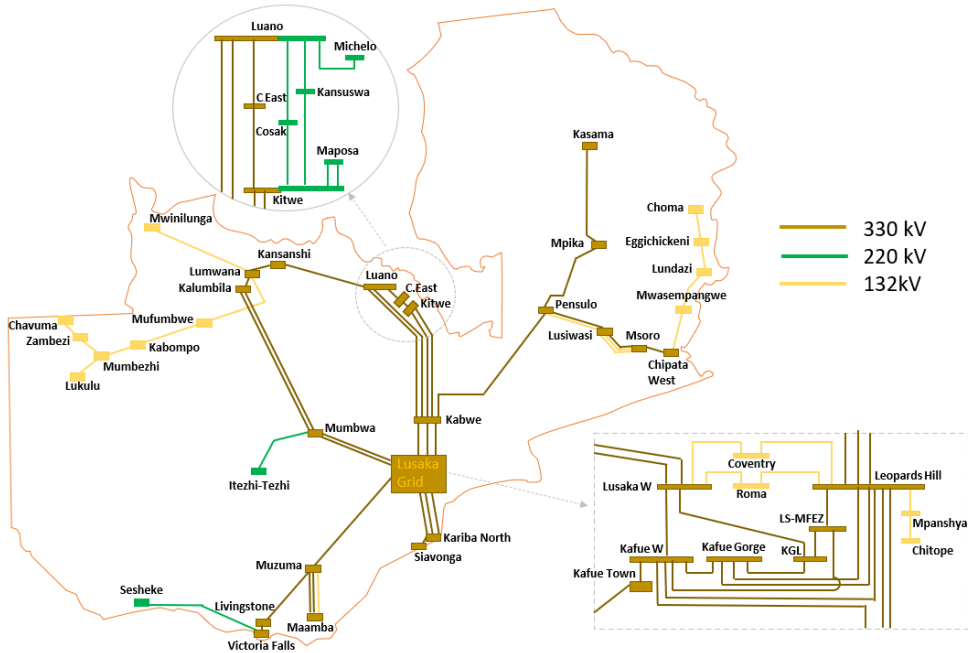


**Figure 12:** The grid used in the grid model in PowerFactory. Source: [91], edited by author

### **Distribution of power plants in the grid**

The thermal power plants and the RoR hydropower plants included in the single-node model were distributed in the grid model based on their existing/planned connection points.

For the Large Hydro power plant, the connection point was set to the node Kafue Gorge. In reality, the three power plants KGU, KNB and KGL that constitute the Large Hydro power plant are located at the nodes Kafue Gorge, KGL and Kariba North. Having the aggregated power plant connected at Kafue Gorge represents a simplification, which is further discussed in Section 6.

Translating the optimal VRE capacity into power plants in the grid was done based on the expected locations of new power plants described in Subsection 5.1. It is out of the scope of this thesis to evaluate the optimal integration strategy for new power plants, and the grid model only includes a single scenario describing how the new capacity can be integrated.

The optimal new solar PV capacity was distributed in two steps. First, capacity corresponding to the currently planned solar PV plants, described in Section 4, was distributed at expected connection points. Second, the remaining new solar PV capacity was distributed equally between the nodes where new solar capacity is planned or expected to be implemented.

The same logic as for the solar PV plants was used for distributing the optimal wind power capacity in the grid. Since only one wind power plant is currently planned, the majority of generation capacity was distributed evenly between the selected nodes. The distribution of VRE power plants is explained in detail in Appendix E.

### **Inflow profiles**

The inflow profiles belonging to each of the nodes were used for the VRE power plants. This is a minor difference from the single-node model, where average inflow profiles representing Zambia as a whole were used. Using the location specific profiles provides a more realistic model of load flows in the system, because it takes into account geographical differences in solar radiation and wind speeds. Only an average climatic year was modeled.

The inflow profiles for the thermal power plants and RoR power plants were the same in the grid model as in the single-node model.

### **Distribution of load in the grid**

The load data for the 48 nodes in the system was extracted from the PowerFactory model, and scaled to represent the 2030 load scenario. Four nodes in the Copperbelt area were identified as nodes dominated by mining loads. These were Kitwe, Luano, Kansanshi and Kalumbila, and the demand at these nodes was scaled to the projected level of mining loads in 2030. Also, the profiles describing load variations were set constant for these loads, because it is assumed that the mining operations provide an almost constant load.

These are the same assumptions as used in [3].

The average levels of all the other loads in the system were scaled to add up to the projected 2030 non-mining demand level. Variations in non-mining loads were modeled with the load profile for the entire system, minus the constant mining load profile. In total, the sum of the constant mining loads and the varying non-mining loads equals the total system load used in the single-node model. Thus, the total load in the grid model represents the same demand scenario as used in the single-node model.

Scaling existing loads with the same factor to reflect the 2030 demand scenario represents a simplification. In reality, the development in existing demand will probably be different at different nodes. At some nodes, the load will likely increase towards 2030, while the load at other nodes could be more stable. Nevertheless, scaling all the loads is considered an acceptable approximation for the purpose of this study.

## 6 Results and discussion

As explained in Section 1, the main goal of this thesis is to identify the optimal portfolio of VRE to be integrated into the Zambian system by 2030. This was done through the three-step procedure; 1.) evaluate the VRE resources, 2.) identify the optimal portfolio and 3.) assess potential overloading in the transmission grid from implementing the optimal portfolio.

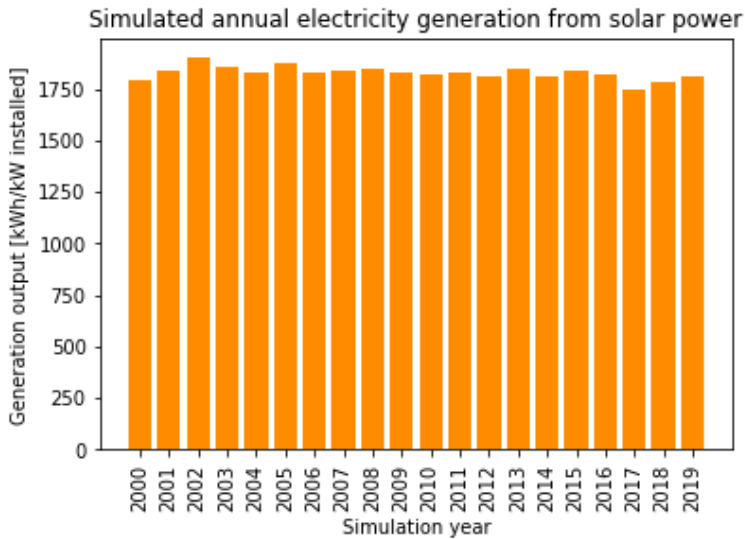
This section shows the results, and discusses them in relation with each other. The observed variations in VRE generation output and precipitation, obtained from Renewables.ninja, are presented first. Based on the results, the potential for diversifying the Zambian generation portfolio with VRE is discussed. Focus is then shifted towards the optimization model. The single-node model used in the optimization model is validated against historical data. Following the model validation, are the results obtained from simulations in the optimization model. These represent the core of this thesis and include evaluations of impacts on load shedding, VRE curtailment and hydropower operations from different VRE portfolios. Results from sensitivity analyses of the most important model parameters are then presented. After the sensitivity analyses, the results from load flow simulations in the grid model are shown. Finally, discussions are made on potential sources of error following the scenario modeling and the use of the PowerGAMA software.

### 6.1 Variations in renewable generation output and precipitation

This subsection presents the results obtained from the simulations in the Renewables.Ninja software. As mentioned, historical data from the years 2000-2019 was used in the simulations.

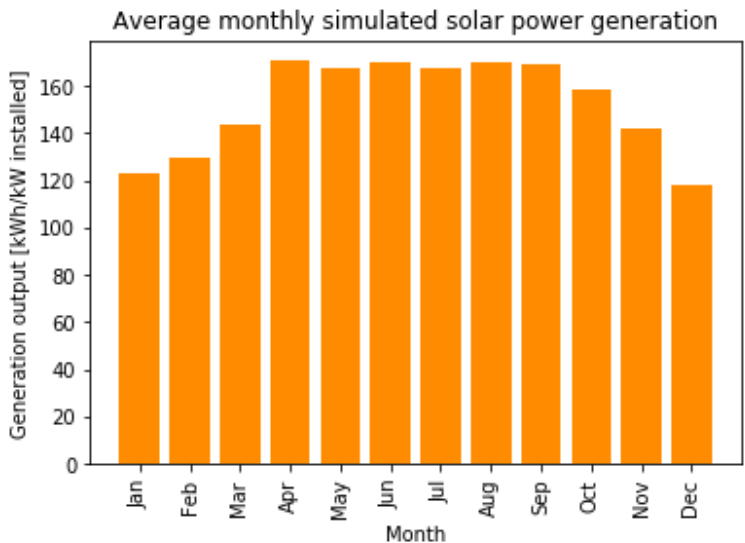
#### 6.1.1 Solar PV

Figure 13 shows the simulated annual electricity generation output per kW installed solar PV capacity in Zambia. As seen from the figure, the annual electricity generation is almost constant, and the standard deviation of the generation output was calculated to only 1.7% for the 20 simulated years. This result underlines the fact that solar power is a stable energy source in an annual perspective. The average capacity factor was calculated to 20.9% based on the simulation results.



**Figure 13:** Simulated annual electricity generation from solar PV in Zambia. The results were obtained as an average of the simulated output from the eight selected locations.

The average monthly electricity generation for the 20 years can be seen in Figure 14. Electricity generation is lower from November to March, which corresponds to the wet season, and higher in the dry season.



**Figure 14:** Average monthly simulated electricity generation from solar power in Zambia for the years 2000-2019.

### 6.1.2 Wind power

Figure 15 shows that the simulated annual electricity generation from wind power is relatively stable. However, a standard deviation of 5.7% in electricity output for the 20 simulated years, makes wind power more variable than solar PV on an annual basis. The average capacity factor was calculated to 40.4% based on the simulation results. A relatively high capacity factor can partly be explained by the wind turbine model selected for the simulations. The Vestas V136 4000 turbine is designed for medium wind speeds, and has a relatively small generator to rotor ratio<sup>10</sup>. This contributes to a high capacity factor, because the turbine is swiping a large area relative to the generator capacity. Selecting another turbine model for the simulations could imply a different capacity factor.

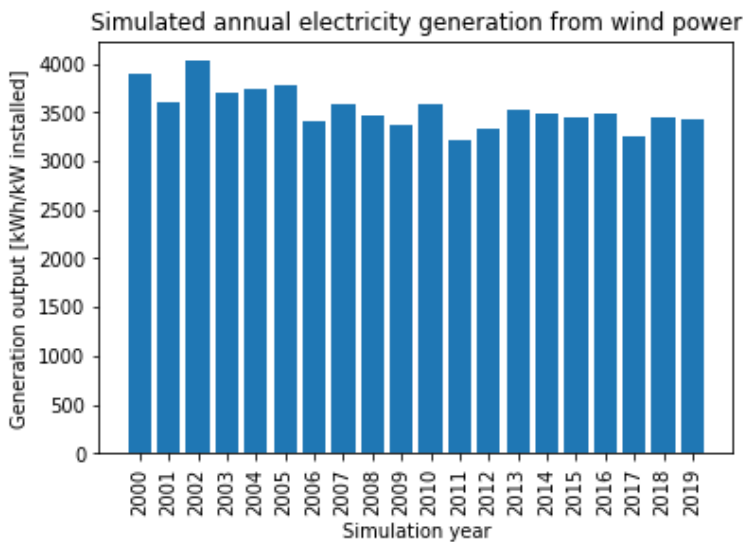


**Figure 15:** Simulated annual electricity generation from wind power in Zambia. The results were obtained as an average of the simulated output from the eight selected locations.

The simulated average monthly electricity generation is shown in Figure 16. As seen from the figure, the electricity generation from wind power varies more on a monthly basis than solar generation. Output is at its highest from July to October, which corresponds to the second half of the dry season. This is often when the inflow to hydropower plants is at its lowest [59].

<sup>10</sup>Generator capacity divided by rotor diameter [92].

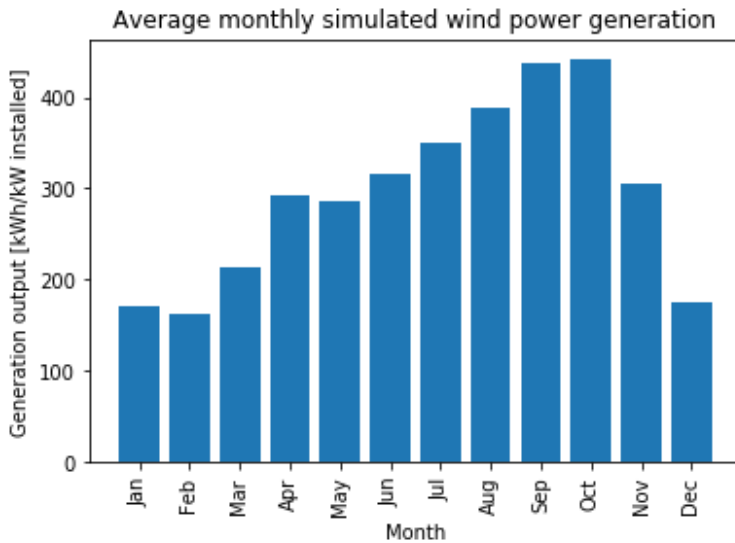


**Figure 16:** Average monthly simulated electricity generation from wind power in Zambia for the years 2000-2019.

### 6.1.3 Daily variations in VRE generation output

The hourly generation output for an average day was obtained for both solar PV and wind power, and is shown in Figure 17. The shape of the solar power generation curve is characteristic with sunrise around 6 am, peak generation around noon, and sunset around 6 pm. On the other hand, wind power generation is highest during night, and has a significant dip during the day. This is a highly interesting finding, because it indicates that solar and wind power could balance out some of the daily variations of one another. In particular, the increase in wind power output around sunset could decrease the magnitude of ramping required from the dispatchable generators in the system.

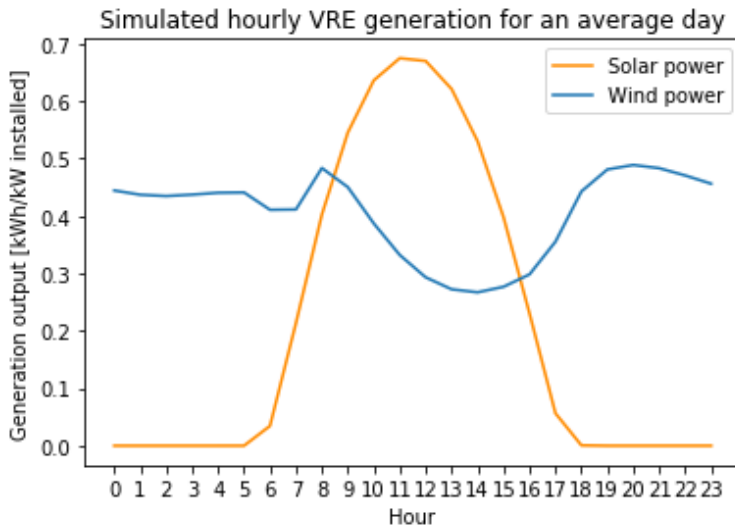


Figure 17: Simulated hourly VRE generation output for an average day (local time).

### 6.1.4 Precipitation

Figure 18 shows the precipitation for the years 2000 to 2019. The standard deviation of the precipitation was calculated to 13.7%, which reflects a high variability compared to the variations found for solar and wind power generation (1.7% and 5.7%, respectively). As mentioned, the annual variability of precipitation cannot be directly translated to variability in inflow to hydropower plants, but can indicate the magnitude of the variations.

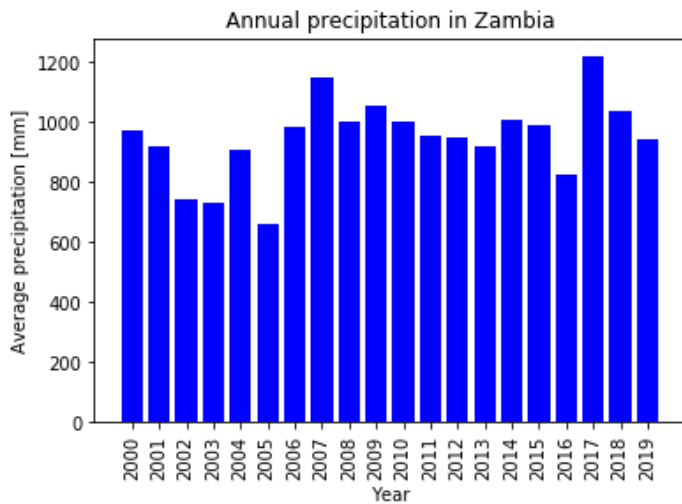


Figure 18: Historical average precipitation in Zambia, weighted by land area.



The average monthly rainfall for the years 2000-2019 is shown in Figure 19. As seen from the figure, there is a clear seasonal pattern with the wet season lasting from November to April, and the dry season lasting from May to October.

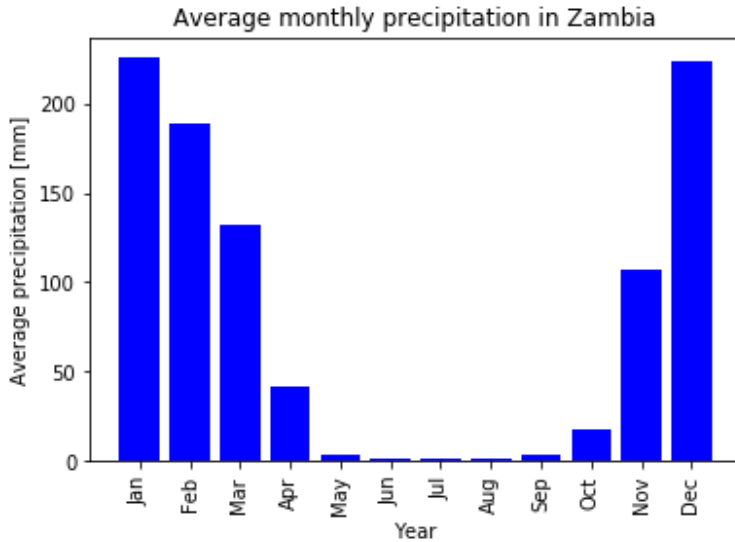


Figure 19: Average monthly precipitation in Zambia.

### 6.1.5 Correlation between VRE generation and precipitation

Finding the correlation between VRE generation and precipitation could indicate how VRE generation output varies in dry and wet years. If negatively correlated with precipitation, increased VRE generation could compensate for some of the reduction in hydropower output in dry years.

Based on the 20 years of simulated VRE generation output and the precipitation data, the correlation coefficients for the annual power output and precipitation were calculated. The coefficients can be seen in Table 14. A correlation coefficient of 1 represents a perfect correlation, a coefficient equal to 0 represents no correlation, and a coefficient equal to -1 represents a perfect negative correlation. As seen from the table, solar PV generation has a negative correlation coefficient of -0.70 with precipitation, which can be translated to a strong negative correlation. Dry years will therefore normally have higher generation output from solar PV power plants than wet years.

The same trend is seen for wind power generation, which has a correlation coefficient of -0.59 with precipitation. This is lower than the correlation between solar PV and precipitation, but the annual variations in wind power output are substantially larger than the variations in solar PV output. This means that despite a lower negative correlation, the increase in output from wind power plants in dry years compared to wet years will in gen-

eral be higher than the corresponding increase in solar PV output.

The correlation between annual solar PV output and annual wind power output is 0.56, which represents a relatively strong positive correlation. Thus, years with high solar PV generation output will in general have high output from wind power plants.

	Precipitation	Solar PV generation
Solar PV generation	-0.70	1.0
Wind power generation	-0.59	0.56

**Table 14:** The correlation coefficients between solar PV generation, wind power generation and precipitation in Zambia.

### 6.1.6 Diversifying the generation portfolio with VRE in a changing climate

As mentioned in Section 4, there is a need for diversifying the Zambian generation portfolio to reduce the risk of power shortage in dry years. Based on the simulations in Renewables.ninja and the existing literature presented in section 2, some key-takeaways can be mentioned.

Solar PV power can provide a stable energy output on an annual basis, and will most likely not change due to climate change, as discussed in Section 2. On a monthly basis, solar generation output is highest in the dry season, and lowest in the wet season. This could potentially compensate for the decrease in generation output from hydropower plants in the dry season. In addition, solar output is highest in dry years.

Wind power output varies slightly more than solar PV on an annual basis, but the variations are relatively small. The literature presented in Section 2 indicates that wind power output could be higher in a changing climate, but it could also remain unchanged. On a monthly basis, wind power varies quite a lot, with highest production in the second half of the dry season. The daily variations in wind power imply higher generation during night, and lower generation during day. Wind power could therefore balance some of the daily variations in solar PV generation, and some of the monthly variations in hydropower generation.

The inflow to hydropower plants depends on rainfall, which has varied substantially historically. Also, literature suggests that the average inflow could decrease as a result of climate change, and that high dependence on hydropower could imply a great risk of electricity supply disruption. Rainfall is concentrated in the rainy season from November to March, and storing water in reservoirs is therefore important for securing electricity supply in the dry months.

As indicated by the name variable renewable energy, solar and wind power output varies in a short term perspective. On an annual basis, the electricity output is however found to be quite stable in Zambia. This is the complete opposite of hydropower plants with reservoirs, which can be dispatched in the short term, but relies on inflow with high variability

on an annual basis. Also, both annual solar PV and wind power output is negatively correlated with precipitation, meaning that the output from these sources is higher in dry years, and lower in wet years. VRE could therefore complement the hydro-dominated system by securing a stable annual energy supply, while hydropower could balance the short-term variations in solar PV and wind power output.

In total, the data extracted and the results obtained from the simulations in Renewables.ninja indicate that implementing both solar PV and wind power plants in the Zambian system could be a good option for diversifying the generation portfolio. The following subsections evaluate the optimal portfolio of VRE capacity to be integrated into the system within 2030.

## 6.2 Single-node model validation

Validating a model describing a future scenario, could be challenging. To validate the single-node model used in the optimization model, the model was adjusted to reflect a 2018 power system scenario. This allowed for comparing the results from the model against historical data. Note that the Large Hydro power plant only includes KGU and KNB in this scenario, since KGL was not in operation in 2018.

The model was validated by comparing the simulated generation at the Large Hydro power plant against historical generation data for KGU and KNB in 2018. This is considered a good measure of the model's ability to replicate the generation dispatch in the system, since the Large Hydro plant is the only dispatchable power plant in the model.

The simulated average daily generation profile for the Large Hydro power plant compared to the recorded average daily generation in 2018, can be seen in Figure 20. On average, the difference between recorded and simulated generation was 11.3% of recorded output. Hence, the model is considered to replicate the generation output of the large hydropower plants in the system quite well on average.

As seen from Figure 20, the generation output in the simulations are, in general, lower than the recorded generation for the off-peak hours, but fits the recorded generation in the peak hours quite well. The main reasons for the observed difference between the simulations and the historical data, are considered the assumptions of monthly variations in RoR generation, instead of hourly variations, and constant output from thermal generators. In reality, the generation output from these sources vary to some degree on an hourly basis. Based on historical data, the nature of these variations are not considered to be governed by a market or any specific rules, and are hence hard to capture in a model. This is explained more thoroughly in [3].

The deviations between the model results and actual system operations are expected to increase when modeling the 2030 scenario. This is primarily because there is more uncertainty associated with the input data in a model representing a future scenario [3]. However, the single-node model was considered applicable for modeling the 2030 scenario, as it seems to capture the main features of the system dispatch.

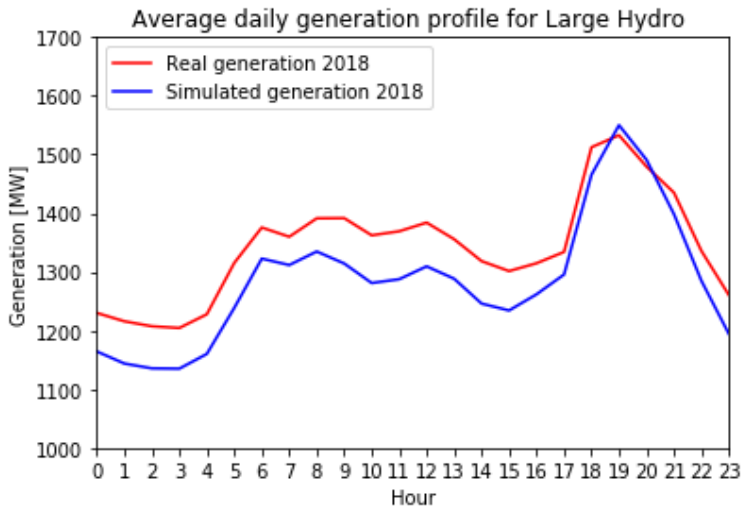


**Figure 20:** The daily average generation output from KGU+KNB in 2018 and simulated output from the Large Hydro power plant in the PowerGAMA model.

## 6.3 Portfolio simulation results

The portfolio optimization model was used for simulating operations for 121 different portfolios of solar PV and wind power capacity for each of the three climatic years. The results of the simulations are described in the following subsections, and a weighted average of the results was used to map out the optimal portfolio. Several of the plots are labeled with "Solar PV share of portfolio" on the y-axis, and the remaining share of the portfolio is hence wind power capacity, since no other VRE technologies were evaluated. A solar PV share of 1.0 thus corresponds to a portfolio consisting only of solar PV capacity, while a solar PV share of 0.0 corresponds to a portfolio consisting of only wind power capacity.

### 6.3.1 Average year results

The system cost for the evaluated portfolios in an average climatic year can be seen in Figure 21. The portfolios implying the lowest system costs can be seen in deep-green color, and the portfolios implying the highest system costs are colored in red. As shown in the plot, many portfolios imply approximately equal annual system costs between 587 and 600 million USD. The lowest system cost is obtained for a portfolio size of 2500 MW, with a solar PV share of 0.8. This corresponds to a portfolio consisting of 2000 MW solar PV capacity, and 500 MW wind power capacity.

The portfolios consisting of only solar PV capacity imply a substantially higher system cost than the portfolios with a 0.9 solar PV share. Only a small fraction of wind power in the portfolio can contribute to a considerably lower system cost. The main reason for the lower cost, is that the magnitude of load shedding occurring during night is reduced when having only a small share of wind power capacity in the system.

The portfolios implying the highest system costs, are the large portfolios with a high share of wind power capacity, seen upmost to the right in Figure 21. For these portfolios, the aggregated reservoir in the model is filled during the simulated year, leading to spillage of water. Adding a unit of VRE generation capacity adds low value to the system, because it mainly leads to less hydropower dispatch and following more spillage at the end of the year. This challenge is greater for portfolios with a high share of wind power, because wind power has almost twice as high capacity factor as solar PV.

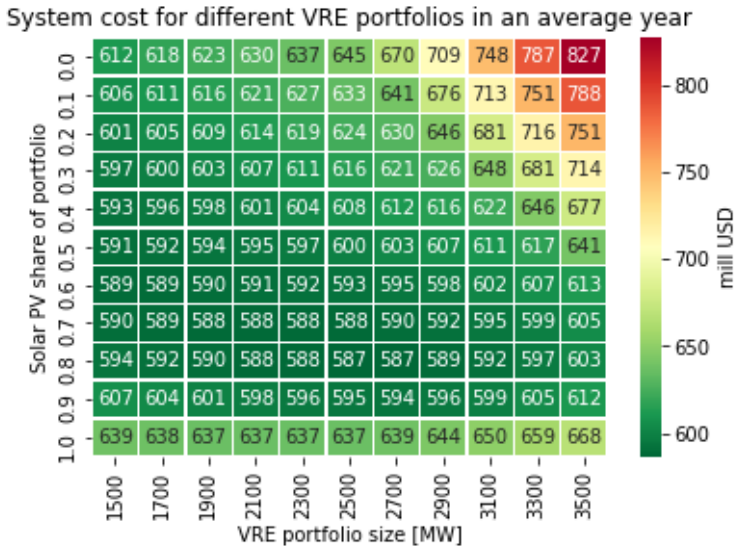


**Figure 21:** Total annual system cost for 121 different portfolios of solar PV and wind power capacity integrated into the system in an average year. The y-axis shows the solar PV share of the portfolio, implying that the upmost row corresponds to VRE-portfolios consisting of only wind power capacity (0.0 solar PV share), while the lowermost row corresponds to VRE-portfolios consisting of only solar PV capacity (1.0 solar PV share).

### 6.3.2 Dry year results

Figure 22 shows the system cost for the evaluated portfolios in a dry year. The lowest system cost for the dry year is obtained for a VRE portfolio of 2700 MW, with a 0.6 share of solar PV. This corresponds to a portfolio of 1620 MW of new solar PV capacity, and 1080 MW new wind power capacity. Compared to the results for the average year, some distinct differences can be seen.

First, the number of portfolios implying almost the same system cost is higher for the dry year. Figure 22 shows a high number of different portfolios implying a system cost in the range 755-765 million USD. The main reason for this result, is the use of a constant water value of 0.052 USD/kWh. This value is relatively close to the LCOE of solar PV and wind power capacity, described in Section 5. Adding an additional unit of VRE capacity will in general lead to lower dispatch from the Large Hydro power plant in the model, implying more water in the reservoir. If neither VRE curtailment, spilling from the reservoir or load shedding occurs, an additional unit of electricity generated from VRE translates directly to an additional unit of energy stored in the reservoir. Hence, the cost of adding a unit of VRE capacity is almost the same as the implied reduction in system cost due to higher reservoir levels. Spilling of water from the reservoir is not a challenge for most portfolios in the dry year, because of the low inflow to the reservoir. The result is a high number of portfolios with similar system costs. This proves the importance of a

correct valuation of water in the reservoir, and is further evaluated in Subsection 6.4.

Another difference from the results obtained for the average year, is higher system costs for all portfolios in the dry year. This is an intuitive result, since the inflow to the reservoir and RoR hydropower plants is lower, leading to less value added to the reservoir and less cheap generation from RoR hydropower plants. Also, the load shedding experienced in the system is higher for some portfolios in the dry year. However, the selected dry year (2003) had a higher wind power capacity factor than the selected average year (2011). Despite the lower output from RoR hydropower plants, the magnitude of load shedding was therefore lower in the dry year, compared to the average year, for all portfolios with a wind power capacity share of more than 30%. This proves the fact that wind power can be of high value in dry years. The value of wind power is reflected in the optimal portfolio for the dry year, consisting of 40% wind power, compared to the 20% wind power capacity share in the optimal portfolio for the average year.

As for the average year, the portfolios consisting of only solar PV capacity imply a substantially higher system cost than portfolios containing only a 10% fraction of wind power capacity. Increasing the VRE generation capacity in the system solely by building solar PV power plants seems to be a suboptimal solution.

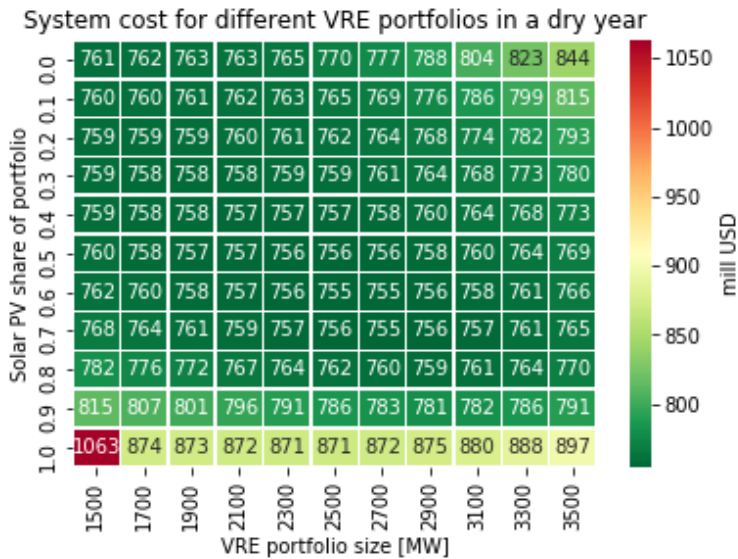


**Figure 22:** Total annual system cost for 121 different portfolios of solar PV and wind power capacity integrated into the system in a dry year. The y-axis shows the solar PV share of the portfolio, meaning that the upmost row corresponds to VRE-portfolios consisting of only wind power capacity (0.0 solar PV share), while the lowermost row corresponds to VRE-portfolios consisting of only solar PV capacity (1.0 solar PV share).



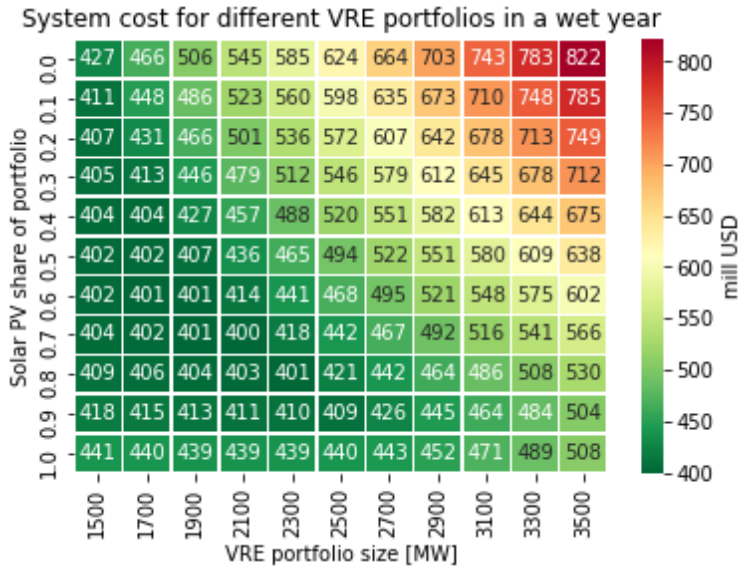
### 6.3.3 Wet year results

Figure 23 shows the system cost resulting from the different portfolios in a wet year. As seen in the figure, the lowest system cost is obtained for a VRE portfolio size of 2100 MW, with a solar PV share of 0.7. This corresponds to a portfolio of 1470 MW of solar PV, and 630 MW wind power capacity.

System costs are lower for all portfolios compared to the average and dry year, because of higher inflow to the reservoir and RoR hydropower plants. The cost of load shedding is also generally lower compared to the average and dry year, due to increased RoR hydropower generation. Nevertheless, the same trend of noticeably higher system cost for the portfolios consisting of only solar PV, compared to portfolios with a share of wind power, can still be seen.

The trend of high system costs for large portfolios with a high share of wind power capacity, seen for the average year, is even stronger for the wet year. With a higher inflow to the reservoir, the challenge of spilling water is greater for a larger fraction of the portfolios.

One of the main reasons for the observed spilling, is the assumption of an initial reservoir level of 75%. This is somewhat high compared to the reservoir level in the Kariba Dam, which makes up the majority of the aggregated reservoir in the model, in recent years [82]. In the sensitivity analyses in Subsection 6.4, an initial reservoir level of 30% is applied, which is more in line with the reservoir levels the last few years. Nevertheless, a 30% reservoir level is considered critically low, and assuming a higher reservoir level could be more relevant in a sustainable operated system in 2030. The 75% filling level applied in the base case, can therefore be viewed as a sustainable future scenario, while the 30% filling level models a scenario similar to the current water level.



**Figure 23:** Total annual system cost for 121 different portfolios of solar PV and wind power capacity integrated into the system in a wet year. The y-axis shows the solar PV share of the portfolio, meaning that the upmost row corresponds to VRE-portfolios consisting of only wind power capacity (0.0 solar PV share), while the lowermost row corresponds to VRE-portfolios consisting of only solar PV capacity (1.0 solar PV share).

### 6.3.4 Weighted average results

A weighted average result was obtained to find the economically optimal portfolio of new VRE capacity to be integrated into the system. As seen in Section 5, the dry year was assumed to represent the 15% driest years, the wet year was assumed to represent the 15% wettest years, and the average year was assumed to represent the 70% median years. By weighting the results obtained for each of the climatic years by the fraction of years they are assumed to represent, a weighted average result was obtained.

Figure 24 shows the weighted average system cost resulting from the evaluated portfolios. The lowest system cost is obtained for a VRE portfolio size of 2100 MW, and a solar PV share of 0.7. This corresponds to a portfolio of 1470 MW of solar PV, and 630 MW wind power capacity, which is also the optimal portfolio obtained for the wet year. Considering the fact that the optimal portfolio size is 2500 MW for an average year, and 2700 MW for a dry year, the weighted average result of 2100 MW might seem low. However, many portfolios imply almost similar system costs in the average/dry year. For the wet year, the differences in system costs are larger. The wet year result is hence tipping the weighted average result towards the 2100 MW portfolio, despite being weighted by a factor of only 15%.

Taking the above considerations into account, care should be taken when determining

an optimal portfolio of VRE to be integrated into the system. Spilling from hydropower reservoirs might not be a challenge in reality, because surplus energy can be exported to neighboring countries through interconnectors. Also, the use of a constant water value leads to a high number of portfolios having almost the same system cost in the dry/average year, as previously explained. Nevertheless, the results are interesting, because they indicate that being able to export or consume excess power could be of high importance, to avoid spilling.

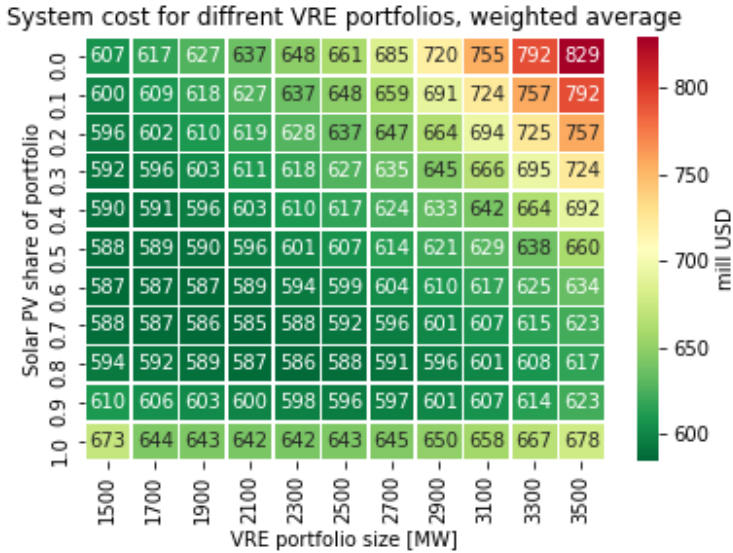


**Figure 24:** Weighted average system cost for the average, dry and wet year.

The optimal portfolios obtained for the three climatic years, and the optimal portfolio for the weighted average result can be seen in Table 15. Including the existing solar PV power plants, the optimal new VRE capacity implies a VRE penetration<sup>11</sup> of 37% in 2030.

As a reference, [11] finds a VRE penetration of 44%, consisting of 1376 MW solar PV and 1400 MW wind capacity, to be optimal in Zambia in a 2030 scenario. However, the authors identify the optimal portfolio as the portfolio minimizing the magnitude of load shedding and VRE curtailment, and the result is not directly comparable with the results obtained in this thesis. Still, some brief comments could be made.

The main difference between the optimal portfolio found in the two projects, is that the wind power capacity found in this thesis is lower than in [11]. When evaluating portfolios based on system cost, the higher LCOE of wind power plants results in a lower optimal capacity than when evaluating portfolios based on only technical parameters. In general, a portfolio proving to be optimal from a technical perspective could be suboptimal in an

<sup>11</sup>Installed VRE capacity as a fraction of total installed generation capacity in the system.

economic perspective, and vice versa. The following subsection aims to supplement the economic results with evaluations of technical impacts on power system operations from different VRE portfolios.

Climatic year	Optimal new solar PV capacity [MW]	Optimal new wind power capacity [MW]
Average year	2000	500
Dry year	1620	1080
Wet year	1470	630
Weighted average result	1470	630

**Table 15:** Economically optimal portfolios of new solar PV and wind power capacity for the three climatic years, and the weighted average result.

### 6.3.5 Impacts on system operations from different VRE portfolios

Evaluating the system costs resulting from the different portfolio combinations can inform about the potential economic benefit from implementing new VRE capacity. However, the impacts on system operations should also be considered when mapping out an optimal portfolio of new VRE capacity to be integrated into the system. In particular, the magnitude of load shedding, VRE curtailment, and the ramp rate required by the dispatchable hydropower plants in the system are interesting parameters.

#### Load shedding

If power plants are not able to meet the system load, load shedding is applied. Figure 25 shows the simulated generation dispatch and load shedding for three selected days in an average climatic year. The optimal portfolio in the weighted average result, consisting of 1470 MW solar PV and 630 MW wind power capacity, was used in the simulations. The purpose of the figure is to illustrate the relation between generation output and load shedding.

The figure shows a constant generation output from the thermal power plants and from the RoR hydropower plants (since the three days are within the same month). Wind power output is low during the whole time period, while the output from solar PV shows distinctive daily variations. Load shedding occurs at the load peaks for the two first days. An interesting observation is that the wind power output is low in the hours of load shedding. During the peak load the third day, the wind output is higher, and load shedding is not conducted. This illustrates how wind power generation during the afternoon peak could reduce the quantity of load shedding. As seen in the figure, the output from solar PV is zero during the afternoon peak, indicating that increasing the solar PV generation capacity in the system does not contribute to meeting the highest load peaks in the system.

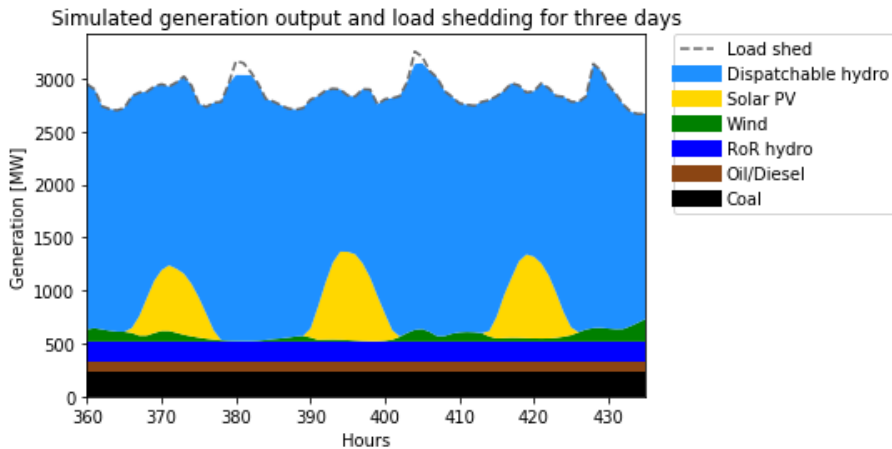


**Figure 25:** Simulated generation output and load shedding for three selected days in January (from hour 360 to hour 432). A VRE portfolio of 1470 MW solar PV and 630 MW wind power capacity in an average climatic year was used in the simulations.

The economic cost of load shedding is included in the system cost, but the magnitude of load shedding resulting from the different VRE portfolios is, nevertheless, an interesting parameter to evaluate. For the sake of simplicity, weighted average results for the three climatic years are presented, with the same weighting factors as used for the system costs.

Figure 26 shows the magnitude of load shedding in GWh for the evaluated portfolios. Load shedding is higher for the portfolios with a high share of solar PV, compared to portfolios with more wind capacity. As previously mentioned, this applies in particular for portfolios consisting only of solar PV. As seen in Subsection 6.1, wind generation increases on average in the afternoon. Having only a relatively small amount of wind power capacity in the system can therefore make up the difference between load shedding and normal operations during the afternoon load peak.

Another interesting observation is that load shedding occurs for all portfolios. This was found to be true also for each of the individual climatic years. For many of the portfolios, load shedding might be considered negligible in an economic perspective, but being able to operate the system without blackouts could be important from an operational standpoint. The optimal portfolio, with a size of 2100 MW and a 0.7 solar PV share, results in 12 GWh of load shedding, as seen in Figure 26. Increasing the share of wind power in the portfolio to e.g. 0.4 could be an option for reducing load shedding. This increases the system cost by only 0.68%, but decreases the load shedding by 33%.

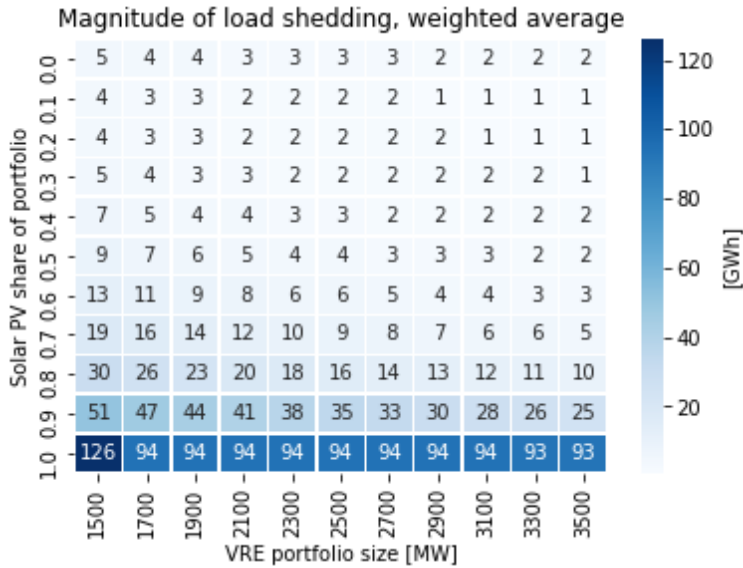


**Figure 26:** Load shedding as a weighted average of the three climatic years.

### **Curtailment of VRE and RoR hydropower**

If the power generated in the model exceeds the load, curtailment of solar PV, wind power and RoR hydropower plants will occur. Figure 27 shows the magnitude of curtailment in GWh for the evaluated portfolios, as a weighted average of the three climatic years. As expected, the magnitude of curtailment is highest for portfolios consisting of a large fraction of either solar PV or wind power, and lower for portfolios with a more equal share between the two technologies. This is because the risk of overgeneration in hours with either high wind speeds or high solar irradiation is higher when relying heavily on one of the two technologies. The highest magnitude of curtailment is seen for the 3500 MW pure wind portfolio. For this portfolio, the curtailed energy adds up to 1144 GWh (9.3% of generated electricity from wind power), which is high.

Comparing the load shedding and the VRE curtailment resulting from the different portfolios is interesting. The portfolios implying the lowest degree of load shedding, result in a relatively high degree of VRE curtailment. This result suggests that meeting the electricity demand growth only by new VRE capacity implies over dimensioning the VRE portfolio. Also, since load shedding is performed for all portfolios, adding dispatchable generation capacity should be done in addition to new VRE capacity. Building new hydropower plants with reservoirs could be an option to ensure that dispatchable generation capacity is high enough to meet the load peaks in the system.

Curtailment, however, does not seem like a significant challenge for most of the portfolios. For the optimal portfolio, no curtailment is performed. One of the main reasons for the relatively low magnitude of curtailment, is the assumed high degree of flexibility

of the Large Hydro power plant in the model. The ramp rate requirements and average daily generation output for the dispatchable hydropower plants in the system are discussed further below.

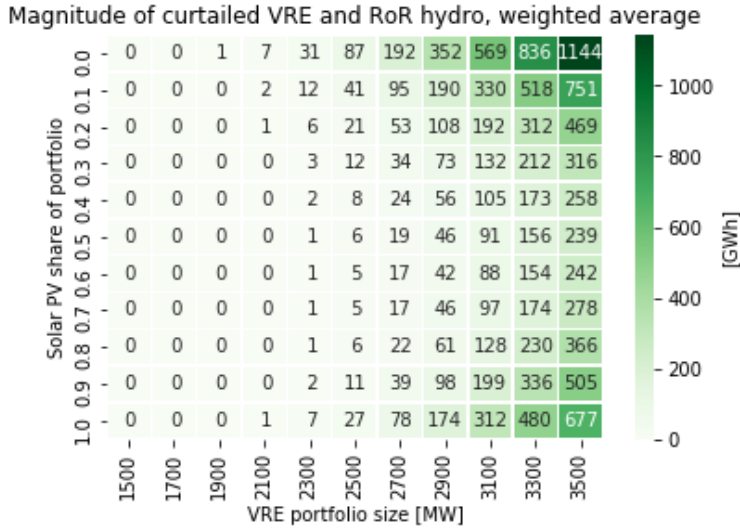


**Figure 27:** Curtailed VRE and RoR hydropower as a weighted average of the three climatic years.

### Hydropower dispatch

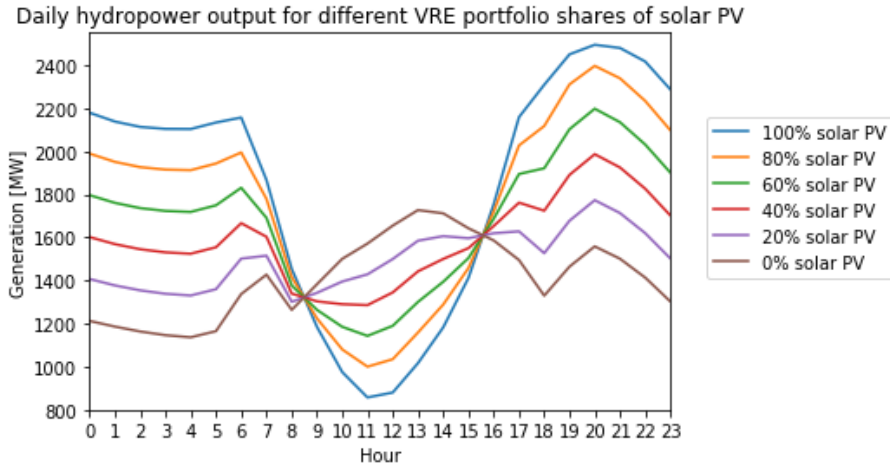
It is out of the scope of this thesis to assess the technical implications at hydropower plants from changed operations. Also, since the large dispatchable hydropower plants are aggregated in the model, the dispatch of each individual power plant is not captured. However, evaluating the cumulative output from the large hydropower plants can inform about the impacts on hydropower operations from different VRE portfolios.

Figure 28 shows the average daily dispatch of the Large Hydro power plant for different combinations of new solar PV and wind power capacity integrated into the system. A portfolio size of 2100 MW was applied. The dry climatic year was chosen for the comparison, since the generation from RoR hydropower plants is lower than for the wet and the average year, requiring a higher ramp rate for the dispatchable hydropower plants. A dry year is therefore considered most critical in terms of dispatchable hydropower operations. The two intersection points for all curves correspond to the two times during the day when the output from solar PV and wind power is the same on average per installed MW. This can be seen as the intersections between the solar PV and the wind power generation curves in the previously shown Figure 17.

As seen from Figure 28, the daily average hydropower dispatch resulting from a VRE portfolio consisting of 100% solar PV capacity varies between 860 MW and 2500 MW during the day. In addition to the large difference between minimum and maximum output, the solar PV portfolio results in a steep decrease in hydropower output in the morning

when the sun is rising, and a steep increase in the afternoon when the sun is setting and the load is increasing. This results in a shape of the curve similar to the previously mentioned "duck curve". A portfolio consisting of only wind power capacity (0% solar PV) results in a completely different hydropower dispatch. For this portfolio, the maximum generation output occurs just after noon, and the hydropower output is lowest during night.

Between these two extremes are the hydropower dispatch profiles resulting from portfolios with both solar PV and wind power capacity. Having wind power capacity in the VRE portfolio could decrease the difference between minimum and maximum output, and make the magnitude of required ramp rates lower. As an example, the three hydropower plants must increase generation with an average rate of 260 MW/hour in the afternoon with a 100% solar PV portfolio. For a portfolio with 60% solar PV and 40% wind power capacity, the rate is reduced to 125 MW/hour.



**Figure 28:** Simulated average daily generation output from the Large Hydro power plant in a dry year. A VRE portfolio size of 2100 MW was used in the simulations. 0% solar PV corresponds to a portfolio consisting of only wind power capacity, while 100% solar PV corresponds to a VRE portfolio with only solar PV. Note that the y-axis is starting at 800.

In addition to the average daily hydropower dispatch in a dry year, scenarios of more extreme days should be evaluated. Assessing whether or not the hydropower plants can physically handle the most extreme daily variations in generation output, is considered important. The assumptions of no ramp rate constraints, and the relatively low limit on minimum output from the Large Hydro power plant in the model, could potentially overestimate the aggregated flexibility of KGU, KGL and KNB. More detailed assessments should be made of the maximum degree of flexibility the three large hydropower plants could provide.

Furthermore, evaluations of other sources of flexibility, such as cycling of the thermal power plants and the Itzhi-Tezhi hydropower plant, should be conducted. The daily gener-



ation output from these plants were set to constant in the model, but they could potentially contribute with flexibility by varying generation to meet changes in net load. Short-term storage technologies, such as batteries, could also be a future option for smoothing out the daily variations in output from VRE, and particularly the output from solar PV plants.

However, all the mentioned flexibility options come with a potential cost, and the cost should be evaluated against the differences in system cost between portfolios. If e.g. the portfolio found optimal in the optimization model implies a high increase in cost of operating existing hydropower plants, selecting another portfolio could be optimal.

Also, the relation between the dispatch of the cascaded power plants KGU and KGL should be evaluated in more detail. In the model, it is assumed that the capacity of KGL is always available. In reality, the power plant depends on sufficient inflow from the KGU power plant upstream, due to the limited reservoir size of KGL. Evaluating this interrelationship is, however, out of the scope of this thesis, and is suggested as further work in Section 7.

## 6.4 Sensitivities

Simulating power system operations involves a large number of model parameters and assumptions, even when aggregating a relatively small system to one node, as done in this thesis. Conducting sensitivity analyses could inform about the impact of changes in important model parameters and assumptions. The optimization model results described so far will from now be called "the base case" to separate it from the results obtained in the sensitivity analyses.

To limit the scope of this thesis, sensitivity analyses were only conducted for the three model input parameters considered to be of highest importance for the results. Also, instead of re-running the heavy computational simulation several times (as often done in sensitivity analyses), only one plausible alternative to each of the three model parameters was evaluated. During the work with the thesis, the model parameters considered most critical for the results have been identified as the valuation of water in the reservoir (water values), the projected 2030 system load and the initial filling level of the Large Hydro power plant reservoir.

### 6.4.1 Dynamic water values

In the base case, the  $\text{ReservoirFilling}_{\text{cost}}$  was calculated as the difference in stored energy between the beginning and the end of the simulation period, multiplied by the constant water value. As described, the use of a constant water value resulted in a high number of portfolios implying close to equal system costs. When using a dynamic water value, the  $\text{ReservoirFilling}_{\text{cost}}$  was calculated as the sum of the net change in reservoir level multiplied by the water value for each time step, as explained in Section 3.

Figure 29 shows the weighted average system cost for the three climatic years when using dynamic water values. Compared to the weighted results obtained in the base case (Figure 24), the main difference is that small portfolios with a high solar PV share imply a higher system cost, relative to the other portfolios. This is due to the fact that reservoir filling decreases during the simulation period for these portfolios. Lower reservoir levels imply higher water values (when using dynamic water values), resulting in a higher system cost for the small portfolios than in the base case.

Another interesting difference from the base case, is that the system cost is in general higher for all portfolios. This is because lower reservoir levels imply a higher cost than in the base case, while higher reservoir levels imply a smaller negative cost (benefit) compared to the base case.

A deep-green area can be seen stretching from the upper left corner to the lower right corner of the figure. These are the portfolios resulting in the lowest system costs. For smaller portfolio sizes, a high fraction of wind power provides low system costs, while a higher fraction of solar PV is optimal for the larger portfolios. The portfolios resulting in low system costs generally imply small changes in net filling of the reservoir during the simulation period. Using a dynamic valuation of water thus seems to reward portfolios

resulting in a stable reservoir level around the initial filling level of 75%. For the Zambian system, using dynamic water values could be advantageous compared to using a constant water value. This is because the dynamic water value method puts a higher cost on low reservoir levels. Low filling levels have proven devastating to the Zambian system in dry years, and portfolios resulting in critically low water levels should therefore imply a high system cost.

A portfolio size of 2700 MW and a solar PV share of 0.7 implies the lowest system cost. This corresponds to a portfolio of 1890 MW solar PV and 810 MW wind power capacity. The portfolio size of 2700 MW is higher than the one obtained in the base case (2100 MW), while the distribution between solar PV and wind power capacity is the same.

Similar plots as the one seen in Figure 29 for each of the three climatic years can be seen in Appendix B.

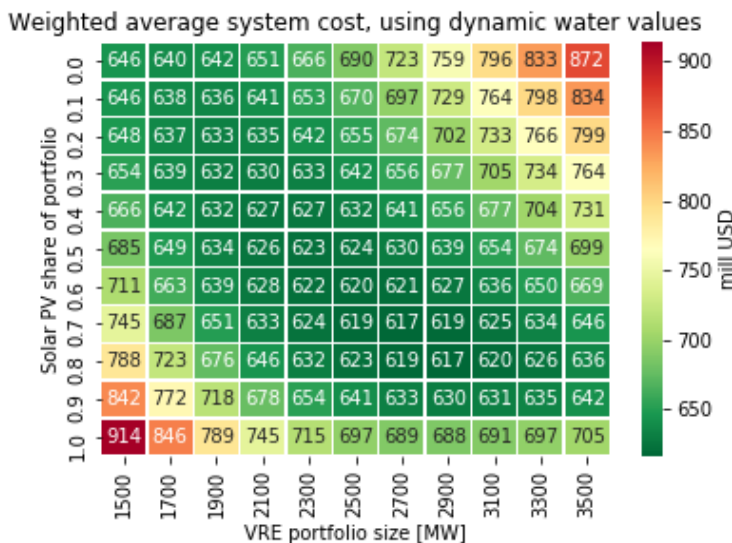


**Figure 29:** Weighted average system cost for different VRE portfolios, when using dynamic water values.

#### 6.4.2 Projected 2030 system load

Predicting future system load can be challenging in developing countries. Several factors such as economic development, increasing electrification rates and development in the use of electricity in households and industry can contribute to the future system load. Previous projections of total electricity demand performed in [59] seem to have overestimated the development in system load. The projected electricity demand used in the base case in this thesis is also relatively high. To evaluate the impacts of a potentially lower electricity demand, an alternative load profile was used in the sensitivity analysis, and it is from now

referred to as the "low load profile".

The low load profile was based on the system demand profile of 2014, but scaled to an average load of 2413 MW, which is 15% lower than the load profile used in the base case. 2014 is the second most recent year not impacted by load shedding, and was therefore chosen as an alternative to the 2018 load profile. Both the hourly profile and the average load were hence different than in the base case. An overview of the differences between the two load profiles can be seen in Table 16.

	<b>Base case</b>	<b>Low load</b>
Historical load profile [year]	2018	2014
Average load [MW]	2839	2413
Max load [MW]	3489	3250
Annual electricity demand [GWh]	24870	21137

**Table 16:** The system load used in the base case and in the sensitivity analysis.

Simulations with the low load profile were run for the three climatic years. All inputs except for the load were the same as in the base case. The weighted average result for the three climatic years can be seen in Figure 30. The x-axis is starting at 500 MW instead of 1500 MW, and the range of portfolios shown are hence not the same as in the base case. This is because the optimal portfolio with low load proved to have a smaller size than the optimal portfolio in the base case, and the range of evaluated portfolios was therefore adjusted. The system costs resulting from the different portfolios in each of the climatic years can be seen in Appendix C.

A portfolio size of only 700 MW and a solar PV share of 1.0 provides the lowest system cost with the low load. Compared to the base case, this is a highly interesting finding for several reasons. The optimal portfolio size is substantially lower compared to the optimal portfolio size of 2100 MW found in the base case. A 15% lower load hence implies a decrease of 66.7% in the optimal VRE portfolio size. Also, the optimal portfolio contains only solar PV capacity, and no wind power.

One of the main reasons for the differences between the base case and the low load case, is that load shedding is only a marginal contributor to system cost for most portfolios in the low load case. Having wind power capacity in the system is therefore less valuable compared to the base case where wind power reduces the quantity of load shedding in the afternoon and night. Having a smaller VRE portfolio size will also be beneficial when load shedding is not an important driver of system cost.

Increased spilling from the reservoir in the low load case is also an important reason for the observed results. The spilling is substantial not only for larger portfolios with a high wind power capacity share, but also for smaller portfolios. In the wet year, nearly all VRE portfolios result in a full reservoir in the model, leading to spilling. This topic is further discussed in the following subsection.

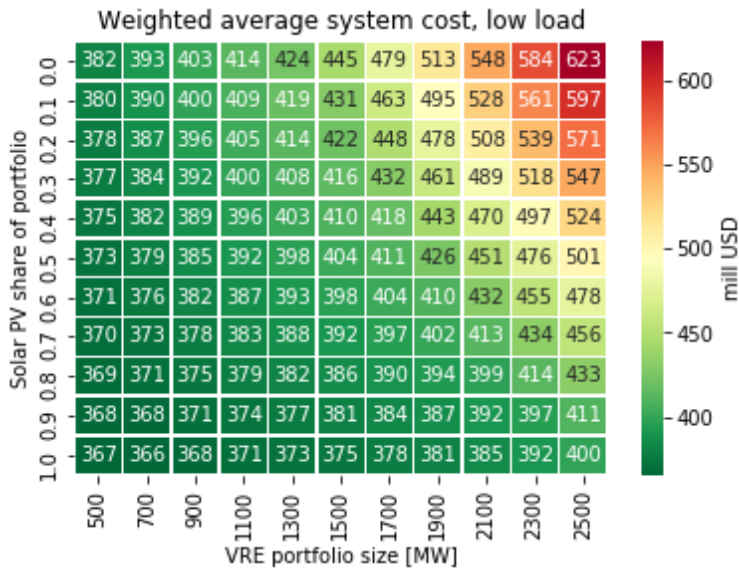


**Figure 30:** Weighted average system cost for different VRE portfolios, when using the low load profile in the simulations. Note that the x-axis is starting at 500 MW instead of 1500 MW used in the previous plots.

### 6.4.3 Initial reservoir filling levels

As seen both in the base case and in the low load case, spilling from the aggregated Large Hydro reservoir occurs for several portfolios. The assumption of an initial reservoir filling level of 75% is an important reason for this. As previously mentioned, this represents a high filling level for January from a historical perspective.

To evaluate the consequences of a lower initial reservoir level, simulations were performed with a starting level of 30%. Figure 31 shows the weighted average system cost resulting from different VRE portfolios when using a low initial reservoir level. A portfolio size of 3100 MW and a solar PV share of 0.7 provides the lowest system cost. This corresponds to a VRE portfolio that is 1000 MW larger than in the base case, but with the same solar PV share. The deviation in portfolio size between the result obtained in the base case and in the low initial reservoir level case, proves that the initial reservoir level is an important parameter when modeling the system.

The difference in optimal portfolio size can be explained by the most significant drivers of system cost in the two cases. For the base case, spilling from the reservoir for the larger portfolios in the wet year leads to large differences in system cost. However, the difference in system cost between many of the portfolios is relatively small in the average year and the dry year. With the low initial reservoir level, the situation is completely opposite. Emptying the reservoir for smaller portfolios in the dry year implies large cost differences. For the average year and the wet year, the cost differences are however relatively small

between many of the portfolios. The initial reservoir level is hence determining if spilling of water or emptying the reservoir is driving the weighted average system cost.

An interesting observation was made by evaluating the system cost in the low initial reservoir level case for each of the three climatic years (shown in Appendix D). For each climatic year, the optimal portfolio size is only 200 MW larger than the same climatic year in the base case. For the low initial reservoir level case, the size of the optimal portfolio in the weighted average is thus larger than the optimal portfolio size for each of the climatic years; 2300 MW (wet year), 2700 MW (average year) and 2900 MW (dry year). This might seem counterintuitive, but is possible since the portfolios are defined by the distribution of capacity between each technology, in addition to size, implying a two-dimensional problem. In the weighted average, a combination of solar PV and wind power capacity that is not optimal in any of the individual climatic years could provide the lowest cost. This portfolio could have a different size, and/or a different distribution between each technology than any of the portfolios found optimal in each climatic year.

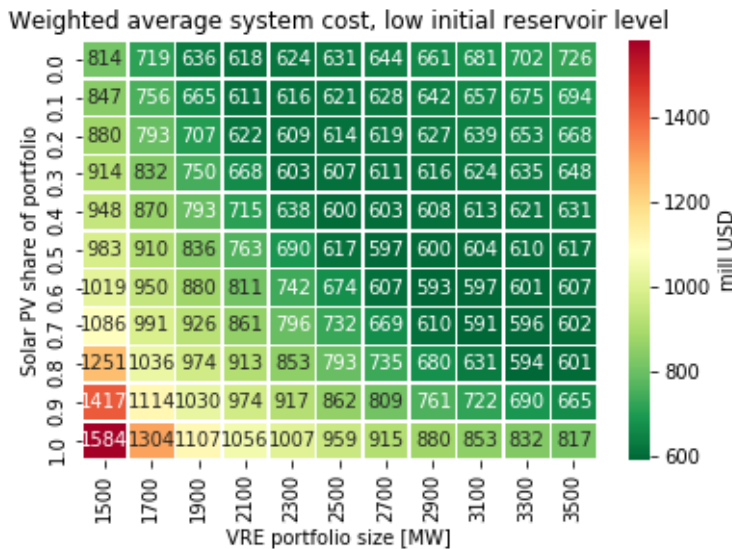


**Figure 31:** Weighted average system cost for different VRE portfolios when having an initial reservoir filling level of 30%.

The results from the sensitivity analyses prove that the portfolio optimization model is highly sensitive to several model parameters. The economic and technical results should be evaluated together, and the results in the base case must be seen in relation to the results from the sensitivity analyses. In the following subsection, an evaluation of potential congestion in the power grid, resulting from integrating the optimal portfolio of VRE capacity, is conducted. Here, the optimal portfolio is referring to the portfolio providing the lowest weighted average cost in the base case.

## 6.5 Grid model simulation results

Hourly operations were simulated in the grid model for an average climatic year. The average utilization of all lines in the model was evaluated. This corresponds to the average load flow in each line as a fraction of the maximum transmission capacity.

Because the line transfer capacities represent constraints in the PowerGAMA model, the load flow in each line will never exceed the capacity. Having a line utilization of 100% corresponds to having transfer capacity as a binding constraint. To evaluate which lines in the system that constrains the power flows, and are in danger of becoming overloaded, the number of hours above 90% utilization was counted for each line. A line with zero hours above 90% utilization (from now referred to as high capacity hours) is never close to overloading. Similarly, a line with many high capacity hours will most likely constrain system operations and/or become overloaded in the real system.

69 out of the 72 lines in the model had an average utilization below 60%, and no high capacity hours. This result indicates that the power flow in most lines stays well within the transfer capacity limits for all hours throughout the year. The three lines having a higher utilization, and also a substantial amount of capacity hours, are all located in the Lusaka area, and are marked with red in Figure 32.

The overloading of the two 330 kV lines between Kafue Gorge and Leopards Hill can be explained by the location of the aggregated Large Hydro power plant at the node Kafue Gorge in the model. As mentioned, KGU, KGL and KNB are in reality located at three different nodes. The high utilization of the lines between Kafue Gorge and Leopards Hill is therefore considered a consequence of the model simplifications, and is assumed not to be a challenge in the real system. This assumption was tested by adding two lines between Kafue Gorge and Leopards Hill in the model. The two lines correspond to the transfer capacity between Kariba North and Leopards Hill in the real system, which withdraws power from KNB. With these two lines integrated into the model, no high capacity hours were seen for the lines between Kafue Gorge and Leopards Hill.

The overloading of the 132 kV line between Roma and Leopards Hill was, however, not considered a result of the model simplifications. Previous studies suggest that overloading of the grid in the Lusaka area is likely to occur with the expected growth in demand. In [20], the Leopards Hill-Roma line is found to be the only line (at the three highest voltage levels) that is overloaded in a scenario with 120 MW new solar PV capacity in the system. The paper argues that the overloading is not due to the integration of solar PV capacity, but rather due to the load increase in the Lusaka area. Similarly, [11] finds that the 132 kV grid in the Lusaka area is likely to become overloaded due to demand growth in the short term. The paper argues that a few network reinforcements are needed in the Zambian system, but that no critical overloads occur from integrating 2776 MW of new VRE capacity within 2030.

None of the observed overloadings were therefore considered to be caused by the integration of the optimal portfolio of new VRE capacity in the system. Also, the similarity

between the results obtained in the grid model and the existing literature suggests that the model captures the main characteristics of the load flows in the system.

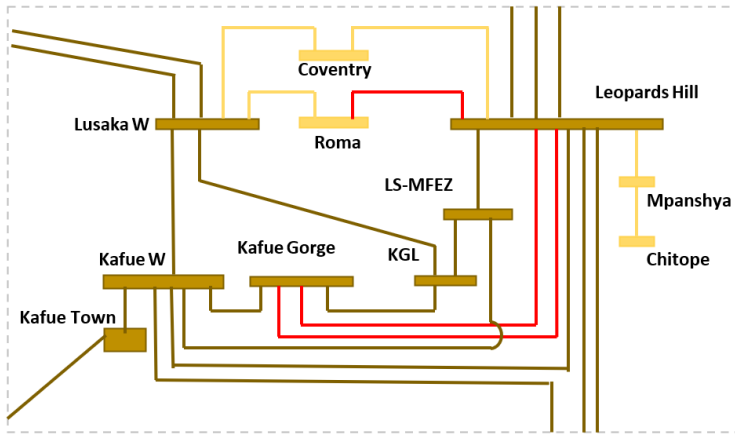


**Figure 32:** The overloaded lines in the Lusaka area market with red color.

In total, the results from the grid model indicate that the optimal VRE capacity can be integrated into the power system without overloading the current transmission grid. Having an uncongested transmission grid also implies that the use of a single-node model in the portfolio optimization likely does not lead to any large errors. Because power can flow relatively unconstrained, modeling the grid as a copper plate seems to be a fair simplification for the purpose of the study. In addition, not including the cost of potential grid upgrades following VRE integration in the system cost, is considered a valid assumption. This is because the need for large transmission system upgrades seems to be limited.

Care should nevertheless be taken when interpreting this result. The grid model represents a relatively distributed VRE integration scenario, and the new capacity is distributed between a total of 14 nodes. Most of these nodes are also located close to Lusaka and the Copperbelt area, where the grid is in general robust. If large new VRE power plants are constructed in e.g. the northeastern part of the country, overloading could occur due to the weaker electricity grid in that part of the system.

The practical implementation of the new power plants is also a factor that is not considered in the model. Both solar PV and wind power plants require a relatively large amount of available land. Experiences from other countries show that particularly wind power could be the subject of a changing public opinion, and become unpopular among the population [93]. In densely populated areas, the limited amount of available land could also be challenging. Therefore, the locations selected for new power plants in the grid model could in reality be inadequate.

Further, the model only considers the three highest voltage levels in the system. If new VRE capacity is connected at lower voltage levels, congestion could occur in the under-



lying grid without being captured in the model. Implementing distributed VRE in the distribution grid could have benefits such as proximity to load with following less losses, and potential reduced investments in transmission infrastructure. Evaluations of different scenarios of centralized versus distributed implementation of VRE capacity should therefore be conducted.

Despite the simplifications made, and the limited scope of the analyses conducted in the grid model, the findings are considered relevant to supplement the results obtained in the optimization model. As discussed, the findings are also supported by current literature.

## 6.6 Potential sources of error

Modeling the 2030 scenario implies using projections for the future development of several parameters. This is considered the potentially largest source of error in this thesis, and the most important assumptions regarding the modeled scenario are discussed below. Sources of error related to the use of the PowerGAMA software are also discussed.

As seen from the results, the optimization model proved to be highly sensitive to the projected system load. A decrease in average load of only 15% shifted the results drastically. The load projection used in this thesis is considered the currently best available projection, but the reader should be aware that the portfolio optimization results could change if load projections are updated in the future.

If new hydropower or thermal power plants not included in the scenario are commissioned before 2030, the results obtained in this thesis could potentially be invalid. This particularly applies if one of the large hydropower projects Batoka Gorge or Devil's Gorge are commissioned. A smaller optimal VRE portfolio would most likely be the result.

Assuming no interconnectors to neighboring countries simplifies the model of the system, but also affects the results. The spilling from full reservoirs and curtailment of VRE generation would most likely not be experienced in an interconnected system, where excess power could be exported. Similarly, load shedding would most likely be reduced when assuming the possibility of importing power during hours with low output from VRE power plants. Nevertheless, the assumption of no interconnectors to neighboring countries can be justified because uncertainty is related to the future export/import market. Also, it provides a good basis for evaluating strategies to make Zambia self-sufficient with electricity. Evaluating an interconnected scenario with export/import could, however, result in a more realistic model of the future system. In [11], the authors find that both the optimal solar PV capacity and the optimal wind power capacity is substantially higher when interconnections with neighboring countries are included. This is mainly because the revenue from exporting power makes increased generation capacity profitable.

Changes in the cost projections for new solar PV and wind power capacity could also change the results. In the model, a tipping point would be the static water value applied in the base case. If the LCOE of new solar PV or wind power capacity reaches lower levels than this value, installing more of that technology would be optimal, as long as spilling from the reservoir does not occur. In the real interconnected system, a similar tipping point could be the electricity price realized from VRE technologies in the SAPP electricity market. If the LCOE of new capacity is lower than this price, installing more VRE capacity would be beneficial.

Weighting the results from different climatic years to obtain an average result could imply error. Uncertainty is related to the fraction of years each of the chosen climatic years actually do represent. This could lead to inaccurate weighting factors. Also, the inflow to reservoirs depends on other factors in addition to precipitation. Modeling the variations in inflow between the climatic years only based on the variations in precipitation could lead

to errors in the modeled variations.

### **6.6.1 Sources of error from modeling the system in PowerGAMA**

Since the PowerGAMA software was used in both the portfolio optimization model, and in the grid model, evaluating the potential sources of error from modeling the system in PowerGAMA is relevant.

As mentioned in the single-node model validation in Subsection 6.2, the assumption of a constant generation output from the thermal generators, and only monthly variations in the output from RoR hydropower plants is considered a potential source of error. In reality, the thermal generators and the Itzhi-Tezhi power plant are likely to vary the daily dispatch to some degree. Increased cycling at these plants could decrease the daily variations in dispatch from the large hydropower plants, and thus enable higher penetration of VRE in the system.

Aggregating the KGU, KGL and KNB power plants was necessary to obtain a proper model of the dispatchable hydropower plants, but could imply sources of error. As seen in the grid model, the aggregation of the power plants at a single node resulted in overloaded lines. In addition, the aggregation does not capture the relation between inflow, dispatch and reservoir level for each of the three plants.

Since the PowerGAMA software does not allow for modeling upward/downward regulating reserves, this was done by setting static upper/lower generation limits for the Large Hydro power plant. This is considered a simplified model of the reserve requirements, since it does not allocate reserves between the upper/lower generation limit. It was therefore assumed that sufficient reserves can be allocated for all levels of generation between these limits. This is a simplification due to the minimum generation output requirement for each individual generator in the real system.

Assuming an availability of 100% for all power plants is another assumption in PowerGAMA. This is a simplification of the real system where most generators will have some time out of operation due to faults and/or scheduled maintenance. Analyzing the impacts of planned/unplanned outages of generators should therefore be conducted. Also, fault analyses, contingency analyses and stability analyses are necessary. These assessments should include evaluations of sub-hourly fluctuations in output from VRE plants, which are not captured in the model.

Despite the simplifications made when modeling the system in PowerGAMA, the models built in the software are considered well suited for replicating the main features of the system. In particular, the coupling in time of reservoirs allows for modeling hydropower-dominated systems. Compared to the potential errors following the 2030 scenario projections, the errors following the modeling of the system in PowerGAMA are considered relatively small. However, more detailed analyses of e.g. hydropower operations and power system stability following a renewable energy integration should be conducted.

## 7 Conclusion

This thesis presents the methodology used and the results obtained from answering the question; *What is the optimal portfolio of new solar PV and wind power capacity to be integrated into the Zambian power system within 2030?*

The optimal VRE portfolio consists of 1470 MW (70%) solar PV and 630 MW (30%) wind power capacity in the base case. This corresponds to a VRE share of 37% of total system generation capacity. When assuming a dynamic valuation of water stored in reservoirs or a lower initial reservoir level, the optimal portfolio size changes to 2700 MW and 3100 MW, respectively. However, the distribution between solar PV and wind power capacity remains at 70/30, suggesting that this could be the optimal distribution of solar PV and wind power capacity. Assuming a lower system load drastically changes the result to a smaller portfolio of 700 MW solar PV, and no wind power capacity.

The optimal portfolio of VRE is considered the single most important result in this thesis. Nevertheless, this result should be seen in relation to the other results, which can be summarized as follows:

- The annual electricity output from solar PV and wind power is relatively stable between years, compared to the inflow to hydropower plants. Also, the generation from VRE is negatively correlated with precipitation. This implies that the output from solar PV and wind power plants is higher in dry years. Literature suggests that future climate change could reduce water availability, but that a decrease in solar irradiation and wind speeds is more unlikely. On a monthly basis, the VRE generation output is highest in the dry season. The sum of these findings demonstrate that diversifying the generation portfolio with VRE could increase energy security in Zambia.
- Meeting the expected growth in electricity demand entirely by implementing new VRE capacity, does not seem like an optimal solution. Load shedding occurs for all portfolios included in this thesis, and for the portfolios resulting in the lowest degree of load shedding, substantial curtailment of VRE capacity is seen. Therefore, increasing the dispatchable generation capacity in the system in parallel with the VRE integration could be necessary.
- Integrating wind power capacity could reduce load shedding and decrease the magnitude of hydropower ramping. On average, the wind power output increases in the afternoon, and this corresponds well with the afternoon load peak. Wind power could thus benefit the system from both an economic and a technical perspective, despite having a higher LCOE than solar PV.
- The current electricity grid is considered suited for integrating the optimal portfolio of VRE, given the assumed distribution of new power plants in the grid. Therefore, the flexibility of existing hydropower plants is considered the most critical factor when integrating renewable energy into the system, from a technical perspective.

## 7.1 Scope of future work

The most important topic to evaluate further, is considered the impact on each of the dispatchable hydropower plants from increased VRE penetration in the system. An assessment of the potential increased wear and tear on the hydropower plants should be conducted. Studying this topic in relation with the reserve requirements, and the system stability, could be interesting. Uncertainty is related to how much VRE capacity that can actually be integrated into the system from a technical perspective, and this relies heavily upon how flexible the hydropower plants can be operated. Also, the hydrological interaction between the cascaded reservoirs belonging to KGU and KGL should be assessed.

Translating the findings in this thesis, and current literature, into a renewable energy integration strategy for Zambia, is another relevant topic for future work. Creating a timeline that secures that power plants can meet the expected increase in demand, is considered important. This should include an evaluation of the need for increased dispatchable generation capacity in addition to new VRE capacity. Also, more detailed grid studies should be conducted to better understand the impact on the transmission system from new power plants.

The sensitivity analyses proved that the optimization model applied in this project is highly sensitive to several input parameters. Further studies of these parameters could therefore be useful. In particular, projections for future system load and studies of the valuation of water in reservoirs, could be interesting. Extending the model to include neighboring countries, could also be an option for future work. The optimal portfolio could then be found as the one minimizing system cost with imports/exports to neighboring countries included in the model.

---

## References

- [1] Unites Nations, *Affordable and clean energy: Why it matters*, 2020. [Online]. Available: %7Bhttps://www.un.org/sustainabledevelopment/wp-content/uploads/2016/08/7\_Why-It-Matters-2020.pdf%7D.
- [2] J. Corfee-Morlot, P. Parks, O. James, and F. Ayeni, “Achieving clean energy access in sub-Saharan Africa,” OECD, Paris, FR, Tech. Rep., 2018.
- [3] L. F. Habostad, “Building a framework for evaluating the impacts on power system operations from increased VRE penetration in Zambia,” Specialization project report, Norwegian University of Science and Technology, Trondheim, NO, Dec. 2020.
- [4] World Data Lab, *World Poverty Clock*, 2018. [Online]. Available: <https://worldpoverty.io/map>.
- [5] The World Bank Group, *Access to electricity, Zambia*, 2018. [Online]. Available: <https://data.worldbank.org/indicator/EG.ELC.ACCS.ZS?locations=ZM>.
- [6] G. Alfred Mwila *et al.*, “Impact of load shedding on small scale enterprises,” Energy Regulation Board, Lusaka, ZM, Tech. Rep., 2017.
- [7] R. Ngoma, A. Tambatamba, B. Oyoo, D. Mulongoti, B. Kumwenda, and H. Louie, “How households adapted their energy use during the Zambian energy crisis,” *Energy for Sustainable Development*, vol. 44, pp. 125–138, 2018.
- [8] Maamba Colliers Limited, *Power Generation*. [Online]. Available: %7Bhttp://maambacoal.com/power.htm%7D.
- [9] IEA (2019), “Renewables 2019,” IEA, Paris, FR, Tech. Rep., 2019.
- [10] A. Mwila *et al.*, “Energy Sector Report 2019,” Energy Regulation Board, Lusaka, ZM, Tech. Rep., 2019.
- [11] A. Prudenzi, A. Venturini, F. Begnis, G. Molino, and M. Armiento, “Integration of variable renewable energy sources in the national electric system of Zambia,” Res4Africa Foundation, Rome, IT, Tech. Rep., 2020.
- [12] Bloomberg Green, *Solar and Wind Cheapest Sources of Power in Most of the World*, 2020. [Online]. Available: %7Bhttps://www.bloomberg.com/news/articles/2020-04-28/solar-and-wind-cheapest-sources-of-power-in-most-of-the-world?sref=Oz9Q3OZU%7D.
- [13] E. G. Hertwich *et al.*, “Integrated life-cycle assessment of electricity-supply scenarios confirms global environmental benefit of low-carbon technologies,” *Proceedings of the National Academy of Sciences of the United States of America*, vol. 112, pp. 6277–6282, 2015.
- [14] H. G. Svendsen, *PowerGAMA User guide (v1.1)*, SINTEF, Trondheim, NO, 2017.
- [15] I. Graabak, S. Jaehnert, M. Korpås, and B. Mo, “Norway as a battery for the future European power system-impacts on the hydropower system,” *Energies*, vol. 10, pp. 1–25, 2017.

- 
- [16] B. Kumwenda, W. Mwakw, D. Mulongoti, and H. Louie, "Integration of solar energy into the Zambia power grid considering ramp rate constraints," *Proceedings - 2017 IEEE PES-IAS PowerAfrica Conference*, pp. 254–259, 2017.
- [17] M. McPherson, M. Ismail, D. Hoornweg, and M. Metcalfe, "Planning for variable renewable energy and electric vehicle integration under varying degrees of decentralization: A case study in Lusaka, Zambia," *Energy*, vol. 151, pp. 332–346, 2018.
- [18] IRENA, "Targeting Residential Electricity Subsidies in Zambia," International Renewable Energy Agency (IRENA), Abu Dhabi, UAE, Tech. Rep., 2013.
- [19] C. Lanfranconi, A. Renzulli, and D. Paladini, "Enhancing the renewable energy transition in Zambia," Res4Africa, Rome, IT, Tech. Rep. November, 2018.
- [20] L. Kalemba, "Cumulative Impact Studies - Integration of 100-120 MW Solar PV projects into the Zambian Grid," Multiconsult Norge AS, Oslo, NO, Tech. Rep., 2019.
- [21] D. Nugent and B. K. Sovacool, "Assessing the lifecycle greenhouse gas emissions from solar PV and wind energy: A critical meta-survey," *Energy Policy*, vol. 65, pp. 229–244, 2014.
- [22] IRENA, "Renewable Power Generation Costs in 2019," International Renewable Energy Agency (IRENA), Abu Dhabi, UAE, Tech. Rep., 2020.
- [23] J. Schmidt, R. Cancelli, and A. O. Pereira, "The role of wind power and solar PV in reducing risks in the Brazilian hydro-thermal power system," *Energy*, vol. 115, pp. 1748–1757, 2016.
- [24] R. Spalding-Fecher, B. Joyce, and H. Winkler, "Climate change and hydropower in the Southern African Power Pool and Zambezi River Basin: System-wide impacts and policy implications," *Energy Policy*, vol. 103, pp. 84–97, 2017.
- [25] D. Conway, C. Dalin, W. A. Landman, and T. J. Osborn, "Hydropower plans in eastern and southern Africa increase risk of concurrent climate-related electricity supply disruption," *Nature Energy*, vol. 2, pp. 946–953, 2017.
- [26] B. H. Hamududu and H. Ngoma, "Impacts of Climate Change on Water Availability in Zambia: Implications for Irrigation Development," Indaba Agricultural Policy Research Institute (IAPRI), Lusaka, ZM, Tech. Rep., 2018.
- [27] G. Falchetta, D. E. Gernaat, J. Hunt, and S. Sterl, "Hydropower dependency and climate change in sub-Saharan Africa: A nexus framework and evidence-based review," *Journal of Cleaner Production*, vol. 231, pp. 1399–1417, 2019.
- [28] C. Fant, A. Schlosser, and K. Strzepek, "The impact of climate change on wind and solar resources in Southern Africa," *Applied Energy*, vol. 161, pp. 556–564, 2016.
- [29] W. Sawadogo *et al.*, "Current and future potential of solar and wind energy over Africa using the RegCM4 CORDEX-CORE ensemble," *Climate Dynamics*, pp. 1–26, 2020.
- [30] B. Kroposki, "Integrating high levels of variable renewable energy into electric power systems," *Journal of Modern Power Systems and Clean Energy*, vol. 5, pp. 831–837, 2017.
-

- 
- [31] G. Magdy, G. Shabib, A. A. Elbaset, and Y. Mitani, "Renewable power systems dynamic security using a new coordination of frequency control strategy based on virtual synchronous generator and digital frequency protection," *International Journal of Electrical Power and Energy Systems*, vol. 109, pp. 351–368, 2019.
- [32] K. Schaps and V. Eckert, *Europe's storms send power prices plummeting to negative*, 2014. [Online]. Available: <https://www.reuters.com/article/instant-article/idINBREA080S120140109>.
- [33] M. Emmanuel, K. Doubleday, B. Cakir, M. Marković, and B. M. Hodge, "A review of power system planning and operational models for flexibility assessment in high solar energy penetration scenarios," *Solar Energy*, vol. 210, 2020.
- [34] M. Hummon *et al.*, "Variability of Photovoltaic Power in the State of Gujarat Using High Resolution Solar Data," NREL, Golden, US, Tech. Rep., 2014.
- [35] California ISO, "Energy and environmental goals drive change," CAISO, Folsom, US, Tech. Rep., 2016.
- [36] J. A. Dowling *et al.*, "Role of Long-Duration Energy Storage in Variable Renewable Electricity Systems," *Joule*, vol. 4, pp. 1907–1928, 2020.
- [37] M. S. Ziegler, J. M. Mueller, G. D. Pereira, J. Song, M. Ferrara, Y. M. Chiang, and J. E. Trancik, "Storage Requirements and Costs of Shaping Renewable Energy Toward Grid Decarbonization," *Joule*, vol. 3, pp. 2134–2153, 2019.
- [38] L. Gaudard and F. Romerio, "The future of hydropower in Europe: Interconnecting climate, markets and policies," *Environmental Science and Policy*, vol. 37, pp. 172–181, 2014.
- [39] I. Graabak, M. Korpås, S. Jaehnert, and M. Belsnes, "Balancing future variable wind and solar power production in Central-West Europe with Norwegian hydropower," *Energy*, vol. 168, pp. 870–882, 2019.
- [40] Y. Gebretsadik, C. Fant, K. Strzepek, and C. Arndt, "Optimized reservoir operation model of regional wind and hydro power integration case study: Zambezi basin and South Africa," *Applied Energy*, vol. 161, pp. 574–582, 2016.
- [41] P. March, "Flexible Operation of Hydropower Plants," Electric Power Research Institute (EPRI), Palo Alto, US, Tech. Rep. June, 2017.
- [42] U. Seidel, C. Mende, B. Hübner, W. Weber, and A. Otto, "Dynamic loads in Francis runners and their impact on fatigue life," *IOP Conference Series: Earth and Environmental Science*, vol. 22, pp. 1–9, 2014.
- [43] W. Yang, P. Norrlund, L. Saarinen, A. Witt, B. Smith, J. Yang, and U. Lundin, "Burden on hydropower units for short-term balancing of renewable power systems," *Nature Communications*, vol. 9, pp. 1–12, 2018.
- [44] ZESCO, *Non-public data received from ZESCO*, Lusaka, ZM, 2020.
- [45] S. Awerbuch, "Portfolio-based electricity generation planning: Policy implications for renewables and energy security," *Mitigation and Adaptation Strategies for Global Change*, vol. 11, pp. 693–710, 2006.
-



- 
- [46] X. Deng and T. Lv, "Power system planning with increasing variable renewable energy: A review of optimization models," *Journal of Cleaner Production*, vol. 246, pp. 1–15, 2020.
- [47] S. Collins, J. P. Deane, K. Poncelet, E. Panos, R. C. Pietzcker, E. Delarue, and B. P. Ó Gallachóir, "Integrating short term variations of the power system into integrated energy system models: A methodological review," *Renewable and Sustainable Energy Reviews*, vol. 76, pp. 839–856, 2017.
- [48] A. Rose, R. Stoner, and I. Pérez-Arriaga, "Prospects for grid-connected solar PV in Kenya: A systems approach," *Applied Energy*, vol. 161, pp. 583–590, 2016.
- [49] J. Hu, R. Harmsen, W. Crijns-Graus, and E. Worrell, "Geographical optimization of variable renewable energy capacity in China using modern portfolio theory," *Applied Energy*, vol. 253, 2019.
- [50] SOLARGIS, *Global solar atlas 2.0, a free, web-based application is developed and operated by the company solargis s.r.o. on behalf of the world bank group, utilizing solargis data, with funding provided by the energy sector management assistance program (esmap)*, 2020. [Online]. Available: <https://globalsolaratlas.info/map>.
- [51] DTU, *Global wind atlas 3.0, a free, web-based application developed, owned and operated by the technical university of denmark (dtu). the global wind atlas 3.0 is released in partnership with the world bank group, utilizing data provided by vortex, using funding provided by the energy sector management assistance program (esmap)*, 2020. [Online]. Available: <https://globalwindatlas.info/area/>.
- [52] *Renewables.ninja*, 2021. [Online]. Available: <https://www.renewables.ninja/>.
- [53] S. Pfenninger and I. Staffell, "Long-term patterns of European PV output using 30 years of validated hourly reanalysis and satellite data," *Energy*, vol. 114, pp. 1251–1265, 2016.
- [54] I. Staffell and S. Pfenninger, "Using Bias-Corrected Reanalysis to Simulate Current and Future Wind Power Output," *Energy*, vol. 114, pp. 1224–1239, 2016.
- [55] E. A. Rye and A. L. Øvrebø, "Analyzing the Integration of Renewable Energy in Interconnected Power Systems Using a Flow-based Market Model," M.S. thesis, Norwegian University of Science and Technology (NTNU), Trondheim, NO, 2016.
- [56] J. Frayer, S. Keane, and J. Ng, "Estimating the Value of Lost Load," London Economics International LLC, Boston, US, Tech. Rep., 2013.
- [57] H. G. Svendsen and O. C. Spro, "PowerGAMA: A new simplified modelling approach for analyses of large interconnected power systems, applied to a 2030 Western Mediterranean case study," *Journal of Renewable and Sustainable Energy*, vol. 8, pp. 1–29, 2016.
- [58] H. Farahmand, S. Jaehnert, T. Aigner, and D. Huertas-Hernando, "Nordic hydropower flexibility and transmission expansion to support integration of North European wind power," *Wind Energy*, vol. 18, pp. 1075–1103, 2014.

- 
- [59] Ministry of Energy and Water Development, “Power System Development Master Plan for Zambia 2010-2030,” Lusaka, ZM, Tech. Rep., 2011.
- [60] A. D. Roberts and G. J. Williams, *Zambia*, 2020. [Online]. Available: <https://www.britannica.com/place/Zambia>.
- [61] Pinterest, *Zambia map*, 2020. [Online]. Available: <https://no.pinterest.com/pin/436356651397805788/>.
- [62] Wikimedia Commons, *Topographic map of Zambia*, 2017. [Online]. Available: [https://commons.wikimedia.org/wiki/File:Zambia%7B%5C\\_%7DTopography.png%7D](https://commons.wikimedia.org/wiki/File:Zambia%7B%5C_%7DTopography.png%7D).
- [63] The World Bank Group, *The World Bank In Zambia*, 2020. [Online]. Available: <https://www.worldbank.org/en/country/zambia/overview>.
- [64] African Forum and Network on Debt and Development, “The case of copper for Zambia,” AFRODAD, Harare, ZW, Tech. Rep., 2016.
- [65] P. Jain, “Coal Power in Zambia : Time to Rethink,” *Southern African Journal of Policy and Development*, vol. 3, pp. 14–24, 2017.
- [66] International Energy Agency (IEA), *Zambia - Countries & Regions - IEA*, 2018. [Online]. Available: <https://www.iea.org/countries/zambia>.
- [67] Multiconsult, *Itezhi-tezhi dam*, 2020. [Online]. Available: <https://www.mynewsdesk.com/no/multiconsult/pressreleases/assessment-of-itezhi-tezhi-dam-in-zambia-2970507%7D>.
- [68] A. Kiganda, *Construction of diesel power plants in Zambia halted*, 2016. [Online]. Available: <https://constructionreviewonline.com/news/construction-diesel-power-plants-zambia-halted/>.
- [69] B. P. Mulenga, S. T. Tembo, and R. B. Richardson, “Electricity access and charcoal consumption among urban households in Zambia,” *Development Southern Africa*, vol. 36, pp. 585–599, 2019.
- [70] M. Tailashi, *We cannot stop exporting power because of Load shedding - ZESCO*, 2020. [Online]. Available: <https://onelovezambia.com/we-cannot-stop-exporting-power-because-of-load-shedding-zesco/>.
- [71] M. Vagliasindi and J. Besant-Jones, “Power Market Structure: Revisiting Policy Options,” World Bank, Washington DC, US, Tech. Rep., 2013.
- [72] Lusaka Times, *Zesco in k2.8 billion loss in 2018 – nkhuwa*, 2019. [Online]. Available: <https://www.lusakatimes.com/2019/11/21/zesco-in-k2-8-billion-loss-in-2018-nkhuwa/>.
- [73] CUTS (2020), “Targeting Residential Electricity Subsidies in Zambia,” CUTS International, Lusaka, ZM, Tech. Rep. January, 2020.
- [74] A. Mwila *et al.*, “Energy Sector Report 2018,” Energy Regulation Board, Lusaka, ZM, Tech. Rep., 2018.

- 
- [75] SOLARGIS, *Global solar atlas 2.0, a free, web-based application is developed and operated by the company solargis s.r.o. on behalf of the world bank group, utilizing solargis data, with funding provided by the energy sector management assistance program (esmap)*, 2019. [Online]. Available: <https://globalsolaratlas.info/download/zambia>.
- [76] M. Z. Jacobson and V. Jadhav, "World estimates of PV optimal tilt angles and ratios of sunlight incident upon tilted and tracked PV panels relative to horizontal panels," *Solar Energy*, vol. 169, pp. 55–66, 2018.
- [77] A. Banda, L. Simukoko, and H. M. Mwenda, "A Review of Wind Resource Potential for Grid-Scale Power Generation in Zambia," UNESCO 6th Africa Engineering Week and 4th Africa Engineering Conference, on the 18th – 20th September, at Avani Victoria Falls Resort, Livingstone, Zambia, 2019.
- [78] SAPP Operating Guidelines Revision Task Team, "Southern African Power Pool Operating Guidelines," SAPP, Harare, ZW, Tech. Rep., 2012.
- [79] E. Ibanez, I. Krad, and E. Ela, "A systematic comparison of operating reserve methodologies," *2014 IEEE PES General Meeting Conference Exposition*, pp. 1–5, 2014.
- [80] SAPP Planning Sub-Committee, "Sapp pool plan 2017," SAPP, Harare, ZW, Tech. Rep., 2017.
- [81] Norconsult, *Kafue Gorge Lower Hydropower Project , Zambia*, 2015. [Online]. Available: <https://www.norconsult.com/projects/kafue-gorge-lower-hydropower-project/>.
- [82] Zambezi River Authority, *Kariba reservoir data*, 2020. [Online]. Available: <http://www.zambezi.org/hydrology/kariba-reservoir-data>.
- [83] C. Arndt, F. Hartley, G. Ireland, K. Mahrt, B. Merven, and J. Wright, "Developments in Variable Renewable Energy and Implications for Developing Countries," *Curr Sustainable Renewable Energy Rep*, vol. 5, pp. 240–246, 2018.
- [84] B. Pillot, M. Muselli, P. Poggi, and J. B. Dias, "Historical trends in global energy policy and renewable power system issues in Sub-Saharan Africa: The case of solar PV," *Energy Policy*, vol. 127, pp. 113–124, 2019.
- [85] M. De Felice, S. Busch, and G. I. Hidalgo, "Analysis of the water-power nexus in the southern african power pool," Publications Office of the European Union, Luxembourg, LU, Tech. Rep., 2020.
- [86] Multiconsult and The Norwegian University of Life Sciences, "Roadmap to the New Deal on Energy for Africa: An analysis of optimal expansion and investment requirements," Multiconsult, Oslo, Norway, Tech. Rep., 2018.
- [87] R. Wiser, M. Bolinger, and E. Lantz, "Assessing wind power operating costs in the United States: Results from a survey of wind industry experts," *Renewable Energy Focus*, vol. 30, pp. 46–57, 2019.
- [88] T. Freyman and T. Tran, "Renewable energy discount rate survey results - 2018," Grant Thornton UK LLP, London, UK, Tech. Rep., 2019.

- 
- [89] J. Chase, "Scaling solar for Africa: Zambia's 6-cent PV," Bloomberg New Energy Finance, New York, US, Tech. Rep., 2016.
- [90] African Energy, *Zambia: Get fit announces \$4c/kwh tariff*, 2019. [Online]. Available: <https://www.africa-energy.com/live-data/article/zambia-get-fit-announces-4ckwh-tariff>.
- [91] Multiconsult, *Data received from Supervisor Thomas Haugstenrød*, Oslo, NO, 2021.
- [92] M. Preindl and S. Bolognani, "Optimization of the generator to rotor ratio of MW wind turbines based on the cost of energy with focus on low wind speeds," *IECON 2011 - 37th Annual Conference of the IEEE Industrial Electronics Society*, pp. 906–911, 2011.
- [93] CICERO, *Norwegian wind power expansion remains contested*, 2019. [Online]. Available: <https://cicero.oslo.no/en/posts/climate-news/norwegian-wind-power-expansion-remains-contested>.

---

# Appendix

## A Sources used for modeling the Zambian system

<b>Input parameters</b>	<b>Sources</b>
Geographical location of new Solar PV plants	[75], [11]
Geographical location of new wind power plants	[51], [77], [11]
Renewable energy generation profiles	[76], [77], [52]
Precipitation data	[52]
Operating reserve requirements	[44], [11]
Thermal power plants	[11], [74], [44]
RoR hydropower plants	[44], [59], [11], [74]
Large hydropower plants with reservoirs	[11], [74], [44], [59]
Existing/planned VRE power plants	[74], [52]
System load	[44], [11]
Marginal cost of generators	[44], [55]
Value of lost load	[80], [6]
Water values	[85], [44], [55]
Annualized CAPEX and OPEX of new VRE capacity	[86], [21], [11]
Electricity grid data	[44]

**Table 17:** Sources used for modeling the Zambian system in PowerGAMA, and the cost parameters used in the portfolio optimization.

## B Sensitivity analysis: Dynamic water values

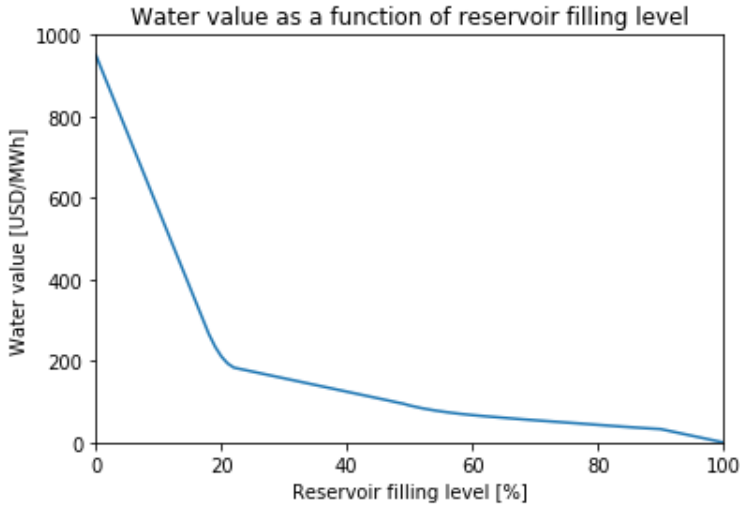


**Figure 33:** Water value profile obtained from [55] and scaled to fit the VoLL in Zambia. The curve shows a steep decrease in water value when the reservoir level is less than 20%. The static water value of 52 USD/MWh used in the base case is obtained for a reservoir level of 73%, which is close to the initial reservoir level of 75% at the beginning of the year.

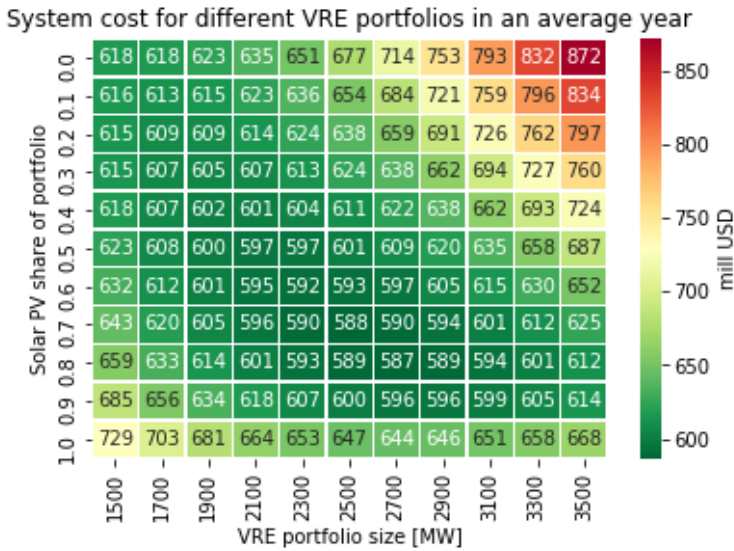


**Figure 34:** System cost for different VRE portfolios in an average year, when using dynamic water values.

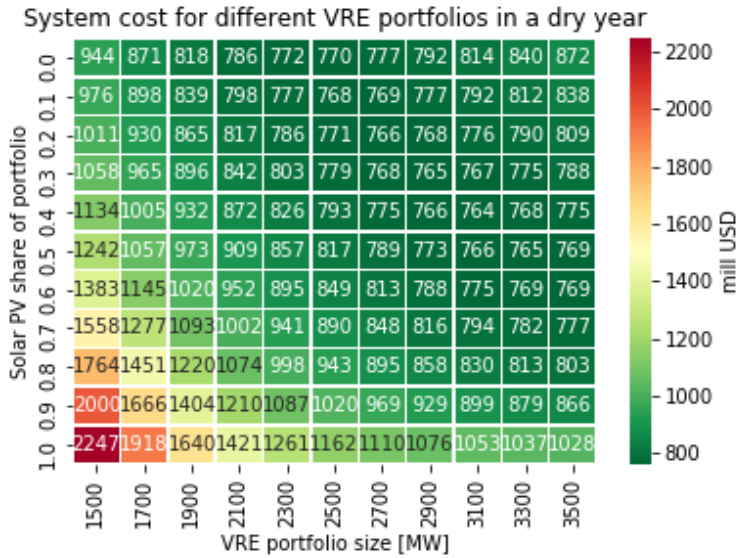


Figure 35: System cost for different VRE portfolios in a dry year, when using dynamic water values.

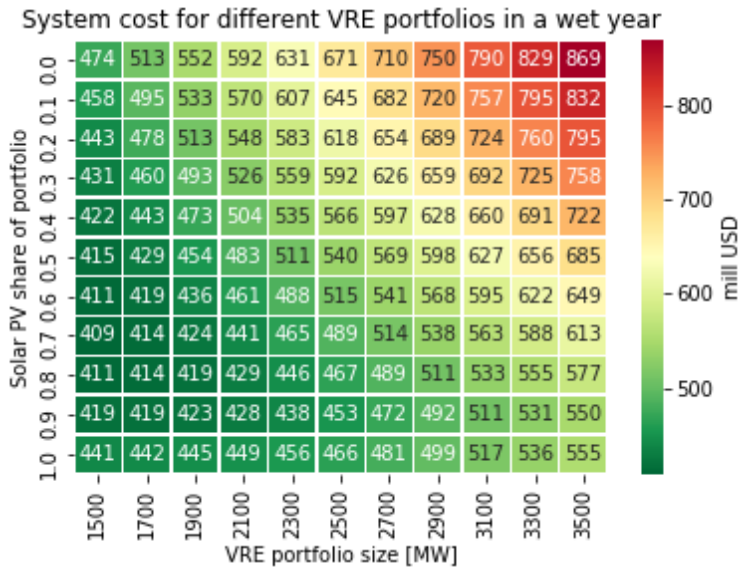
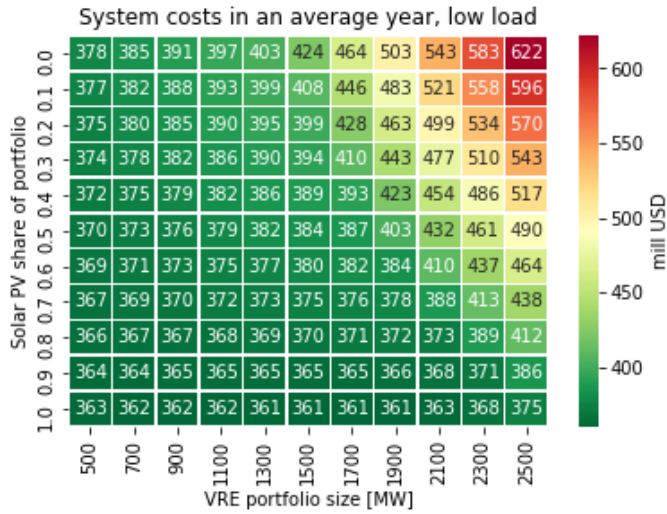
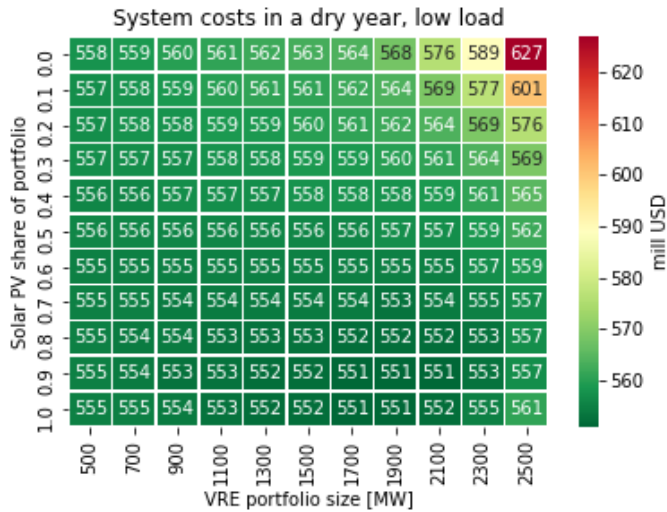


Figure 36: System cost for different VRE portfolios in a wet year, when using dynamic water values.

## C Sensitivity analysis: Low load



**Figure 37:** System cost for different VRE portfolios in an average year, when modeling the system with low load.



**Figure 38:** System cost for different VRE portfolios in a dry year, when modeling the system with low load.



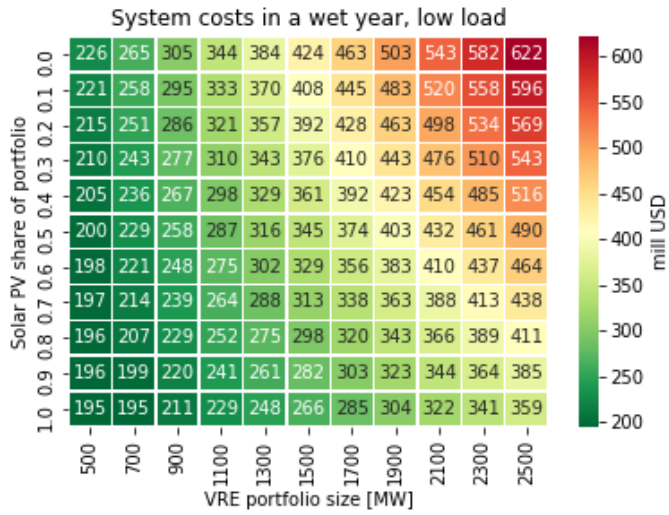


**Figure 39:** System cost for different VRE portfolios in a wet year, when modeling the system with low load.

## D Sensitivity analysis: Low initial reservoir level

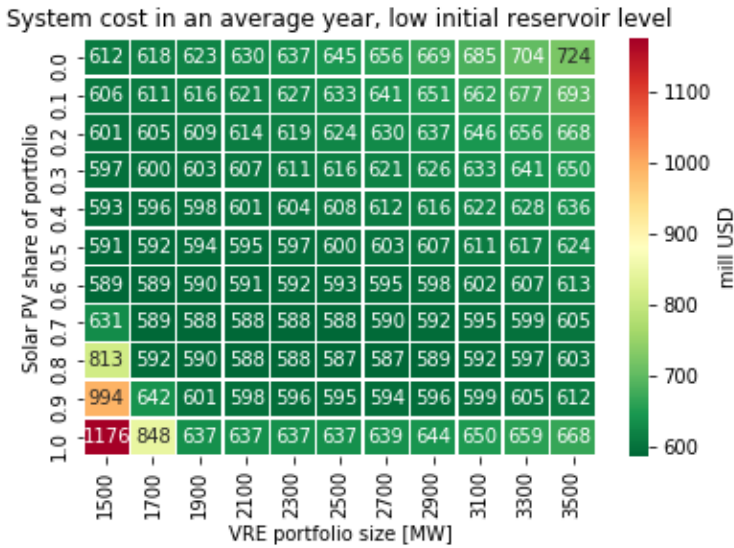


**Figure 40:** System cost for different VRE portfolios in an average year with a low initial reservoir level.

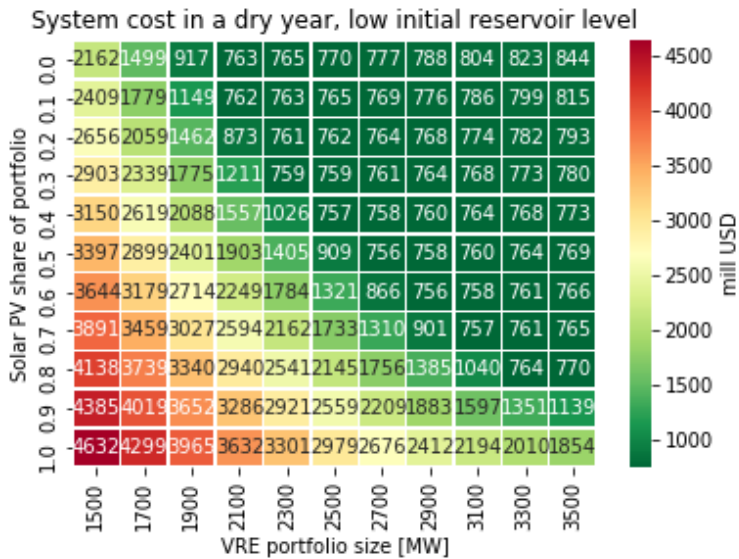


**Figure 41:** System cost for different VRE portfolios in a dry year with a low initial reservoir level.

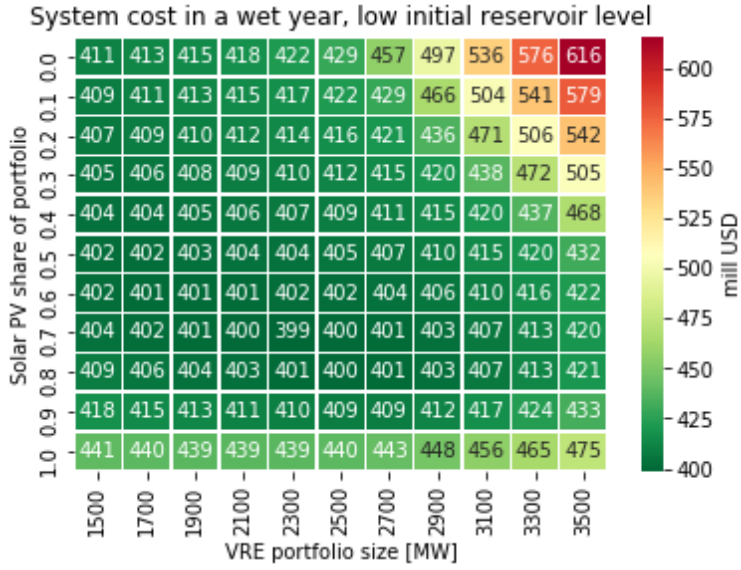


**Figure 42:** System cost for different VRE portfolios in a wet year with a low initial reservoir level.

## E Distribution of VRE power plants in the grid model

The solar PV plants included in the grid model can be seen in Table 18. The optimal new solar PV capacity of 1470 MW was distributed in two steps. First, the currently planned solar PV plants, described in Section 4, were distributed at expected connection points (Planned cap.). Second, the remaining new solar PV capacity was distributed equally between the nodes where new solar capacity is planned or expected to be implemented (Added cap.). This included adding capacity at Livingstone and Kasama where no solar PV capacity is currently planned. The capacity at each node can be viewed as the sum of capacity of the power plants connected to that node. In reality, this could be a single power plant, or several plants.

Node	Planned cap. [MW]	Added cap. [MW]	Total cap. [MW]
Kabwe	40	81	121
Kafue Town	40	81	121
Kitwe	40	81	121
Pensulo	100	81	181
Muzuma	100	81	181
Leopards Hill	150	81	231
Mumbwa	100	81	181
Kariba North	90	81	171
Livingstone	0	81	81
Kasama	0	81	81
<b>Total</b>	<b>660</b>	<b>810</b>	<b>1470</b>

**Table 18:** The optimal new solar PV capacity distributed in the grid model.

The same logic as for the solar PV plants was used for distributing the optimal wind power capacity in the grid. Table 19 shows the resulting distribution. Since only one wind power plant is currently planned, the majority of generation capacity was distributed evenly between the selected nodes.

Node	Planned cap. [MW]	Added cap. [MW]	Total cap. [MW]
Kabwe	0	62.5	62.5
Lusaka West	0	62.5	62.5
Chipata West	0	62.5	62.5
Pensulo	130	62.5	192.5
Mpika	0	62.5	62.5
Leopards Hill	0	62.5	62.5
Mumbwa	0	62.5	62.5
Kafue West	0	62.5	62.5
<b>Total</b>	<b>130</b>	<b>500</b>	<b>630</b>

**Table 19:** The optimal new wind power capacity distributed in the grid model.

